PD
539.7
G 326
V. 3, No. 1

POWER REACTOR TECHNOLOGY

A Quarterly Technical Progress Review

Prepared for U. S. ATOMIC ENERGY COMMISSION by GENERAL NUCLEAR ENGINEERING CORP.

ILLINOIS STATE LIBRARY
JAN 6 - 1960
U. S. Dept. of Documents Division

December 1959

VOLUME 3

NUMBER 1

TECHNICAL PROGRESS REVIEWS

To meet the needs of industry for concise summaries of current atomic developments, the Atomic Energy Commission is publishing this series, Technical Progress Reviews. Issued quarterly, each of the reviews digests and evaluates the latest findings in a specific area of nuclear technology and science.

The four journals published in this series are:

Nuclear Safety, W. B. Cottrell, editor, R. A. Charpie, advisory editor, and associates, Oak Ridge National Laboratory

Power Reactor Technology, Walter H. Zinn and associates, General Nuclear Engineering Corporation

Reactor Core Materials (covering solid material developments), R. W. Dayton, E. M. Simons, and associates, Battelle Memorial Institute

Reactor Fuel Processing, Stephen Lawroski and associates, Chemical Engineering Division, Argonne National Laboratory

Each journal may be purchased ($2.00 per year for subscription and individual issues $0.55) from the Superintendent of Documents, U. S. Government Printing Office, Washington 25, D. C. See back cover for remittance instructions and foreign postage requirements.

●

Availability of Reports Cited in This Review

Unclassified AEC reports are available for inspection at AEC depository libraries and are sold by the Office of Technical Services, Department of Commerce, Washington 25, D. C.

Unclassified reports issued by other Government agencies or private organizations should be requested from the originator.

Unclassified British and Canadian reports may be inspected at AEC depository libraries. British reports are sold by the British Information Service, 45 Rockefeller Plaza, New York, N. Y.; Canadian reports (AECL series) are sold by the Scientific Document Distribution Office, Atomic Energy of Canada, Ltd., Chalk River, Ontario, Canada.

Classified U. S. and foreign reports identified in this journal as Secret or Confidential may be purchased by properly cleared Access Permit Holders from the Technical Information Service Extension, U. S. Atomic Energy Commission, P. O. Box 1001, Oak Ridge, Tenn. Such reports may be inspected at classified AEC depository libraries.

PD
539.7
G326
V.3, No.1

POWER REACTOR TECHNOLOGY

A REVIEW OF RECENT DEVELOPMENTS

Prepared for U. S. ATOMIC ENERGY COMMISSION
by GENERAL NUCLEAR ENGINEERING CORP.

● DEC. 1959
● VOLUME 3
● NUMBER 1

foreword

This quarterly review of reactor development has been prepared at the request of the Division of Information Services of the U. S. Atomic Energy Commission. Its purpose is to assist interested organizations in the task of keeping abreast of new results in reactor technology for civilian application.

The report is a concise discussion of selected phases of research and development for which there have been significant advances or a heightened interest in the past few months. It is not meant to be a comprehensive abstract of all material published during the quarter, nor is it meant to be a treatise on any part of the subject. The intention is to cover the various areas of reactor development from the general viewpoint of the reactor designer rather than from the more detailed points of view of specialists in the individual areas. However, papers which are thought to be of particular significance or particular usefulness in specialized fields will be mentioned in short notes. In the overall plan of the report, it is intended that various subjects will be treated from time to time and will be brought up to date at that time.

Any interpretation of results which is given represents only the opinion of the editors of the report, who are General Nuclear Engineering Corporation personnel. Readers are urged to consult the original references in order to obtain all the background of the work reported and to obtain the interpretation of the results given by the original authors.

W. H. ZINN
General Nuclear Engineering Corporation

contents

ii Foreword

1 **GENERAL RESEARCH AND DEVELOPMENT**

1 I REACTOR APPLICATIONS: PROCESS STEAM GENERATION

1 Uses of Process Heat
1 Process Heat Generation and Consumption
2 Reactors for Producing Process Steam
5 References

6 II THERMIONIC ENERGY CONVERSION

6 Basis of Operation
7 Efficiency Equation
7 Estimates of Attainable Efficiencies
8 High-vacuum Thermionic Converter Performance
9 Experiments on a Cesium-vapor-filled Thermionic Converter
10 Applications
11 Los Alamos Plasma Thermocouple
13 References

15 III REACTOR PHYSICS: H_2O-MODERATED CRITICAL ASSEMBLIES AND ANALYSES

17 References

18 IV HEAT TRANSFER AND FLUID FLOW

18 Collapse of Parallel-plate Fuel Assemblies
19 Nucleate Boiling
21 Liquid-metal Heat Transfer
22 Liquid Metals with Internal Heat Generation
22 Water Flowing Parallel to Tube Bundles
23 References

24 V REACTOR KINETICS AND DYNAMICS

24 Delayed Neutrons in Reactor Kinetics
25 Reduced Delayed-neutron Group Representations
25 Approximations for Reactor Accident Calculations

contents (continued)

26 Oscillation Experiments on Large Heavy-water Reactors
26 Transfer Functions of Distributed Parameter Systems
27 References

28 VI REACTOR SAFETY AND CONTAINMENT

28 AEC Reactor Safety Program
30 Metal-Water Reactions
33 SRE Shutdown
33 References

36 VII SHIELDING

36 Review of Shielding Art
36 Reference

37 VIII MATERIALS

37 Radiation Effects on Semiconductors
37 Radiation Effects on Magnetic Materials
38 Corrosion of Stainless Steel in a Nitrogen Atmosphere
40 References

41 **PROGRESS ON SPECIFIC REACTOR TYPES**

41 IX LIGHT-WATER REACTORS

41 The Belgian BR-3
41 Reference

42 X BOILING-WATER REACTORS: STABILITY

42 Design Considerations
44 Experimental Boiling Water Reactor
47 BORAX Reactors
51 Review of ANL Experience
53 References

54 XI FLUID-FUEL REACTORS

54 Report of the Fluid Fuel Reactors Task Force
58 The Homogeneous Reactor Test
60 References

61 XII NEW REACTOR CONCEPTS: THE FLUIDIZED-BED REACTOR STUDY

63 References

Issued quarterly by the U. S. Atomic Energy Commission. Use of funds for printing this publication approved by the Director of the Bureau of the Budget on November 1, 1957.

GENERAL RESEARCH AND DEVELOPMENT

REACTOR APPLICATIONS: PROCESS STEAM GENERATION

A recent Argonne report[1] on process steam generation directs attention to the question of nuclear process heat.

A brief discussion of the possible future magnitude of nuclear process heat applications, based on references 2 and 3, was given in *Power Reactor Technology*, 2(3): 4-5 (June 1959). The questions of more immediate importance to the reactor designer are the magnitude of the present process heat demand, the requirements of a process heat plant, and the probability of meeting those requirements with nuclear power at the present stage of nuclear technology. A brief discussion of the first two questions, based on references 4 to 7, is given below; the Argonne report may be regarded as a consideration of the third.

Uses of Process Heat

In general, the possible applications of process heat fall into two broad categories defined by operating temperature: a low-temperature range of 400°F or less for use in manufacturing processes requiring low-quality steam, and a high-temperature range of 1500°F or more for use in certain specialized chemical and metallurgical operations. The latter applications are outside the range of existing reactor technology and will not be considered further here.* The practicability of using nuclear reactors for the generation of low-temperature process steam depends on economic factors since the technical feasibility of reactor operation under somewhat more severe conditions is well established.

Large quantities of low-temperature process steam are presently consumed in the processing of products such as textile fibers, chlorine and alkalis, fertilizers, petroleum, antibiotics, pulp and paper, aluminum, and corn products. In the majority of applications, the amount of heat required for an individual plant is under 80 Mw(t), and the user pays less than 70 cents per 10^6 Btu for energy in the form of steam. Although the low unit capacities of the plants do not favor the use of nuclear power, there are certain characteristics of these applications which are favorable. Almost all the plants operate at a load factor of 90 per cent or greater, which is, of course, desirable for a nuclear plant because of the comparatively high contribution of capital investment to the total steam production cost. A second consideration is that the low temperature and pressure requirements may allow cheapening of the reactor. They may, for example, make possible the use of inexpensive materials, such as aluminum or its alloys in the fabrication of the core, or of carbon steel instead of stainless steel in the primary system. Finally, many of the industries using process steam are located in remote areas near their sources of raw materials. The use of a nuclear reactor would provide greater flexibility in the location of plants since transportation of fuel would not be a great problem. The remote location might also conceivably ease the requirements on containment.

Process Heat Generation and Consumption

Certain other aspects of the process steam application appear unfavorable to the introduction of a new energy source. Since in most of the applications proposed the cost of the steam is a small fraction of the cost of producing the end product, proven reliability of the steam

*Some specific high-temperature applications are discussed in references 4 to 6.

generator is usually mandatory. If standby equipment must be provided to ensure against loss of production in case of reactor failure, the economic picture probably becomes quite discouraging. Furthermore, the potential customers for process steam have no great incentive to pursue or support any developmental programs for steam generators, since their interests lie primarily in their finished products.

Reference 7 gives more detailed data on the quantity of process steam used in past years, its cost, and unit sizes of installations. In 1954, approximately 8.7×10^{15} Btu of energy was used as process heat in manufacturing industries in the United States. Of this, about one-third was used in the application of direct firing of fuels to the process, that is, in general, at high temperatures. The remaining two-thirds was used as steam. The process energy used as steam corresponds to approximately 180,000 Mw-years per year, an amount roughly equal to the energy consumption for the production of electricity in that year. Most of the installations fell in the size range below 250,000 lb of steam per hour (~80 Mw(t)), and only about 5 per cent of the capacity was in units having individual capacities greater than 500,000 lb per hour (~160 Mw(t)). The distribution of boiler capacity for process steam units added from 1945 to 1956 is given, over the range of steam pressures and unit capacities, in Table I-1.

Table I-1 PERCENTAGES OF BOILER CAPACITY ADDED IN VARIOUS CAPACITY AND PRESSURE RANGES[7]
(United States Manufacturing Industries, 1945 to 1956)

Pressure range, psi	Percentages of boiler capacity added for the steam capacity ranges (in 10^3 lb/hr) indicated				
	Under 100	100–250	250–500	500 +	Total
Under 250	29.1	5.5			34.6
250–600	8.8	11.8	3.6	0.5	24.7
600–1000	2.3	19.2	10.1	0.2	31.8
1000 +	0.1	0.4	4.2	4.2	8.9
Total	40.3	36.9	17.9	4.9	100.0

It is estimated[7] that, for the smaller coal-fired process steam boilers operating at 90 per cent load factors, the cost of steam generation is about 70 cents per 1000 lb, whereas for a large boiler in the 600,000 lb/hr capacity range, the generating cost under the same conditions would be about 47 cents per 1000 lb. These costs, in terms of energy, correspond to approximately 65 cents and 44 cents per million Btu, or 2.2 and 1.5 mills/kw(t)-hr, respectively.

Reactors for Producing Process Steam

The Argonne report[1] covers a feasibility study of nuclear reactors for process steam which was undertaken at the request of the Atomic Energy Commission. The area defined for study was characterized by the production of saturated steam at 380°F and at a rate of 125,000 lb/hr, with shielding and containment of the plant suitable for location on an industrial site. Four reactor types were studied: a pressurized-water reactor (PWR) with stainless-steel primary system, a similar PWR with carbon-steel primary system, a boiling-water reactor (BWR), and an organic-moderated reactor (OMR). The estimated steam production costs (in cents per 1000 lb of steam) for the designs studied were as follows:

PWR	64–150
BWR	83–172
OMR	75–154

The PWR listed is the one employing the stainless-steel primary system. The ranges in production costs result primarily from differences in assumptions as to rates of capital charge and plant factors. Table I-2 gives a breakdown of production costs for a capital charge rate of 15 per cent per year and a plant factor of 90 per cent. It is stated in the report that none of the reactor types studied has dominant characteristics which show it to be a clear-cut choice over the others for the application. It is implied that the considerably higher fuel cost for the boiling-water reactor is a consequence of the specific reactor design chosen rather than a characteristic of the reactor type.

Other conclusions reached in the study are that carbon or low alloy steels should be acceptable materials of construction for water-cooled reactors having operating temperatures of 500°F or lower, provided that the *p*H is maintained at 10 to 11, that hydrogen is added to the water, and that dissolved and suspended solids are maintained at low levels. It is also concluded that aluminum-clad fuels with surface temperatures as high as 500°F may be acceptable in stainless-steel systems where the *p*H of the water can be

Table I-2 STEAM GENERATION COSTS[1]

	PWR, stainless steel	PWR, carbon steel	BWR	OMR
Capital cost of plant, including land and escalation, dollars	2,763,000	2,486,000	2,226,000	2,260,000
Capital charge at 15 per cent per year and 90 per cent plant factor, cents/10^3 lb steam	42	38	34	34
Nonfuel operating charge, cents/10^3 lb steam	15	15	15	21
Fuel operating charge, cents/10^3 lb steam	20	20	28	24
Fuel inventory charge, at 4 per cent per year on uranium, 6 per cent per year on fabrication cost of fuel inventory not yet loaded, and 15 per cent per year on fabrication cost of core in reactor	12	12	32	17
Total, cents/10^3 lb steam	89	85	109	96

Table I-3 SUMMARY OF PROCESS-STEAM REACTOR DESIGN DATA[1]

	PWR	BWR	OMR
Power, Mw(t)	40.6	40.6	40.6
Fuel	UO_2 in Zr	UO_2 in Zr	U plates in Al
Coolant	H_2O	H_2O	Diphenyl
Core diameter × length, in.	42 × 42	56.3 × 60	48 × 48
Core volume, liters	953	2442	1475
Power density, kw/liter of core	42.6	16.6	27.5
Fuel enrichment, %	1.8	1.5	1.5
Initial fuel loading, kg of U	3380	10,300	7650
Specific power, kw/kg of U	12.0	3.9	5.3
Burn-up, Mwd/metric ton	17,200	12,300	8900
Nonwater to water ratio in fuel region	1.35 : 1	1.2 : 1	
Nonorganic to organic ratio in fuel region			1 : 1
Initial conversion ratio	>0.8	>0.8	>0.8
Void coefficient of reactivity, $\frac{\Delta k}{k} \frac{\Delta \text{ void}}{\text{water volume}}$	−0.2284	−0.1884	
Average steam volume fraction in core		0.18	
Average heat flux, Btu/(sq ft)(hr)	9.08×10^4	4.36×10^4	1.65×10^4
Maximum heat flux, Btu/(sq ft)(hr)	4.74×10^5	1.30×10^5	7.6×10^4
Primary flow rate, lb/hr	4.22×10^6	1.39×10^5	7.9×10^6
Inlet temp., °F	400	239*	421
Outlet temp., °F	430	427	450
Reactor pressure, psi	900	333	75
Process steam conditions:			
Flow rate, lb/hr	1.25×10^5	1.25×10^5	1.25×10^5
Temp., °F	380	380	380
Pressure, psia	196	196	196
Condensate return temp., °F	150	150	150
Make-up water, lb/hr at 60°F	35,000	35,000	35,000

*Inlet temperature into reactor vessel.

5 to 6, but further experience with aluminum corrosion is needed before a definite recommendation for its use under these conditions can be made.

The main characteristics of the designs arrived at for the three reactor types are given in Table I-3. The pressurized-water reactor uses a two-pass flow system through the core, and its heat-removal characteristics are defined by the condition that no fuel-element surface temperature shall be higher than the water saturation temperature. The boiling-water reactor is a natural-circulation system. The process steam is generated in a reboiler whose primary side is fed only by primary steam from the reactor. The reactor employs absorbing control rods with

fuel bundles as followers, but these do not appear to have any great effect on the economic evaluation. The organic reactor is moderated and cooled by diphenyl; it employs a plate type fuel element of uranium −3.5 wt.% molybdenum−0.5 wt.% silicon alloy, nickel-plated, and clad with finned 2S aluminum. Both of the water reactors are provided with steel secondary containment shells; the organic reactor is housed in an insulated sheet-steel building with reinforced-concrete basement (in which the reactor and its primary system are located) and special sealing to minimize leakage through the walls of the steel building.

If a steam production cost of about 70 cents per 1000 lb can be considered a reasonable economic target for a reactor of this size, then the study would appear to indicate that the reactors considered have some chance of approaching this goal. Since it is probable that there is a greater variation in process-steam generating costs than in electric power generating costs in this country, it may well be that there are individual instances in which the use of nuclear process steam would appear economically attractive. This, of course, could be determined only by making a more detailed reactor design for the particularly favorable case selected.

In view of the simplicity of the natural-circulation boiling reactor and its low operating pressure for the process-steam application, and in view of the encouraging experience that has been had with the construction costs and operating behavior of EBWR and other experimental boiling reactors, it comes as a surprise that the study should show a substantially higher steam production cost for the boiling reactor than for either the pressurized-water or the organic-moderated reactor. Although this difference is de-emphasized in the report as being attributable to the specific design study, it must nevertheless be presumed to have some meaning if the study has significance as a comparative study. A consideration of the cost breakdown of Table I-2 shows that the boiling reactor does have the lowest estimated capital cost, that most of the excess cost of steam generated by the boiling reactor is due to a very high fuel inventory charge, and that the remainder of the excess is due to a high fuel operating charge. The latter difference between the boiling and the pressurized reactors appears to stem from the fact that the two reactors were designed with equal quantities of initial excess reactivity, with the fuel lifetime defined as the reactivity lifetime in a uniform flux (obtained by radial and axial fuel shuffling), single-batch, reloading cycle. This appears to be a rather arbitrary way of defining the fuel lifetime, unless it could be shown that a real limitation is involved which could not be circumvented either by the provision of more control-rod capacity or by the use of a partial reloading scheme.

The very high inventory charge against the boiling reactor reflects the low specific power of 3.9 Mw(t) per metric ton of uranium (Table I-3), which in turn is consistent with the low power density of 16.6 kw/liter of core. These low values evidently result from the high value of fuel-to-water ratio used in the reactor. The ratio of nonwater to water volume in the core is 1.2. Thus the power density per liter of coolant is $16.6 \times 2.2 = 37$ kw/liter, a value which is not high for a boiling reactor but nevertheless is not so strikingly low as the power density per liter of core. The second effect of the high fuel-to-water ratio is a relatively high negative steam void coefficient of reactivity (−0.188 per cent k_{eff}/per cent void). As a result of this rather high coefficient, the reactivity held by steam apparently amounts to 3 per cent k_{eff} or more even at the low design power density. The high fuel-to-water ratio was evidently used in order to attain a high conversion ratio. Indeed, the conversion ratios quoted in the report for the three reactor types—which were computed as part of a parametric study rather than for the specific reactor designs described—are surprisingly high for reactors of such small size.

The conflicting demands of conversion ratio and steam void coefficient of reactivity have been pointed out before in this Review, *Power Reactor Technology*, 2(1): 16 (December 1958) and 2(4): 13-16 (September 1959), and are discussed further in the section on boiling reactor stability in the present Review, p. 41. Although a compromise must usually be made between conversion ratio and power density, and the optimum may very well vary with the specific reactor design and application, it would seem improbable that the optimum would swing so far toward high conversion ratio as to result in an inventory charge which accounts for some 30 per cent of the energy generation costs. If the boiling reactor in question were designed for a "wetter" core and were given sufficient excess reactivity to achieve a fuel life equal to that in

the pressurized-water reactor, the inventory charge would decrease, the net fuel burn-up cost would increase to some extent, and there should be some decrease in capital cost. The net effect would probably be a reduction of steam production cost.

References

1. R. H. Armstrong et al., Study of 40 Mw Pressurized Water, Boiling Water, and Organic Moderated Reactors for Production of Process Steam, ANL-6009, June 1959. (Unclassified AEC report.)
2. P. L. Geiringer and M. J. Goodfriend, Potential Applications of Nuclear Energy for Process and Space Heat in the United States, NYO-2332, October 1958. (Unclassified AEC report.)
3. K. M. Mayer, The Economic Setting for World Nuclear Power, A/CONF.15/P/2163, Second United Nations International Conference on the Peaceful Uses of Atomic Energy, Geneva, September 1958.
4. The Outlook for Industrial Heat Reactors, *Nucleonics*, 16(2): 62-71 (February 1958).
5. C. M. Nicholls, Nuclear Heat, *Nuclear Power*, 3(22): 64-68 (February 1958).
6. B. W. Gamson, Nuclear Process Heat Reactors, *Chemical Engineering Progress*, 54(2): 74-78 (February 1958).
7. W. Lawrence Prehn, Jr., and Richard R. Tarrice, Process Heat Generation and Consumption, 1939 to 1967, AECU-3364, January 1958. (Unclassified AEC report.)

Basis of Operation

The thermionic energy converter is a device which converts heat energy directly into electrical energy. It is shown in its simplest form in Fig. 1. Basically, the thermionic energy converter consists of a hot cathode which emits electrons thermionically and a cold anode which collects the emitted electrons. The energy input to the device shown in Fig. 1 is heat which is directed into the cathode. From this heat, useful electrical power can be obtained, under the proper circumstances, by connecting a resistive load between the cathode and the anode. The operation of the converter can be viewed as a thermodynamic cycle wherein the working fluid is the electron gas which is made to flow from the hot plate to the cold plate with a resultant electrical work output.

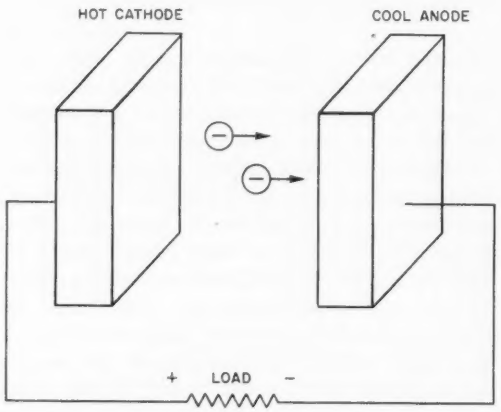

Figure 1 — The simplest form of a thermionic converter.

The thermionic converter utilizes the so-called "Edison effect," which is probably the oldest observed electronic phenomenon. It has been only in the past two years, however, that the device has received serious attention as a possible efficient and practical heat engine.

The basis for operation of the thermionic converter may be better understood by referring to the potential-energy diagram of Fig. 2.

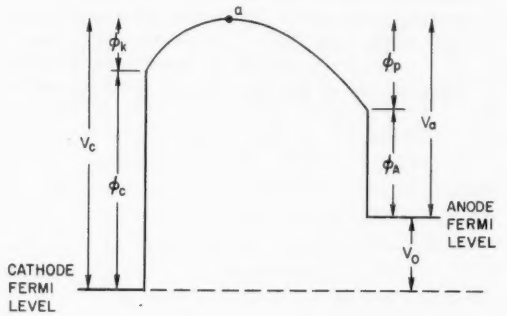

Figure 2 — A potential-energy diagram of a thermionic converter.

The vertical distance on the diagram represents the potential energy of the electron. Heat increases the temperature of the electrons in the cathode, and, therefore, some of the electrons acquire sufficient energy to escape from the plate. The minimum energy required for escape is ϕ_c, which is the energy difference between the Fermi energy level of the electron within the plate and the energy of the electron at rest in a vacuum outside the plate. An additional amount of energy must be supplied to the emitted electron to hurdle the space-charge potential barrier, ϕ_k. Hence, at position *a* in Fig. 2, the electron has potential energy (relative to the cathode Fermi energy level) equal to $\phi_c + \phi_k$. In addition, the electron has kinetic energy $2kT_c$, which is only a few per cent of the potential energy. In effect, then, heat has lifted the electrons over the cathode work-function barrier and the space-charge barrier to the high potential required for the electrons to cross over to the anode. If the electron falls back into the cathode, this energy is given back to the cathode. However, from position *a* in Fig. 2, the electrons can slide

down the potential energy curve toward the anode, thereby converting potential ϕ_p into kinetic energy of the electrons. This kinetic energy goes into the heating of the anode when the electrons strike the anode. At the anode surface, the electrons fall into the metal and, as a result, lose potential ϕ_A as the electrons join those at the Fermi energy level of the anode. Note that ϕ_A is the work function of the anode. At the Fermi energy level of the anode, the electrons have potential energy relative to the Fermi energy level of the cathode; it is this potential difference V_0 which is available as electrical voltage to do work in an external circuit.

The desirable arrangement is a high cathode work function ϕ_c and a low anode work function ϕ_A. However, if the two plates were at the same temperature, the anode would then emit more electrons than the cathode. Hence the anode must be kept colder. With plate spacings of the order of 0.01 in. in a vacuum, the space-charge barrier limits the electron flow to a very small value. In this case, ϕ_k is so large that, at practical cathode temperatures, only a small fraction of the electrons emitted have sufficient energy to penetrate the space-charge barrier. As the space-charge barrier is reduced, the electron flow is increased and is limited finally by the emission capabilities of the cathode at its operating temperature. One way of reducing the space-charge barrier is to place the anode and the cathode very close together.[1,2] Another method is to introduce heavy positive ions to neutralize the electron space charge.[3,4] Introduction of a positively charged grid between the cathode and the anode would also be helpful if the grid did not draw excessive current. Electric and magnetic fields can be employed to conduct the electrons from the cathode to the anode as described by Hatsopoulous.[5] The space-charge barrier problem is one major obstacle which must be overcome in order to make the thermionic device look promising for further development.

Efficiency Equation

This Review is based mainly on the information given in references 1, 4, 6, and 7. The Los Alamos plasma thermocouple,[8,9] which is also a thermionic device, is treated in a separate section.

The general analysis of reference 7 establishes approximate upper limits—which may be achieved in practice—on the efficiency of thermionic converters. The analysis also provides a guide as to which experimental parameters can be profitably varied to improve efficiency. No details of the space-charge potential barrier are considered in the analysis; instead, the space-charge considerations are circumvented by analysis of the problem in terms of the potentials V_c and V_a indicated in Fig. 2.

The efficiency of a thermionic converter is simply the ratio of the electrical power output to the power input, as given by the following equation:[6,7]

$$\eta = \frac{(V_c - V_a)(J_c - J_a) - r_w(J_c - J_a)^2}{J_c\left(V_c + \frac{2kT_c}{e}\right) - J_a\left(V_c + \frac{2kT_a}{e}\right) + K + R + I}$$

The numerator is the product of the output voltage $(V_c - V_a)$ and the net current $(J_c - J_a)$, minus the joule losses in electrodes and leads, $r_w(J_c - J_a)^2$. Here, J_c is the electron-emission current from the cathode to the anode, J_a is the back-emission current from the anode, r_w is the electrical resistance of electrodes and leads, and $(V_c - V_a)$ is as indicated in Fig. 2. The first term in the denominator represents the energy required to lift the electrons from within the cathode material and over the space-charge barrier. The second term is the energy returned to the cathode by anode back-emission. Here, e is the electronic charge, T_c and T_a are the cathode and anode temperatures, respectively, and k is Boltzmann's constant. The term K represents the heat-conduction losses from the cathode, the term R represents the radiation losses from the cathode, and the term I represents the energy input required to produce positive ions for space-charge neutralization.

Estimates of Attainable Efficiencies

Houston[7] first treats the idealized case of no radiation and no conduction losses and where there is zero energy input for positive ion production. His results show that there exists an optimum value of V_a for specified V_c, T_c, and T_a values. At this optimum, the efficiency is roughly 90 per cent of the Carnot efficiency.

Note that since the device is a heat engine, its efficiency can never exceed the Carnot efficiency as given by $T_c - T_a/T_c$. At high anode temperatures ($T_a \sim 1000°K$), the optimum V_a is in the neighborhood of 1.5 volts; this is within the realm achievable with presently known materials. However, for anode temperatures in the vicinity of room temperature, the optimum V_a value is near 0.5 volt, which is unattainably low.

Houston[7] also considers more practical cases in which the extraneous energy losses are included in analysis of over-all efficiency. An anode temperature T_a of 500°K was assumed. However, this assumption is unimportant in that the results obtained are valid for fairly wide variations in anode temperature from the assumed value (T_a should be low enough so that back-emission is negligible). For a given value of V_a and J_c (where J_c is in amperes per square centimeter of cathode surface area), optimum values of T_c and V_c are shown to exist. If a V_a value of 2 volts can be achieved, a maximum η of 16 per cent is indicated as possible at J_c = 10 amp/cm^2. If a V_a value of 1 volt were possible, the maximum η would increase to 34 per cent at J_c = 10 amp/cm^2. For V_a = 2 volts, values of T_c = 2200°K and V_c = 3.4 volts are indicated as optimum. A conclusion is that a low value of V_a and, hence, of the anode work function ϕ_A and space-charge potential barrier ϕ_p, is vital in obtaining high efficiency from a thermionic converter.

It is evident that a crucial question arises in the attainment of the lower limit of V_a. For a cesium-on-oxidized-silver surface, Houston's[7] interpretation of Koller's[9] measurements indicates ϕ_A = 1 volt at 400°K. Since $V_a = \phi_A + \phi_p$, there seems to be little hope of achieving a V_a value less than 1 volt with presently known materials. Hence the value of η = 34 per cent which is calculated as maximum for an assumed V_a = 1 volt may represent an upper bound of the achievable efficiency.

High-vacuum Thermionic Converter Performance

The results of calculations of the performance of a high-vacuum thermionic energy converter are presented in reference 1. The calculations include the effect of the space charge as determined from Langmuir's work.[8] The pertinent features of the analysis and the results obtained are outlined below.

To determine the performance of the converter, it is necessary to know how the output voltage V_0 varies with current I flowing through the device. The anode is assumed to be cold enough so that no electrons are emitted from it. Then, with reference to Fig. 2,

$$V_0 = (\phi_c - \phi_A) + (\phi_k - \phi_p)$$

Both ϕ_c and ϕ_A are functions, respectively, of the cathode and anode materials used and are independent of current flow. However, the space-charge potentials, ϕ_k and ϕ_p, vary with current.

If the cathode temperature T_c, the saturated-emission density I_s available from the cathode, and the separation d of the cathode and anode are known, then both ϕ_p and ϕ_k can be calculated[10] as functions of I. The generalized results obtained were used to predict the performance that can be expected of energy converters operating at T_c = 1000 to 1200°K with saturated-emission densities characteristic of oxide-coated cathodes run in clean environments.[11] Figure 3, taken from refer-

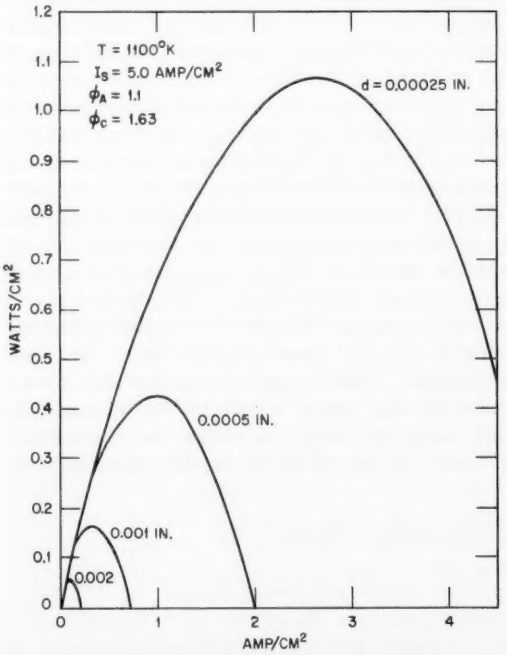

Figure 3 — The output power density versus the current density for four different cathode-anode spacings.[1]

ence 1, is a plot of output power density (watts per square centimeter of cathode surface area) versus current density. First, there is a particular value of external load resistance for which maximum power is transferred to the load. Second, the power density delivered to the load increases rapidly as the cathode-anode separation distance d decreases. In Fig. 4, output power density at maximum power transfer, i.e., using a matched load, is plotted versus cathode-anode spacing d for various values of work-function difference ranging between 0 and 1 volt. The output power density increases rapidly with increase in work-function difference ($\phi_c - \phi_A$).

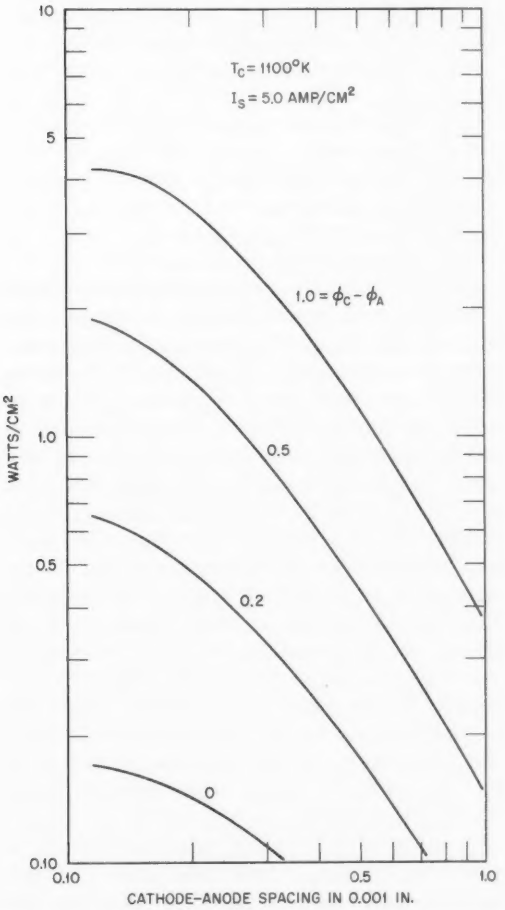

Figure 4—The output power density into a matched load versus cathode-anode spacing for various work-function differences.[1]

Webster[1] points out that some of his predictions have been checked experimentally in energy converters built by Beggs,[11] and satisfactory agreement was obtained. Beggs' work on construction techniques of thermionic converters makes the small cathode-anode spacings (less than 0.001 in.) feasible. An estimate of the efficiency of the high-vacuum thermionic converter is given by Webster.[1] With T_c = 1100°K, I_s = 5.0 amp/cm², d = 0.00044 in., and $\phi_c - \phi_A$ = 0.7 ev, Webster quotes an efficiency of 10 to 20 per cent as attainable with average emissivities and average conductive heat losses.

Experiments on a Cesium-vapor-filled Thermionic Converter

Reference 4 gives the results of experiments on an experimental thermionic converter which utilizes partially ionized cesium vapor for space-charge neutralization. As indicated in Fig. 2, the space-charge potential (ϕ_k) constitutes a barrier to the flow of electrons from the cathode to the anode. If the electrons are moving through a vacuum, the total space charge is simply the sum of the negative electrical charges on all the electrons in the space between the cathode and the anode. It will be distributed in this space in a manner determined by the variation in electron velocity across the space, which in turn depends upon the potential distribution resulting from the space-charge distribution. If the electron current across the space is increased simply by increasing the emission from the cathode, the number of electrons in the space will increase and the space-charge and the resulting negative potential resulting from it will also increase. As the space-charge potential becomes higher and higher, only the more energetic electrons emitted by the cathode can cross the space. Thus the space-charge potential imposes a limit on the current density across the space which may be lower than the limit on the density of electron emission from the cathode.

If positive ions can be introduced into the space, their positive charges will tend to neutralize the negative electron space charge, and the current-limiting effect can be greatly reduced. Since the positive ions, with their much greater masses, move across the space much slower than the electrons, a positive ion charge equal to the electron space charge can be

Table II-1 RESULTS OF EXPERIMENTS ON A CESIUM-VAPOR-FILLED THERMIONIC CONVERTER[4]

			Input power				Output power				
Condition	Cs temp., °C	Cs pressure, mm Hg	Cathode, watts	Ion source,* watts	Correction for half-time output, watts	Total input, watts	Load resistance, ohms	Potential, volts	Current, amps	Power output, watts	Efficiency, %
1	261	0.6	5.35	7.35	1.87	14.57	1.0	1.1	1.1	1.2	8.3
2	261	0.6	8.80	†	0.75	9.55	2.5	1.1	0.44	0.48	5.1
3	291	1.5	5.35	7.35	1.22	13.92	1.0	0.72	0.72	0.52	3.7
4	291	1.5	8.80	†	2.09	10.89	0.6	0.78	1.3	1.0	9.2

* Estimated input power for the central 2 cm of water.
† Tube operated as a diode with only the cathode hot.

maintained with an ion production rate which is very much smaller than the rate of electron emission from the cathode. The attractive method of producing positive ions is by the introduction of neutral atoms whose ionization potential is low enough that they may be ionized by thermal energy at the temperature existing in the thermionic device. Among the chemical elements, the alkali metals are the most easily ionized; of these metals, cesium has the lowest ionization potential (3.87 volts). Consequently, cesium vapor is an attractive substance for promoting space-charge neutralization. The presence of the cesium also affects the work functions of the two electrode surfaces so that, by adjustment of the cesium vapor pressure, the work functions of the cathode and the anode can be varied. On the cold anode the cesium presents a low-work-function collector. A description of one of the several thermionic converter tubes built is presented in reference 4. It is a three-electrode tube consisting of a cylindrical anode and two hot wires running through the cylinder. One wire (of molybdenum) is the cathode when the tube is operated as a diode. For operation as a triode, the other wire (of tungsten) is run hotter than the molybdenum wire and serves as an ion source. The anode surface is a cesiated silver oxide surface, described by Koller,[9] which is the lowest work-function photoemissive surface. The tube is enclosed in an electric oven maintained at an adjustable elevated temperature to produce the desired cesium pressure. The anode is cooled by radiation and by cesium convection to the glass wall of the tube.

Table II-1 shows the results of some tests on this tube. It is evident that the power consumed by the ion source accounts for a substantial fraction of the input power in those cases when the ion source is used (conditions 1 and 3). If, for example, in condition 1 the power to the ion source is not included in computing the efficiency, the efficiency increases to 16.8 per cent. This suggests what can be gained by a more efficient ion generator or by making more efficient use of the ions that are formed. For condition 4 in the table, the open-circuit voltage is 2.75 volts. Hence the internal voltage drop is about $2.75 - 0.78 = 1.97$ volts and suggests that the power dissipated in the plasma is $1.97 \times 1.3 = 2.6$ watts, which is 2.6 times the output power. Any reduction in the plasma potential will appear as an increase in the output potential and in the over-all efficiency. If, for example, the plasma drop could be reduced to 0.2 volt, the efficiency would increase from the measured value of 9.2 to 30 per cent. Unfortunately, this appears to be difficult to achieve. At present, it is impossible to give an accurate physical picture of low-voltage plasma. The true source of the positive ions, as well as their lifetimes and their concentrations in a temperature and voltage potential field, is unknown.

Applications

Possible applications of the thermionic energy converter are discussed in reference 4. The thermionic converter is a high-temperature heat engine whose optimum cathode temperature appears to be between 1300 and 2500°K. The anode temperature must be considerably lower, but there appears to be no advantage to be gained by anode temperatures below 650°K. Since present coolants in nuclear reactors operate in the 600°K range, the thermionic converter could conceivably operate as a top-

ping device for nuclear reactors. One way this might be accomplished is through the use of a reactor fuel element having a double-walled jacket with cesium vapor in a gap between the two walls. The inner wall would be the cathode heated by fission, and the outer wall would be the anode cooled by the conventional coolant. Direct production of electrical energy would accompany the flow of the fission heat through the cesium-vapor space to the coolant. The heat absorbed by the coolant would be converted to electricity by means of the conventional heat cycle with the conventional coolant and turbine-generator system.

As an example of the potentialities of such a topping device, one might consider a thermionic converter efficiency of 20 per cent, a value about halfway between that presently attained in working models and that indicated as theoretically possible. All of the reactor fission heat flows through the device, and, hence, 20 per cent of this heat appears as direct electrical energy. Eighty per cent of the heat is rejected to the coolant. If this heat is utilized with 30 per cent efficiency in a conventional system, the resulting electrical energy amounts to $0.8 \times 30 = 24$ per cent of the original fission heat. Hence the total efficiency of the system would be $20 + 24 = 44$ per cent. The practical problems involved in using thermionic conversion in the reactor are, of course, numerous.

Other applications might result from the need for electrical power sources with no moving parts either for very long life or for quiet operation. Reference 6 presents a preliminary evaluation of the thermionic power plant with a nuclear reactor as heat source for outer space applications. The heat is transferred by conduction from the reactor core to the reactor surface and thence to the cathode surface by radiation. The reactor must therefore be capable of high-temperature operation (4000 and 3000°F as temperatures of reactor centerline and surface, respectively). The anode is cooled by radiation to the space environment. Weight considerations favor relatively small radiator areas, and, consequently, high anode temperatures are required (2200°F in the reference design). The electrical power output of the power-plant package is limited to about 30 kw(e) by the conduction heat-transfer process from reactor core volume to reactor surface. The efficiency of the thermionic converter power plant was estimated as 9.7 per cent. The specific power in electrical watt-output per pound of total power-plant weight was estimated as 18.8 (not including weight of any shadow shielding that may be required for an instrumented space probe).

The thermionic converter has interesting potential applications as a simple small electric generator converting heat from a high-temperature flame. In this case its operation is independent of an electrical distribution system. For example, such a device could use the exhaust flame in an airplane or missile for auxiliary power generation. In some such applications the energy storage problem becomes important.

Los Alamos Plasma Thermocouple

A program has been under way at the Los Alamos Scientific Laboratory to develop a thermionic energy device for converting heat from fissioning material directly into electricity.[12,13] The converter is referred to as a "plasma thermocouple." From a general point of view, the thermionic cell can be considered as a special case of thermoelectric converter with the cesium plasma forming one branch of the thermocouple. The hot junction is the interface between the cathode and the cesium gas, and the cold junction is the interface between the anode and the cesium gas. This alternate representation of the energy converter is given in Fig. 5 (from reference 14).

Two experimental thermionic cells have been constructed and operated. In the first, indirect heating of the tantalum emitter plate is accomplished by electron bombardment with an electron-gun beam. In the second, the emitter is a ZrC:UC rod within which fission heat is produced by insertion in the core of the Omega West Reactor (OWR) at Los Alamos. A cross section of the fission-heated thermionic cell is given in Fig. 6. Reference 12 presents a short review of the initial work and results obtained on the Los Alamos plasma thermocouple. Since the reference is readily available, the information given therein is not reviewed here.

Reference 15 presents data obtained on the vacuum emission characteristics of UC, ZrC, and $(ZrC)_{0.8}(UC)_{0.2}$. Uranium carbide is found to be an exceptionally good emitter over the

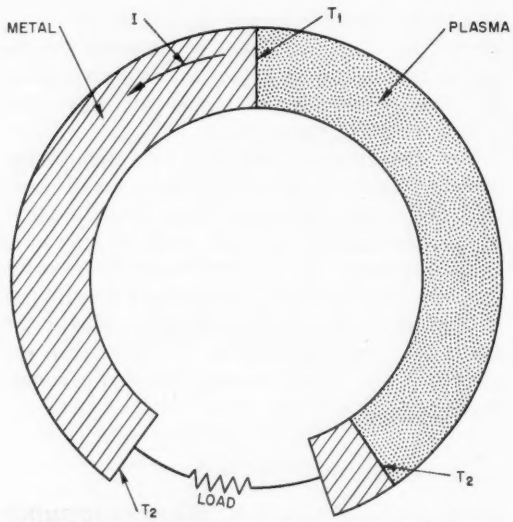

Figure 5—Representation of a thermionic device as a thermocouple. T_1 = hot junction at cathode temperature, T_2 = cold junction at anode temperature.

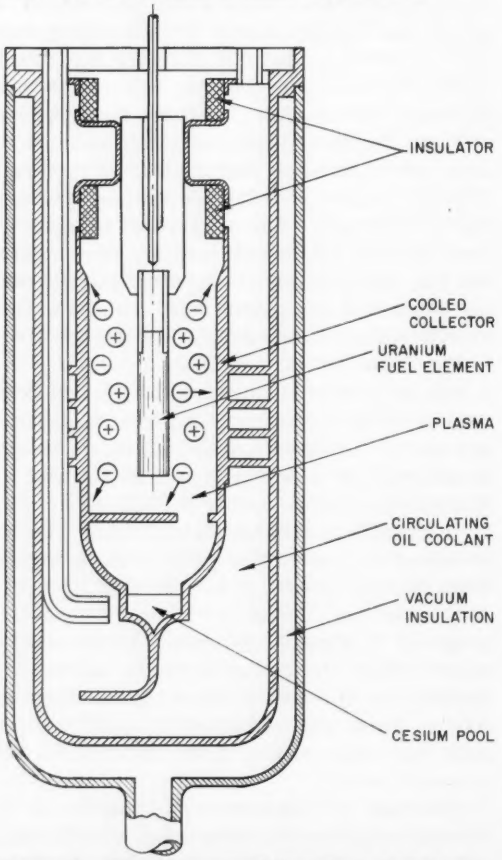

Figure 6—Fission-powered thermionic device operated at Los Alamos.

observed temperature range from 1400 to 1800°K. Pure UC is, however, unsatisfactory as a structural element because of its poor thermal-shock resistance. By contrast, ZrC is much more resistant to thermal shock and thermal cycling. The same resistance to shock and cycling is observed for ZrC:UC mixtures. The experiments show that a solid-solution form of uranium carbide and zirconium carbide gives substantially the same thermionic emission as uranium carbide. Compatibility of UC and ZrC with cesium vapor was said to be demonstrated, although no details are included in reference 15. At 1800°K, the electron emission for ZrC:UC is 1600 times higher than for tantalum (in a vacuum).

Short-circuit current, obtained by placing a low-impedance ammeter directly across the terminals of a thermionic cell, is a useful guide to cell performance. Roughly speaking, the current delivered to a matched external load is about one-half the short-circuit current. Reference 14 presents short-circuit current data for cells containing three different emitter substances: Ta, ZrC, and ZrC:UC for a range of emitter temperatures from 1600 to 2600°K and of cesium pressure from 10^{-5} mm Hg to 2 mm Hg. At the lowest pressure to 10^{-5} mm Hg, the short-circuit current with the tantalum emitter is almost identical with the saturated emission from the tantalum surface in vacuum. As the cesium pressure is increased, the cesium atmosphere greatly enhances the emission of tantalum. At 4×10^{-1} mm Hg, short-circuit current exceeds saturated emission by a factor of 100 at 1800°K and by a factor of 3 at 2600°K.

No enhancement of current emission by the cesium atmosphere (at 3×10^{-1} mm Hg) occurs with the ZrC:UC emitter. Up to 2000°K, the short-circuit data agree with the saturated-emission data, as shown in Fig. 7. The solid curve represents the measured saturated-emitter curve in vacuum; the dashed curve is an extrapolation of the vacuum emission data; the data points represent the measured short-circuit densities at 3×10^{-1} mm Hg cesium vapor pressure. At 2000°K, the ZrC:UC cell produces 40 times the current density of the tantalum cell operated under the same conditions. On this basis it is concluded that the plasma drop is negligible for the current densities obtained in the tantalum cell at 2000°K and, hence, that the tantalum-cell current at

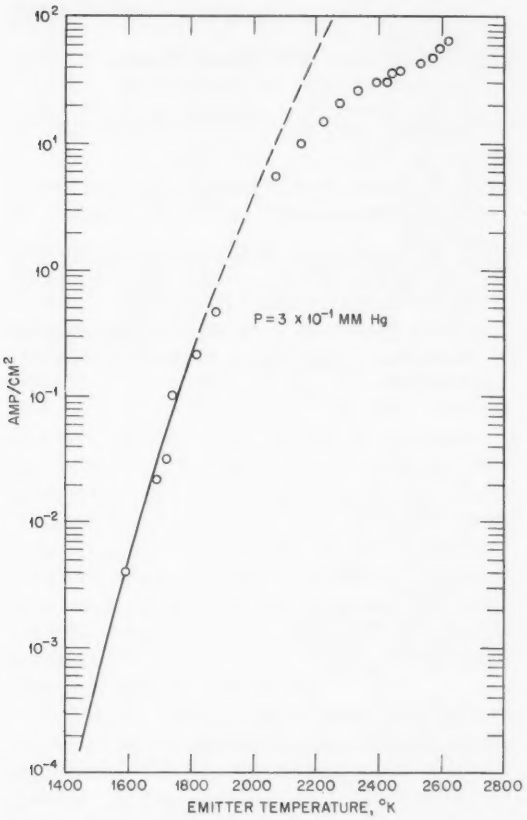

Figure 7 — Comparison of saturated current emission as measured in vacuum (solid curve and extrapolated dashed curve) with short-circuit current for cell with ZrC : UC emitter operated with cesium atmosphere.

2000°K is wholly emission limited. Also, from the agreement between saturated-emission and short-circuit current at values as high as 3 amp/cm², it is tempting to say that even in the ZrC:UC cell the current is still primarily emission limited.

At 2100°K and above the short-circuit current is substantially depressed below that expected from the saturated-emission curve. Reference 14 considers this as a first direct demonstration of a plasma-limited current rather than an emission-limited current.

The highest short-circuit current observed at 2620°K is 124 amp for the 2-cm² emitter area. The power density is about 30 watts/cm². The efficiency of the device is estimated as 15 per cent.

Reference 16 discusses the thermoelectric properties of a gas-filled diode containing a high density of positive ions. The thermoelectric power of the metal with respect to the plasma is negligible when considering a thermocouple made up of metal and plasma. The thermoelectric power of the plasma is estimated from an approximate solution of the Boltzmann equation in the presence of an electric field and a temperature gradient. For representative plasma conditions covered in the experimental work, the analysis gives a thermoelectric power of 1.46×10^{-3} volt/°K. For a temperature difference of 2000°K, this gives a Seebeck emf of the order of 3 volts; this is the order of magnitude of open-circuit voltage observed in the various experiments, thus giving reasonable agreement with the thermocouple theory used.

An attempt is made in reference 16 to obtain an understanding of the characteristics of the plasma. Four principal current-limiting factors in the operation of the plasma thermocouple are involved. The factors are as follows:

1. The current-emission limit of the emitter electrode.
2. The ohmic resistance of the plasma, due primarily to multiple scattering of electrons by the plasma ions.
3. The space-charge region in the vicinity of the cathode surface (the main body of the plasma is electrically neutral on the average).
4. The reduced ion density in the vicinity of the anode surface where the gas temperature is relatively low.

Work is continuing at LASL to explore experimentally the relative importance of these current-limiting factors and to determine more fully the performance capabilities of the thermionic cell.

References

1. H. F. Webster, Calculation of the Performance of a High-vacuum Thermionic Energy Converter, *Journal of Applied Physics*, 30: 488 (1959).
2. G. N. Hatsopoulous and J. Kay, *Journal of Applied Physics*, 29: 1124 (1958).
3. K. G. Hernqvist, M. Kanefsky, and F. H. Norman, Thermionic Energy Converter, *R.C.A. Review*, 19: 244-258 (1958).
4. V. C. Wilson, Conversion of Heat to Electricity by Thermionic Emission, *Journal of Applied Physics*, 30: 475 (1959).

5. G. N. Hatsopoulous, Doctor's Dissertation, M.I.T., June 1956.
6. R. J. Harvey, F. N. Huffman, and C. Eicheldinger, A Preliminary Evaluation of Nuclear Thermoelectric and Thermionic (Secondary) Power Plants for Space Use, MND-1666, Martin Co., Nuclear Div., 1958.
7. J. M. Houston, Theoretical Efficiency of the Thermionic Energy Converter, *Journal of Applied Physics*, 30: 481 (1959).
8. I. Langmuir, *Physical Review*, 21: 426 (1923).
9. L. R. Koller, *Physical Review*, 33: 1082 (1929).
10. I. Langmuir and A. H. Compton, *Reviews of Modern Physics*, 3: 241 (1931).
11. J. E. Beggs, *Institute of Radio Engineers, Transactions on Electron Devices*, ED-3: 93 (1956; ED-5: 55 (1958).
12. G. M. Grover, Los Alamos Plasma Thermocouple, *Nucleonics*, 17: 54 (July 1959).
13. G. M. Grover, D. J. Roehling, and E. W. Salmi, Properties of a Thermoelectric Cell, *Journal of Applied Physics*, 29: 1611 (1958).
14. G. M. Grover et al., Characteristics of a Plasma Thermocouple, *Journal of Applied Physics* (in press).
15. G. M. Grover et al., Characteristics of UC, ZrC, and $(ZrC)_{0.8}(UC)_{0.2}$ as Thermionic Emitters, *Journal of Applied Physics* (in press).
16. H. W. Lewis and J. R. Reitz, Thermoelectric Properties of the Plasma Diode, *Journal of Applied Physics* (in press).

REACTOR PHYSICS:
H_2O-MODERATED CRITICAL ASSEMBLIES AND ANALYSES

The results of a number of critical experiments with water-moderated assemblies have been reported recently. Three of these, the experiments on the Martin Power Reactor,[1] the Yankee critical experiments,[2] and the critical experiments for the N.S. *Savannah*[3] core, are directed toward the investigation of specific reactor designs. They treat the usual quantities involved in such an investigation: critical masses, thermal-flux distributions, control-rod effectiveness, reactivity coefficients, the appropriate lattice characteristics, and effects of water channels. Aside from their usefulness in the experimental design of the reactors in question, these investigations add to the general body of experimental knowledge of H_2O-moderated reactors and are useful for the general understanding of such reactors and for the testing of theoretical methods.

The Martin critical experiment investigated mock-ups of two full-scale core configurations, both about 22 in. in diameter, as well as smaller clean assemblies. The reactor is highly enriched, using fuel elements of tubular shape, 0.375-in. O.D. and 0.315-in. I.D., composed of a UO_2–stainless steel–B_4C (burnable poison) cermet clad with 0.006-in.-thick stainless steel. The active core length is 23 in. Among the measurements of general interest are measurements of the effectiveness of (1) rare earths as control-rod materials and (2) thermal-neutron- and gamma-flux traverses through the relatively thin H_2O reflector, steel-H_2O thermal shield, pressure vessel, and surrounding H_2O.

The Yankee experiments cover assemblies which approximate the Yankee fuel-element and control-rod lattice but which do not mock up the full-size core. The fuel elements are composed of UO_2 pellets, 0.30 in. in diameter, jacketed in stainless steel. The active length is 49.42 in. Three different lattice pitches giving water to equivalent uranium volume ratios of 2.19, 2.93, and 3.87 were investigated. The measurements of lattice characteristics, temperature and void coefficients of reactivity, water channel effects, and resonance absorption in stainless steel are of general interest.

No comprehensive report has yet been issued on the N.S. *Savannah* experiments, but a paper has been presented at a meeting of the American Nuclear Society. The fuel is uranium oxide of 4 per cent enrichment, and jackets of both stainless steel and aluminum have been investigated, at water/UO_2 volume ratios of 1.15 and 1.54. The experiment mocks up the full-size N.S. *Savannah* core.

Reference 4 describes a more general type of experiment which was carried out to study the general properties of seed-and-blanket type reactors, and to verify the nuclear design techniques for such reactors. The experiments were carried out in slab geometry. The H_2O-moderated seed region was a slab, made up of highly enriched uranium-zirconium plates, the slab being approximately 7 in. thick, 54 in. high, and of variable length up to approximately 40 in. This slab, which was supercritical, was provided with cruciform control rods; blanket regions composed of water-moderated natural-uranium plates could be placed adjacent to it on both its large faces. Reactivity measurements were made and power distributions were plotted for various seed-and-blanket combinations. Temperature coefficients and lattice characteristics were also investigated.

A peculiarity which is perhaps worth noting, although its practical effect in power reactors is probably small, is what appears to be anomalous behavior of the temperature coefficients of reactivity for all these assemblies in the temperature range near room temperature. The Martin coefficients show the most regular behavior, but the measured reactivity losses with increasing temperature over the range from 20 to 60°C are about twice as large as those calculated theoretically. In the Yankee case, when the coefficients are plotted as functions of temperature, the curves appear to go through minima, or possibly plateaus, near

50 or 60°C, before continuing to decrease with higher temperatures. The N.S. *Savannah* experiments show positive temperature coefficients of reactivity up to temperatures of about 60°C, and the seed-and-blanket experiments show a positive coefficient for the seed slab alone, up to a temperature of about 50°C, but a negative coefficient over this temperature range when the seed slab has blanket slabs adjacent to it. Whether or not these rather unexpected behaviors are easily understandable in terms of the peculiarities of the assembly is not apparent, but it is possible that some general theoretical investigation of the temperature coefficient behavior in the temperature range below boiling would be worthwhile.

Reference 5 describes a set of critical experiments and an accompanying analysis which were undertaken for the purpose of making a rather rigorous test of the accuracy with which present calculation methods can determine thermal-neutron fluxes in water-moderated assemblies. The assembly consisted of a nearly homogeneous slab core completely surrounded by water reflector. The core, composed of water, zirconium, plastic, and highly enriched U_3O_8, had dimensions roughly 6 by 40 by 31 in. Flux traverses—or more accurately, activation traverses—were made with bare and cadmium-covered detectors along the line which coincided with the short axis of the core. Three configurations were investigated: the clean core surrounded by reflector; the core with a 1-in. water gap bisecting its short dimension, and surrounded by H_2O reflector; and the core–water gap configuration with 0.03-in. cadmium plates lining the boundaries of the water gap, and the core again surrounded by water reflector. The uranium density in the core was relatively high, and consequently thermal-flux peaks, of height two to three times the average thermal flux in the core, existed in the reflector and in the unpoisoned water gap. The arrangement thus represented a rather difficult test for theory because of the large differences in properties of the adjacent regions and the small sizes of the regions.

Since the spatial activation distribution of foils is proportional to the spatial thermal-neutron-flux distribution only if the neutron spectrum is constant over the region investigated, the comparison between experiment and theory was made, not on the basis of neutron flux, but on the basis of the spatial distribution of foil activation. The neutron flux was calculated theoretically, and for each foil type (manganese, gold, U^{235}) the subcadmium activation distribution was calculated, using the theoretical thermal-neutron spectrum, for comparison with the experimental distributions.

The following calculational techniques (plus some corrections for the small degree of inhomogeneity which existed in the core region) were the major ones involved in the theoretical determination of the activation distribution:

1. A four-group diffusion theory calculation of the epithermal neutron-flux distributions was used in order to arrive at the spatial distribution of thermal-neutron source strength. For this calculation the epithermal constants of the assembly regions were calculated by an infinite-medium, multigroup P-1 code (MUFT). Since there was some question as to the validity of the infinite-medium constants in the narrow regions involved, check calculations of the thermal-neutron source distribution were made using a P-1 multigroup code which did not assume separability of space and energy. The difference between the two methods amounted to only 1 per cent in the calculated distributions.

2. The thermal-neutron constants for the several regions were taken as the Wigner-Wilkins averages over infinite mediums of the same composition (SOFOCATE code).

3. The transport of thermal neutrons was approximated both by the double P-1 approximation and by the diffusion approximation.

4. Once the thermal-neutron-flux distribution was determined, a problem remained in determining the activation distribution because of spectrum differences from region to region. For example, the subcadmium activation of a $1/v$ absorber is proportional to the total number of neutrons per cubic centimeter in the subcadmium energy region, rather than to the subcadmium neutron flux. Far from the core-water interfaces, the average neutron velocity ($\bar{v}$), as determined by the Wigner-Wilkins calculation, was 20 per cent greater in the core region than in the reflector region. To determine a $\bar{v}$ for the calculation of activation in the region near the interface, $\bar{v}$ was assumed to vary linearly between the two values, over a distance of one diffusion length on each side of the core-reflector boundary.

The agreement between measured and calculated activation distributions was gratifying

and leaves little doubt that the calculational methods tested are entirely adequate for reactor design calculations involving situations comparable to those investigated. Even the diffusion-theory results are quite good in terms of the accuracies needed for design. It appears that only in special cases, or in connection with fundamental neutron-transport studies, would further refinements on the methods—such as a point-by-point variation of the neutron spectrum—be called for.

Reference 6 reports an investigation of the neutron-spectrum characteristics of a small subregion embedded in a reactor core of different composition, and particularly of the degree to which measurements of the microscopic core constants in the subregion can be considered to duplicate those of a core having a composition the same as that of the subregion. The conclusion is that such measurements are possible and valid and that the scheme offers a means of investigating microscopic core parameters over a wide range of core compositions without the use of large quantities of experimental fuel elements.

The subregions investigated had radii of 5.8 and 9.0 cm and were located at the center of a core having a total radius of approximately 30 cm. Both core and subregion were water moderated; slightly enriched uranium and UO_2 were used as fuel alternatively for the core and/or the subregion.

Theoretical calculations were made by a four-group method and indicated that, for the larger subregion, the ratios of flux densities of the four energy groups maintained a nearly constant value out to a radius of 5 or 6 cm. This indicates, of course, that the neutron-energy spectrum is nearly constant near the center of the subregion and approaches very closely the equilibrium distribution which would characterize a complete core having the composition of the subregion. These are the only requirements for the validity of the method. In the experimental part of the investigation, fast and thermal activation distributions were measured through the subregion and the surrounding core and were found to check rather closely with the calculated distributions. Thermal utilization, resonance escape probability, and the fast-fission effect were measured in the subregions of two different sizes and also in a core having the same composition as the subregion. The subregion results checked very closely with the full-core results for all quantities except resonance escape probability, where there was a discrepancy of 3 or 4 per cent in $(1-p)$. This was thought to be consistent with the small spectrum variations indicated by the theoretical calculations.

References

1. H. B. Rosenthal and E. A. Scicchitano, eds., Nuclear Studies on the MPR Zero Power Test Core, MND-MPR-1646, Dec. 23, 1958. (Unclassified AEC report.)
2. P. W. Davison et al., Yankee Critical Experiments, Measurements on Lattices of Stainless Steel Clad Slightly Enriched Uranium Dioxide Fuel Rods in Light Water, YAEC-94, April 1959. (Unclassified AEC report.)
3. R. M. Ball et al., Critical Experiments for the N. S. *Savannah* Core, BAW-1131, Dec. 10, 1958. (Unclassified AEC report.)
4. S. H. Levine et al., Critical Experiments with a Seed and Blanket Slab Geometry Assembly, WAPD-TM-130, July 1959. (Unclassified AEC report.)
5. M. Goldsmith and T. M. Ryan, Thermal Activation Shapes in a Water-moderated Critical Assembly, *Nuclear Science and Engineering*, 5(5): 299 (May 1959).
6. John J. Volpe et al., Two Region Studies in Slightly Enriched Water-moderated Uranium and Uranium Dioxide Lattices, *Nuclear Science and Engineering*, 5(6): 360 (June 1959).

Collapse of Parallel-plate Fuel Assemblies

The design of high specific power reactors involves choosing a coolant mass flow rate that is as high as possible, consistent with an acceptable pressure drop and with a continuing structural integrity of the fuel element. With respect to this latter item, reference 1 presents an analytical study of the flow velocities necessary to collapse parallel-plate fuel assemblies, such as are found in MTR-ETR fuel elements. The assumptions used in the derivations are as follows:

1. The plates are homogeneous, isotropic, elastic, initially flat or uniformly curved, uniform in spacing and dimensions, and free of unidentified sources of deformation.
2. The coolant is incompressible; all channels have the same mass flow; at any cross section normal to the longitudinal axis, the flow within any channel is uniform; and leakage between channels is suppressed.
3. Plates are broad enough (in comparison with their thickness) so that shear deformation is negligible, and they are long enough (in comparison with their breadth) to enable them to deflect locally without significant redistribution of flow among the coolant channels.
4. Side plates or supports are rigid.

The various cases and resulting formulas are presented below:

Case A: Flat Plates with Built-in Edges

$$V_c = \left[\frac{15\ gEa^3h}{\rho b^4\ (1-\nu^2)}\right]^{1/2}$$

Case B: Flat Plates with Simply Supported Edges

$$V_c = \left[\frac{15\ gEa^3h}{\rho b^4\ (1-\nu^2)}\right]^{1/2}$$

Case C: Flat Plates with Longitudinally Spaced Supports

$$V_c = \left[\frac{\pi^4\ gEa^3h}{48\ \rho l^4 (1-\nu^2)}\right]^{1/2}$$

Case D: Curved Plates with Fixed Edges

$$V_c = \left[\frac{2\ gh\ a^3 E \beta_1 \sin^5 \alpha}{3\rho b^4\ (1-\nu^2)\left(\frac{1}{6} - \frac{\sin 2\alpha}{8\alpha} + \frac{\cos 2\alpha}{12}\right)}\right]^{1/2}$$

Case E: Curved Plates with Hinged Edges

$$V_c = \left[\frac{4\ ghEa^3\ \beta_2 \sin^5 \alpha}{3\rho b^4\ (1-\nu^2)\ C}\right]^{1/2}$$

where V_c = linear velocity of coolant for which collapse occurs due to flow-induced effects alone, ft/sec
g = gravitational acceleration, ft/sec^2
E = Young's modulus, lb/sq ft
a = plate thickness, ft
h = initial flow channel thickness at midspan, ft
ρ = coolant density, lb/cu ft
b = width of flat plate or chord of curved plate, ft
ν = Poisson's ratio
l = longitudinal distance between plate-edge supports, ft

$$\beta_1 = \frac{AR^2}{I} f_2(\alpha) + f_1(\alpha)$$

$$\beta_2 = \frac{AR^2}{I} f_3(\alpha) + f_1(\alpha)$$

R = initial mean radius of curvature, ft
I = moment of inertia of beam cross section per unit width of beam, ft^4/ft
A = area of beam cross section per unit width of beam, ft^2/ft

$$f_1(\alpha) = \frac{1}{2 \sin^2 \alpha}\left(\frac{\alpha}{2} + \frac{\sin^2 \alpha}{4}\right)$$

$$f_2(\alpha) = f_1(\alpha) - \frac{1}{2\alpha}$$

$$f_3(\alpha) = \frac{1}{2 \sin^2 \alpha}\left(\alpha - \frac{3}{4}\sin 2\alpha + \frac{\alpha \cos^2 \alpha}{2}\right)$$

2α = curved-plate arc between supports

The effect of different pressures on either side of the plate is discussed, as is the case where the fuel plates are subjected to external transverse loadings in addition to hydraulic forces. Some experimental justification for the approach is presented in reference 1, but the author recommends additional experiments to validate the analytical study.

Additional data on collapse of parallel-plate assemblies are presented in reference 2. Plexiglas parallel plates were tested in a flow facility wherein the side plates were rigid. The Case A equation predicted a collapse velocity of 21 ft/sec. Results are as follows:

> Flow through the test section was gradually increased until plate-to-plate contact was seen. Slight plate contact was visible at 21 ft/sec; full contact occurred at 31 ft/sec at the leading edge of the plates. At 41 ft/sec, contact extended downstream and gradually tapered off until it ceased 4 to 5 in. above the inlet edge of the plates. A definite flow disturbance existed across the plates and was made visible when air was injected into the flow stream.

The work of reference 1 is also extended to include the effect of flow redistribution on the critical flow velocity.

Nucleate Boiling

In the design study[3] of the large organic-cooled and -moderated reactor which was made as part of the AEC survey of large power reactor types under Public Law 85-590 (reviewed in *Power Reactor Technology*, 2(4): (September 1959)), one of the anticipated technological advances was the use of nucleate boiling of the organic coolant in the hot-coolant channels. Since the thermal performance of the design depended rather strongly on this feature, it would appear that the question of nucleate boiling in organic coolants is one of considerable importance. Reference 4 concerns nucleate boiling characteristics under conditions of pool boiling at atmospheric pressure. The following coolants were investigated:

1. Diphenyl.
2. Metaterphenyl (Santowax-M).
3. Orthoterphenyl (Santowax-O).
4. Mixture of 4.35 wt.% paraterphenyl in metaterphenyl.
5. Eutectic mixture of 32 wt.% diphenyl in orthoterphenyl.

The data were presented in graphical form and will not be reproduced here. A peak heat flux was found for all coolants studied except orthoterphenyl.

The case of pool boiling is not directly applicable to organic-cooled power reactors since the reactor coolant would be under conditions of forced convection, probably at elevated pressure, and subject to varying degrees of subcooling. Hence the authors presented methods of estimating the effects of pressure, velocity, and subcooling as well as compared their data with other pool boiling investigations.

The effects of velocity and subcooling were examined by using the equations of Core and Sato[5] for diphenyl and Santowax-R extrapolated to zero velocity. The results of the present study showed peak fluxes of 95,000 Btu/(hr)(sq ft) for diphenyl and from 97,000 to 135,000 Btu/(hr)(sq ft) for the other substances; extrapolations of Core and Sato's equations yield values of 116,000 Btu/(hr)(sq ft) for diphenyl and 152,000 Btu/(hr)(sq ft) for Santowax-R. The lowest diphenyl velocity used by Core and Sato in their experiments was 0.5 ft/sec, whereas that for Santowax-R was 5 ft/sec.

The correlations of Rohsenow[6] and Forster and Greif[7] for pool boiling of other liquids were examined as to their applicability for use with diphenyl, orthoterphenyl, and metaterphenyl. The Rohsenow correlation was found to be satisfactory for diphenyl and metaterphenyl, but the correlation did not hold for the case of orthoterphenyl. One of the correlations suggested by Forster and Greif was found to be satisfactory for diphenyl and metaterphenyl, but it too was unsatisfactory for use with orthoterphenyl. Several coefficients used in the correlations were determined.

An interesting phenomenon was observed during the runs with diphenyl. During one of the runs, the test section was allowed to film boil for 15 to 30 sec, and a thin film of amorphous carbon deposited on the heater. After the test section was brought back to the nucleate boiling regime, the heat-transfer coefficient showed

marked improvement. Figure 8 shows the improvement after film boiling. These data were found to be reproducible in test runs conducted over a year apart. It was concluded by the authors that the thin layer of carbon so improved the nucleation mechanism that, for a given heat flux, the temperature difference requirements were lowered. A pertinent question concerns the

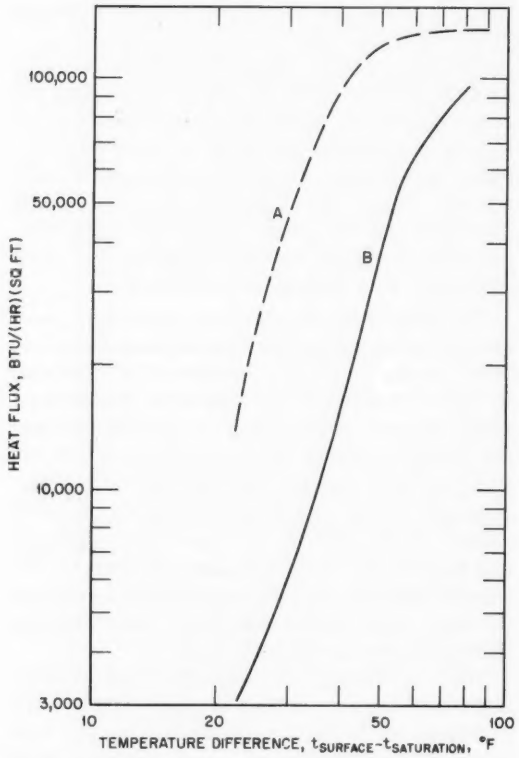

Figure 8 — Comparison of heat flux versus temperature difference for diphenyl, before and after film boiling.[4] *A*, diphenyl after boiling. *B*, diphenyl before boiling.

significance of the observations to organic-cooled power reactors employing boiling. One point is that the modified surface appears to be more stable to nucleate boiling, since it appears that the test section did not film boil at heat fluxes well over the peak heat flux recorded for the clean surface. Thus an organic-cooled reactor design that is power limited by the onset of film boiling might profit if element surfaces could be modified to give the heat-transfer coefficients implied by the upper curve of Fig. 8. A further question, of course, is whether the carbon deposit, helpful in a thin layer, might be harmful in thicker layers, and whether the presence of nucleate boiling might favor the build-up of deposits over a long period of time.

The last issue of this publication (Vol. 2, No. 4, September 1959) discussed the role of surface condition in boiling water and cited Argonne National Laboratory (ANL) data which revealed that surface irregularities tend to increase the peak heat flux because of increased turbulence and more numerous nucleation points. References 8 and 9 are reports of recent research in the area. The reports will not be reviewed in detail since they are of primary interest to the specialist in boiling heat transfer. Reference 9 describes a new approach to the determining of the number of active sites present during nucleate boiling by simultaneously electroplating a layer of metal on the boiling surface during boiling and subsequently by counting the pinholes where no metal was deposited. The conclusions of the two reports are believed to be of sufficient general interest that they are reproduced herein; those of reference 8 are as follows:

1. Nucleation occurs from pre-existing gas-filled cavities on the surface.
2. A single dimension in general is sufficient to characterize such an active cavity.
3. The wall superheat at which such a cavity will become active is fixed by surface tension and other known fluid properties.
4. The mean surface temperature is not equal to the temperature felt by an active cavity.
5. For surfaces made of the same material and treated in the same way, a single plot of the number of cavities versus a group with the dimensions of length can be developed which is appropriate to apply to a variety of fluids at various pressures.

The conclusions of reference 9 are:

1. The relation between heat flux and active site population is

$$Q/A = 1400\ (N/A)^{0.47}$$

where Q/A = heat flux, Btu/(hr)(sq ft)
N/A = number of active sites on heated surface per square foot of heat-transfer area

2. At active site populations greater than 500 per square foot, the heat-transfer coefficient, h, can be represented by

$$h = 49\,(N/A)^{0.43}$$

3. The amount of heat attributed to each active site becomes less as the population of active sites increases. At the beginning of boiling, although most of the heat is transferred by free convection, the first active site in the 1.77-sq in. test area (or 81 sites per square foot), was *associated* with 11,000 Btu/hr. By comparison, at a heat flux of 317,000 Btu/(hr)(sq ft), each active site was *associated* with only 1.95 Btu/hr.

4. Electroplating during boiling is a new tool for boiling research. The populations of active sites on a heated surface can now be determined at much greater heat fluxes than possible by previous techniques. An analysis of information from additional experiments could lead to a unified theory for the entire range of nucleate boiling in which the surface condition, as well as nucleation and bubble growth, is treated as a variable.

Liquid-metal Heat Transfer

Reference 10 is an analytical study of turbulent liquid-metal heat transfer in channels. The case considered is restricted to the entrance region of a channel, where boundary layers are not, by definition, fully established. The idealized system investigated is the following:

1. The wall temperature distribution is a simple step function, $t = t_0$ for $x < 0$ and $t = t_w$ for $x > 0$. The fluid approaching the entrance region has an established temperature, t_0.
2. Longitudinal heat conduction is small compared to convection and is neglected.
3. The established turbulent velocity profile is represented by a uniform distribution $u = U$.
4. The eddy diffusivity distribution varies linearly with distance from the wall and as the nine-tenths power of the Reynolds modulus, $\epsilon/\nu = C_1 \mathrm{Re}^{0.9}(y/b)$.
5. The fluid properties are invariant with temperature.
6. Steady state exists.

Here ϵ = eddy diffusivity, sq ft/hr
ν = viscosity, sq ft/hr
C_1 = dimensionless constant
Re = Reynolds number
b = channel half-thickness, ft
y = distance measured into channel from wall perpendicular to the channel boundary, ft

Several of the above postulates bear discussion. The effects of axial conduction and a nonuniform velocity profile were investigated and found to be unimportant over the range of variables studied. The diffusivity function shown was formulated under the assumption that the heat-transfer and momentum-transfer eddy diffusivities are identical, and the postulated function is a linear approximation to the actual momentum-transfer eddy diffusivity. Since the actual momentum-transfer eddy diffusivity is constant in the turbulent layer, the postulated function departs radically from the actual function as distance into the turbulent layer is increased; however, the postulated function is a good approximation in the laminar and buffer layers. It was calculated that the Nusselt moduli obtained with the linear function were within 10 per cent of the moduli when the actual momentum-transfer eddy diffusivities were employed in the calculations. The linear approximation makes the equations more tractable, and the resulting answers are of sufficient accuracy because the heat-transfer limitations are not set by the turbulent layer.

The differential equation for the convective transfer of heat was solved by a separation-of-variables technique, and the symmetry boundary condition resulted in the typical infinite series solution, since the differential equation yielded zero-order Bessel functions of the first and second kind for its general solution. The eigenvalues and series coefficients were evaluated for a range of Reynolds and Prandtl moduli, and Nusselt numbers and mixed-mean fluid temperatures were calculated. Prandtl numbers from 0.002 to 0.06 and Reynolds numbers from 5000 to 1×10^6 were used. Figure 9, typical of the results, illustrates the fact that entrance

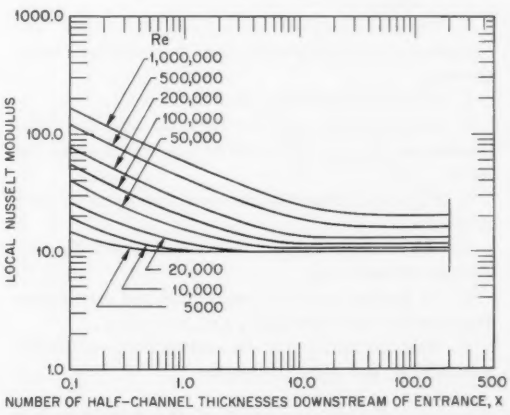

Figure 9—Nusselt modulus versus X and Re; Pr = 0.002 (reference 10).

effects are present for many channel thicknesses downstream, particularly at high Reynolds numbers. The calculated results were compared with other work, both experimental and analytical, and good agreement was obtained.

Liquid Metals with Internal Heat Generation

The system studied in reference 11 consists of a long, smooth, insulated pipe with liquid metal flowing under internal heat-generation conditions. Guard heaters were used around the insulation to achieve adiabatic operation.

A general theory of heat transfer with internal heat generation was derived, and experiments were conducted to validate the theory. The solution for the conservation-of-energy equation yielded an analytical expression for the following parameter T as a function of N_{Re} and N_{Pr}:

$$\frac{k\,(T_w - T_m)}{q'''_m\, r_w^2} \equiv T$$

where k = fluid thermal conductivity, Btu/(hr)(ft)(°F)
T_w = wall temperature at fluid interface, °F
T_m = mixed mean fluid temperature, °F
q'''_m = mean volumetric heat generation rate, Btu/(hr)(cu ft)
r_w = pipe radius, ft

The analytical expression was derived under the following assumptions:

1. A steady state exists.
2. Temperature and velocity distributions are independent of axial position and symmetrical about the axis.
3. Constant radial heat flux at the wall.
4. Heat sources exist in the fluid and are independent of axial position and symmetrical about the axis.
5. Physical properties are not functions of temperature.
6. Physical properties are not affected by conditions of fluid flow.
7. An analogy exists between heat and momentum transfer for turbulent flow; i.e., $\epsilon_h = \alpha\epsilon_m$.
8. Heat is transferred by convection, molecular conduction, and eddy conduction.

Since one of the purposes of the paper was to study the relations between ϵ_h and ϵ_m, the derivation employed a value of unity for α.

The experiments were conducted with mercury for N_{Pr} from 0.0191 to 0.0224 and N_{Re} from 29,000 to 164,000. The fluid was internally heated electrically, and values of T were determined by measuring appropriate temperatures and other necessary parameters.

The experimental values of T, T_{expt} were found to be on the average 49 per cent higher than the values calculated using the $\alpha = 1$ analogy. Based on this result, the author concludes: "Thus, it may be concluded that, on the average, the radial conductances are smaller than those calculated from the heat-momentum-transfer analogy. This is essentially the same result as ordinary heat-transfer tests with liquid metals have shown. Thus it appears that the ratio α is not unity but somewhat smaller."

The difficulty with the experiment lies in the fact that the modulus T is calculated by measuring the difference between two large numbers of nearly the same value, T_w and T_m. Typical differences of 2 to 6°F were measured, and values of wall temperature ranged from about 100 to nearly 200°F. This difficulty is reflected by the fact that the value of T_{expt} showed a maximum of ±35 per cent variation from the mean. Temperature differences were stated to be accurate to ±40 per cent at the worst.

Water Flowing Parallel to Tube Bundles

The fuel element consisting of bundles of fuel rods cooled by water which flow parallel to the axes of the rods is of continuing interest to the reactor design engineer. Recent experimental and analytical data[12] have shown that the Colburn equation may not be correct for determining turbulent, nonboiling heat-transfer coefficients.

The recommended equation is as follows:

$$\frac{hD_e}{k} = C\ (\mathrm{Re})^{0.8}\ (\mathrm{Pr})^{1/3}$$

where h = heat-transfer coefficient
D_e = 4 × hydraulic radius
k = thermal conductivity based on film temperature
Re = Reynolds number based on film temperature
Pr = Prandtl number based on film temperature except C_p, which is based on bulk temperature
C = empirical constant

Values of C are given by the following equations for $2.5 \times 10^4 < \mathrm{Re} < 10^6$:

Triangular pitch,

$$C = 0.026\ (S/D) - 0.006 \text{ for } 1.1 < S/D < 1.5$$

where S = center-to-center distance between tubes
D = tube diameter

Square pitch,

$$C = 0.042\ (S/D) - 0.024 \text{ for } 1.1 < S/D < 1.3$$

This new correlation usually yields higher heat-transfer coefficients than does the Colburn equation; at large values of S/D, the improvement is about 40 per cent. Also, the square lattice, at a given S/D, shows improved coefficients compared to the triangular lattice.

References

1. D. R. Miller, Critical Flow Velocities for Collapse of Reactor Parallel-plate Fuel Assemblies, KAPL-1954, August 1958. (Unclassified AEC report.)
2. Reactor Technology Report No. 9—Engineering, KAPL-2000-6, June 1959. (Unclassified AEC report.)
3. Organic Cooled Reactor Study, TID-8501, Parts 1-5, April 1959. (Unclassified AEC report.)
4. D. P. Jordan and G. Leppert, Nucleate Boiling Characteristics of Organic Reactor Coolants, *Nuclear Science and Engineering*, 5(6): 349-359 (June 1959).
5. *Power Reactor Technology*, 2(3): 20 (June 1959).
6. W. M. Rohsenow, Heat Transfer Symposium, University of Michigan Press, 1953.
7. K. E. Forster and R. Greif, *Transactions of the American Society of Mechanical Engineers*, 81: 43-53 (1959).
8. P. Griffith and J. D. Wallis, The Role of Surface Conditions in Nucleate Boiling, Storrs Heat Transfer Conference, Preprint 106 (1959).
9. R. F. Gaertner and J. W. Westwater, Populations of Active Sites in Nucleate Boiling Heat Transfer, Storrs Heat Transfer Conference, Preprint 105 (1959).
10. H. F. Poppendiek, Turbulent Liquid-Metal Heat Transfer in Channels, *Nuclear Science and Engineering*, 5(6): 390-404 (June 1959).
11. G. L. Muller, Experimental Forced-convection Heat Transfer with Adiabatic Walls and Internal Heat Generation in a Liquid Metal, ORNL-2669, Aug. 28, 1959. (Unclassified AEC report.)
12. J. Weisman, Heat Transfer to Water Flowing Parallel to Tube Bundles, *Nuclear Science and Engineering*, 6(1): 78 (July 1959).

Delayed Neutrons in Reactor Kinetics

Although extreme accuracy in the calculation of kinetic behavior is not often required for reactor design purposes, many reactor experiments depend, for the measurement of reactivity, on kinetic measurements. The most common of these is the measurement of an asymptotic positive reactor period in the range from a few seconds to a few hundred seconds. In such cases an accurate knowledge of the kinetic characteristics of the reactor is essential for accurate results. Three main types of effects must be taken into account: uncertainties in the delayed-neutron characteristics for a given fissionable isotope, the effect of neutron importance in determining the effective values of the delayed-neutron fractions, and delayed-neutron production by sources other than the main fissionable isotope (e.g., by fast fission in U^{238} or by γ-n reactions). Reference 1 treats the first two of these questions.

The value of a delayed neutron to the chain reaction is, in general, greater than that of an average prompt neutron because the delayed neutrons are produced at lower average energies than the prompt neutrons and, therefore, have a lower probability of leaking from the reactor. For this reason the effective delayed-neutron fractions may be larger than the true fractions. This effect is small in large low-leakage reactors but may be appreciable for small reactors, particularly those moderated by H_2O, in which the slowing-down length is quite sensitive to neutron birth energy. The kinetic effects of delayed-neutron importance can be discussed conveniently in terms of the inhour equation, which relates the asymptotic reactor period to the reactivity.

For long periods the inhour equation

$$\rho = \frac{l^*}{\tau} + \sum_i \frac{\overline{\beta}_i}{1 + \lambda_i \tau}$$

can be reduced to

$$\rho = \sum_i \frac{\overline{\beta}_i}{1 + \lambda_i \tau} \qquad (1)$$

where ρ is the reactivity, l^* is the effective prompt-neutron lifetime, τ is the asymptotic reactor period, λ_i is the decay constant of the ith species of delayed-neutron precursor, and $\overline{\beta}_i$ is the effective fraction of total fission neutrons resulting from the ith precursor species. The $\overline{\beta}_i$ is, in general, different from β_i, the true ith delayed fraction, but is, of course, dependent on β_i.

The reference rewrites Eq. 1 in the form

$$\rho = \beta \left[\frac{\overline{\beta}}{\beta}\right](\tau) \sum_i \Gamma_i(\tau) \qquad (2)$$

where β is the true total delayed fraction and $\Gamma_i(\tau)$ is given by

$$\Gamma_i(\tau) = \frac{\beta_i/\beta}{1 + \lambda_i \tau}$$

Thus the two terms, β and $\Sigma\, \Gamma_i(\tau)$, depend only on the true delayed-neutron fractions, and all the effects stemming from the importance of the delayed neutrons in the reactor are lumped into the term $[\overline{\beta}/\beta]\,(\tau)$, defined as

$$\left[\frac{\overline{\beta}}{\beta}\right](\tau) = \frac{\sum_i \frac{\overline{\beta}_i}{\beta_i} \Gamma_i(\tau)}{\sum_i \Gamma_i(\tau)}$$

It is thus an average of the (effective β_i)/(true β_i) weighted by $\Gamma_i(\tau)$. It is evidently a function of τ, as indicated, and as is to be expected, since the relative importance of the various delayed groups in determining τ varies as τ varies. The term $[\overline{\beta}/\beta](\tau)$ would be expected to be insensitive to variations in the experimental values of β_i, although sensitive to the energies of the delayed groups. Therefore Eq. 2 has separated the terms which (1) involve experimental uncertainties in β_i and λ_i and (2) are common to all reactors

employing a given fissionable isotope, from the term which (1) involves the delayed-neutron importance, (2) is subject to experimental error only with respect to delayed-neutron energies, and (3) will vary from reactor to reactor.

Reference 1 investigates the effective delayed-neutron fractions for a case in which the ratios $\overline{\beta}_i/\beta_i$ would be expected to be relatively large: a thin (7-in.) highly enriched water-moderated slab, reflected by water, and the same slab, reflected by a natural-uranium and water blanket. The ratio $\overline{\beta}_i/\beta_i$ was determined for each delayed group by making four-group criticality calculations in which the effects of the ith group, with its appropriate birth energy, was treated as a separate fast-neutron source. From the ratios so obtained, the quantity $[\overline{\beta}/\beta](\tau)$ was computed for various values of τ from 20 to 300 sec. The values obtained for the H_2O-reflected slab were all approximately 1.26, and the variation over the range of τ was no greater than the uncertainties in birth energy of the delayed groups. It may therefore be concluded that an effective value of the total delayed fraction, $\overline{\beta}$, can be derived for a given reactor and that the ratio $\overline{\beta}/\beta$ can be used as a correction term for the inhour equation using true values of β_i, to take account of delayed-neutron importance over the range of periods normally used in experiments.

The reference also tabulates, for various values of τ from -5000 sec to $+200$ sec, the values of Γ_i and $\beta \sum_i \Gamma_i$ as derived from three different sets of experimental data: the Hughes data[3] of 1948, the Keepin data[3] of 1955, and the Keepin data[4] of 1957.

Reference 2, which is a rigorous general discussion of the application of reactor kinetics as a tool in experimental reactor physics, is also of interest in connection with this subject.

Reduced Delayed-neutron Group Representations

Reference 5 reports an analytical study of the validity of representing the six delayed-neutron groups by a smaller number of groups in kinetic calculations. The kinetic behavior as calculated with "equivalent" one-group, two-group, and three-group representations are compared with those calculated using the six actual delayed groups for a variety of different cases. These cases include the behavior of the asymptotic reactor period (as given by the inhour equation), the reactor transfer function, and the behavior after step increases and step decreases of reactivity. It is shown that the two-group and three-group approximations duplicate reasonably well the behavior with the full six groups. The principal advantage of the three-group representation over the two-group is that, by choosing the characteristics of the third group to duplicate those of the actual delayed group having the longest half life, the asymptotic rate of decay of power in the subcritical reactor can be duplicated.

Approximations for Reactor Accident Calculations

Reference 6 discusses methods of approximating the behavior of reactor power during a typical start-up accident or during similar transients. The typical assumed accident is one in which reactivity is added continuously to the initially subcritical reactor (usually at a constant rate) until the reactor is made subcritical by the over-power scram circuit or by other means. In the reference the accident is divided into three stages: the increase of reactivity to delayed critical, the interval from delayed critical until the shutdown mechanism begins to function, and the shutdown period. Different approximations, which are not amenable to brief summary, are applied in the three stages.

Although accidents of this type can be investigated to any desired degree of numerical accuracy by machine computation, the uncertainties in the physical processes involved do not often justify very great accuracy of computation. Consequently, the approximations discussed in the reference may be found to be useful for many practical cases as well as helpful for the insight they give into the kinetic behavior of the reactor.

Reference 7 also treats approximate methods for calculating the effects of hypothetical reactivity accidents. Specifically, it covers the calculation of rates of reactivity removal necessary to limit reactor power to a specified value when the power is rising on a period τ because of the step insertion of an excess reactivity δk_p.

For $\delta k_p < \beta$, with reactivity reduced at a constant rate γ sec^{-1} after time $t = 0$ and power P_0, the power P at any time $t > 0$ is given by

$$\frac{P}{P_0} = 1 + \left(\frac{\delta k_p\, \alpha l^* \lambda}{\beta^2}\right)(1 - e^{-\beta t/l^*}) + \frac{(1-\alpha)\,\delta k_p\, \lambda}{\beta} t - \left(\frac{\alpha\, \lambda^2\, l^2\, \delta k_p}{\beta^3}\right)(1 - e^{-\beta t/l^*}) + \frac{\alpha \lambda^2 l^* \delta k_p}{\beta^2} t - \frac{\alpha \lambda^2\, \delta k_p}{2\beta} t^2$$

where $\alpha = \gamma/(\lambda \delta k_p)$, l^* is the effective prompt-neutron lifetime, β is the delayed-neutron fraction, and λ is the decay constant of a single group of delayed neutrons equivalent to the six actual delayed groups. The reference states that an approximation which will give conservative results (i.e., a high value of P) is $\lambda = \Sigma\, \lambda_i \beta_i / \beta$. The equation above is based on the linearized kinetic equations; consequently, it should be valid only if γ is chosen large enough that the maximum value of P is not greatly larger than P_0. It is stated that values of γ which will reduce the reactivity to zero in about $2\frac{1}{2}$ sec or less will limit P to values not substantially greater than P_0, provided $\delta k_p < \beta$.

In the case of $\delta k_p > \beta$ the power will rise above the value P_0 unless the reactivity can be reduced nearly instantaneously. If reactivity is reduced at the rate γ $\sec^{-1}$, the maximum power P_m is approximated by

$$\log_e \frac{P_m}{P_0} = \frac{(\delta k_p - \beta)^2}{2\gamma l^*}$$

If reactivity is reduced at an accelerated rate a, where a has the units $(\delta k_{\text{eff}}/k_{\text{eff}})/\sec^2$, the maximum power is given by

$$\log_e \frac{P_m}{P_0} = \frac{2\sqrt{2}\,(\delta k_p - \beta)^{3/2}}{3l\sqrt{a}}$$

The reference compares the results of the above approximations with digital computer results, using the exact space-independent kinetics equations to demonstrate their validity.

Oscillation Experiments on Large Heavy-water Reactors

Oscillation experiments and their analyses to determine temperature coefficients of reactivity for a large, natural-uranium reactor, cooled and moderated by D_2O, are reported in reference 8. The experiments are interesting primarily for the techniques they establish, especially since they were made on a large reactor which had no special provisions for reactivity oscillation.

A trapezoidal reactivity oscillation was used, produced by periodically withdrawing a gang of control rods at constant speed for a time interval t (the drive time), holding the rod position constant for a time interval t_2 (the wait time), driving the rods in again at the same constant speed for a time interval t_1, and again holding position constant for a time interval t_2. Values of 2 and 4 sec were used for t_1, and values of 1, 2, 4, 6, and 8 sec were used for t_2. The reactivity coefficients were derived from the observed behavior of the neutron-flux level during the latter three-fourths of the wait time. The observed behavior was taken as the average for 10 to 15 consecutive oscillations.

The purposes of the wait time and of the variations in wait time are to separate the effects on the neutron detector of changes in flux shape resulting from the displacement of the control rods from the effects on the detector of changes in over-all power resulting from the reactivity transients brought about by changes in the temperatures and in the control-rod positions. Such a separation is necessary in a large reactor.

The temperature coefficient was derived by fitting the observed flux-level variation with a mathematical model in which the temperature coefficient of reactivity was treated as an adjustable parameter. In the particular reactor investigated, the moderator temperature coefficient of reactivity did not appear in the frequency range investigated because of the long time constant associated with the coefficient. Apparently, the coolant coefficient of reactivity was small; the observed coefficient, which was negative, with a delay of 2.3 sec, was attributed to the fuel temperature.

Transfer Functions of Distributed Parameter Systems

In reference 9, transfer functions are derived for a solid-fuel reactor—as approximated by two different models—and for a counterflow heat exchanger. The reactor and heat exchanger are considered as distributed-parameter (rather than lumped) systems in so far as heat transfer, flow, and temperature distributions are concerned, although the power distribution in the

reactor is considered to be constant. Lumped network approximations to the distributed-parameter transfer functions are given in an appendix.

References

1. R. L. Ewen and R. S. Wick, Delayed Neutrons in Reactor Kinetics Calculations, in Bettis Technical Review: Reactor Physics and Mathematics, WAPD-BT-13, p. 1, May 1959. (Unclassified AEC report.)
2. A. F. Henry, The Application of Reactor Kinetics to the Analysis of Experiments, *Nuclear Science and Engineering*, 3(1): 52 (January 1958).
3. G. R. Keepin, Delayed Neutrons, in "Progress in Nuclear Energy," Series I, McGraw-Hill Book Co., Inc., New York, 1956.
4. G. R. Keepin et al., Delayed Neutrons from Fissionable Isotopes of Uranium, Plutonium, and Thorium, LA-2118, February 1957. (Unclassified AEC report.)
5. R. E. Skinner and E. R. Cohen, Reduced Delayed Neutron Group Representations, *Nuclear Science and Engineering*, 5(5): 291 (May 1959).
6. H. Hurwitz, Jr., Approximate Analysis of Reactor Start-up Incidents, *Nuclear Science and Engineering*, 6(1): 11 (July 1959).
7. John MacPhee, On the Termination of Reactor Excursions, *Nuclear Science and Engineering*, 5 (5): 273 (May 1959).
8. H. Dean Brown and William E. Loewe, Analysis of Reactor Oscillations for Coefficients of Reactivity, *Nuclear Science and Engineering*, 5(6): 376 (June 1959).
9. Elias P. Gyftopoulos and Henry B. Smets, Transfer Functions of Distributed Parameter Nuclear Reactor Systems, *Nuclear Science and Engineering*, 5(6): 405 (June 1959).

AEC Reactor Safety Program

The U. S. Atomic Energy Commission has issued a document (reference 1) which outlines the comprehensive research and development program of the AEC on reactor safety and containment. The document also summarizes briefly the results that have been obtained in the several projects which make up the program and illustrates these results with some of the data that have been obtained. Since it is important to the nuclear plant designer to factor into his reactor and containment designs the most up-to-date safety and containment information, Table VI-1 has been prepared, summarizing the program, indicating the agencies carrying out the various projects, and repeating most of the references from the AEC document.

Table VI-1 AEC REACTOR SAFETY PROGRAM

Program	Main activity or objective	Status	Agency	Selected references (from ref. 1)
Reactor experiments on kinetics and control	Dynamic measurements on experimental reactors			
SPERT-I	Atmospheric pressure; natural-circulation H_2O; highly enriched core	Operating since 1955	Phillips Petroleum Co. (NRTS)	2–5
SPERT-II	Pressure to 300 psi; H_2O or D_2O with circulation to 20,000 gal/min; various cores and reflectors	Critical 1959	Phillips Petroleum Co. (NRTS)	6,7
SPERT-III	Pressure to 2500 psi; circulating H_2O for power up to 60 Mw(t); various cores; boiling or subcooled operation	Critical December 1958	Phillips Petroleum Co. (NRTS)	6,7
KEWB	Homogeneous water boiler (H_2O); graphite reflected; normal operating power 50 kw(t)	Operating since 1956	Atomics International	8,9
EBR-I	NaK-cooled fast breeder; normal operating power 1.4 Mw(t), 250 kw(e); reactor dynamics with various cores by means of oscillator tests	Operating since 1951	Argonne National Laboratory (NRTS)	10–14
Safety-system performance	Measure practical limits of safety-system response and develop reliable fast-acting systems which approach these limits; work to date primarily for pool type reactors	In progress	Oak Ridge National Laboratory	
Development of self-actuating safety devices (reactor fuses)	Develop self-actuating reactor shutdown devices for research and power reactors	In progress	Atomics International	15–17
Theoretical reactor kinetics	Develop and test analytical procedures; identify and understand basic sources of reactivity change; advance technique of safety calculations	In progress	Phillips Petroleum Co. and Ramo-Wooldridge Corp. (SPERT-I analysis); Atomics International	

Table VI-1 (Continued)

Program	Main activity or objective	Status	Agency	Selected references (from ref. 1)
Energy and fission-product release caused by fuel melting	Predict realistically the form and quantity of fission-product release following core meltdown; obtain understanding of factors influencing initiation, propagation, and rate of metal-water and metal-gas reactions			
Fission-product release upon melting of irradiated fuel samples	Species and quantity of fission products released as affected by nature of fuel element, concentration of fission products in element, atmosphere of meltdown, time at melt temperature, agitation and disposal of melt	In progress	Oak Ridge National Laboratory	18–21
Meltdown of zirconium-uranium subassemblies	Investigation of effects of melting subassemblies of plates in steam atmosphere; fission-product release, chemical reaction, and physical distribution of melt and fission products	In progress	MSA Research Corp.	
Field release of fission products from melted fuel	Release and dispersion of fission products in the field from melted fuel	First tests in 1958, to be reported in 1959–60	Convair, Fort Worth (NRTS)	
Transient reactor test facility (TREAT)	Meltdown of fuel elements and core segments in a special transient reactor to study melting behavior, fission-product release, and chemical reactions; initial program directed at fast-reactor safety	TREAT Critical February 1959	Argonne National Laboratory (NRTS)	22
Metal-water reaction studies	Studies of chemical reactions between water and molten metals of types used in reactor construction and the rates and magnitudes of resulting energy releases; theoretical, laboratory, engineering, and reactor investigations	In progress	Argonne; General Electric (Valle-citos); Stanford Research Institute	23–27
Metal-gas reaction studies	Fundamental study of ignition and burning of metals in gaseous atmospheres; work presently concentrated on uranium and its alloys	In progress	Argonne National Laboratory	28
Containment studies	Develop methods for determining the loads which might be generated in a reactor accident and for designing containment structures which will resist these loads			
Energy sources	Present work includes experimental study of explosive decompression of hot water (ARF), external effects of pressure vessel rupture (APG), and methods of simulating reactor energy releases (SRI, NOL)	In progress	Armour Research Foundation; Aberdeen Proving Ground; Stanford Research Institute; Naval Ordnance Laboratory	29,30

Table VI-1 (Continued)

Program	Main activity or objective	Status	Agency	Selected references (from ref. 1)
Pressure transmission and reflection	Study of hydromechanics of blast-wave propagation in various media; mathematical description of pressure-volume characteristics; experimental crushing of materials under shock loads; velocity of sound in gas-water dispersions	In progress	Armour Research Foundation	29,31
Missiles	Study of penetration of materials by rod type missiles	In progress	Stanford Research Institute	32
Earthquakes	Study of possible effects of earthquakes on reactors	Report expected 1959	Lockheed Aircraft Corp. and Holmes and Narver, Inc.	
Primary containment	Experimental investigation of the mechanics of large deformation and rupture of pressure vessels	In progress	Naval Ordnance Laboratory	33
Blast shields	Study of use of blast shields to reduce loading on outer containment structure; experimental investigation of dynamic strength of crushable materials	In progress	Armour Research Foundation	34
External containment structures	Investigation of response of outer containment structures to transient internal loads; establish design criteria by measuring elastic and plastic response and comparing with theory; verify the usefulness of scale-model testing	In progress	Aberdeen Proving Ground	35–37

Metal-Water Reactions

The possibility of a reaction of the metals contained in a reactor with its coolant influences many areas of reactor design. Two classes of reactor accidents may be conceived in which metal-water reactions might be important. The first of these would involve the sudden melting of the metal in an environment of more or less liquid water, as the result, for example, of a rapid power excursion. This type of accident, which could conceivably lead to an explosive chemical energy release, has been considered not applicable in many water reactor cases. The second class is typified by the loss-of-coolant accident, in which the melting occurs rather slowly, in a steam atmosphere, and molten metal may drop into a pool of residual water at the bottom of the reactor vessel. Reference 38 illustrates a method for determining the extent of a metal-water reaction in an accident of this type and applies the method to calculate the amount of reaction for a particular accident occurring to a particular reactor. The method of treating the problem is believed to be of sufficient interest to warrant discussion.

The problem can be divided into two sections:

1. The application of high-temperature zirconium-water reaction data to determine the temperature excursion (and extent of reaction) of the reactor core when it is being affected by a combination of heat produced by the oxidation process together with the decay heat.

2. Determination of a cooling curve, and extent of oxidation, for the reaction between a molten drop of uranium alloy and/or zirconium and steam. This assumes the clad has been ruptured, releasing molten drops of fuel. The basic method used is that of Lustman.[39]

The kinetics of the reaction of Zircaloy and water are contained in the following equations:

$$\Delta W = k(T)t^{n(T)}$$

$$k(T) = Ae^{-Q/RT}$$

where W = oxygen weight gain, g/cm^2
$k(T)$ = temperature-dependent rate constant
t = time, sec
$n(T)$ = temperature-dependent exponent of the time
A = constant
Q = activation energy, cal/mole
R = gas constant, cal/deg-mole
T = absolute temperature, °K

These functions are plotted in Figs. 10 and 11. It should be noted that some extrapolation has been done in Fig. 10, and this carries over to Fig. 11 also.

The procedure starts with the assumption of some sort of credible accident, and this obviously is a function of the detailed reactor design; the loss-of-coolant accident studied in reference 38 is probably one of the most severe accidents that can happen to a power reactor, since it assumes a rupture somewhere in the primary coolant loops such that the core is left bare with a pool of water standing in the bottom of the pressure vessel. Thus water is available for a metal-water reaction but not for cooling.

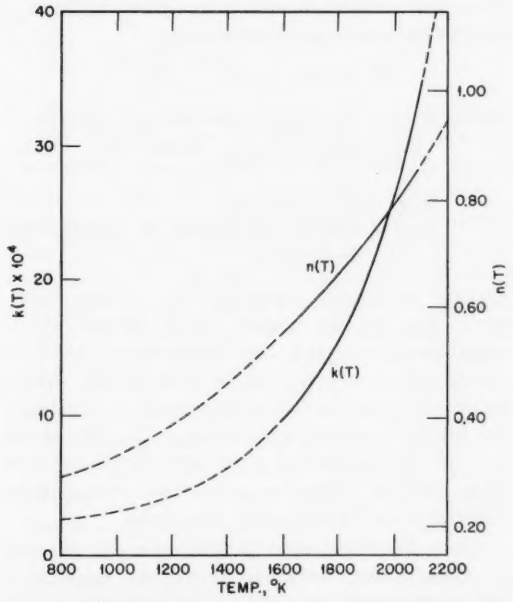

Figure 10 — $k(T)$ and $n(T)$ versus T. Dotted lines are extrapolations of data.[38]

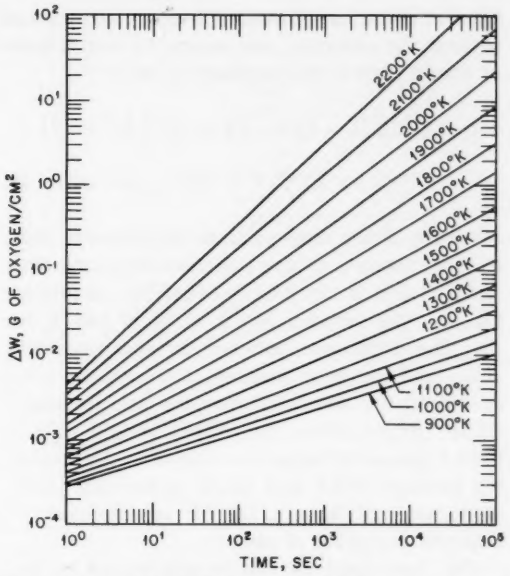

Figure 11 — Metal-Water reaction curves for Zircaloy-2.[38]

After loss of coolant the temperature history is divided up into increments of temperature, ΔT. For each ΔT the sum of decay and reaction heats is equated to the heat required to raise the core temperature ΔT degrees, and the kinetics at the temperature of the upper limit of ΔT are used to compute the amount of reaction over the whole ΔT range. The basic chemical reaction is

$$Zr_{solid} + 2H_2O_{gas} \rightarrow ZrO_{2\,solid} + 2H_{2gas} \qquad (1)$$

Because Eq. 1 is exothermic, the metal-water reaction can become autocatalytic, heating the metal to its melting point (about 2200°K). The amount of heat produced by Eq. 1 is

$$\Delta H_R = -149{,}120 + 8.5T - 1.44 \times 10^{-3}T^2 + \frac{2.41 \times 10^5}{T} \qquad (2)$$

where ΔH_R = calories released from Eq. 1 as written*
T = temperature, °K

All the heat released by Eq. 1 does not go into the metal, however, since some heat must go into heating 2 moles of steam to the tempera-

*Reference 38 shows the units as calories per mole of reactant, but from reference 39 it appears that the enthalpy change is for Eq. 1 as it is shown.

ture in question. Equation 3 gives the amount of heat, in calories, necessary to heat a mole of steam from a temperature T_1 to T.

$$\Delta H_S = 7.219\,[T - T_1] + 1.187 \times 10^{-3}\,[T^2 - T_1^2] + 8.9 \times 10^{-8}\,[T^3 - T_1^3]^* \quad \text{cal/mole} \quad (3)$$

Since Eq. 2 was derived from free-energy data, it is necessary to use the same standard state and T_1 value in Eq. 3 as were used in calculating Eq. 2. The authors use a value of 298°K for T_1. The difference between the heat liberated, ΔH_R, and the heat passing to the steam, ΔH_S, is called the "heat entering the solid phase," HESP. Since ΔW is the oxygen weight gain in time t (grams of oxygen per square centimeter), the product of ΔW and HESP is the heat liberated per unit area if HESP is expressed in calories per gram of oxygen.

The heat balance can be expressed as follows:

Specific heat = decay heat + oxidation heat

or

$$\Delta T \times Cp_{Zr} \times W = H_D \times t \times W + \text{HESP} \times [k(T)\,(t + t_0)^{n(T)} - k(T)\,t_0^{n(T)}] \quad (4)$$

In this equation:

1. ΔT is the temperature rise of the element during time t, °K.
2. Cp_{Zr} is the specific heat of the cladding, cal/g/°K.
3. W is the weight of a half-section, g/cm^2.
4. H_D is the decay heat liberated, cal/g/sec.
5. $k(T)t_0^{n(T)}$ represents the total number of grams of oxygen reacted prior to the temperature interval in question.
6. t_0 is the time (in seconds) at the new temperature that it would take to oxidize the section to the extent it has reached prior to the temperature interval in question.
7. $k(T)(t + t_0)^{n(T)}$ is the total amount of oxidation that has taken place, including the temperature interval in question.
8. The difference between 7 and 5 is equal to the amount of oxidation taking place during the temperature interval in question.

Equation 4 is solved for t by trial and error, and the amount of oxidation taking place during the interval is calculated. This procedure is repeated until the melting temperature of the cladding is reached. At this point the left side of Eq. 4 is replaced by the heat of fusion, and the calculations are continued. The calculations would continue until the core had melted or some external mechanism (e.g., water sprays) had terminated the excursion.

The second part of the problem is started when the cladding ruptures exposing the fuel to the water. In the particular reactor design studied in reference 38, the fuel, an alloy of uranium, had a lower melting temperature than Zircaloy. Hence, when the Zircaloy melted, it was assumed that this molten fuel suddenly dropped into the pool of water. If the fuel were UO_2, this part of the problem, of course, would not exist. In addition, molten drops of Zircaloy would be dropping off fuel elements and into the water pool at the bottom of the pressure vessel. The heat balance is again the basic equation to solve, using the method of dividing the total temperature interval into increments of width ΔT. It is assumed that heat is lost from the molten drops entirely by radiation, and the balance equation becomes

$$H_{\text{rad}} = H_R + H_{DH} + H_{SH}$$

where H_{rad} = energy transferred by radiation
H_R = energy from metal-water reaction
H_{DH} = decay energy
H_{SH} = energy liberated in cooling an amount ΔT

Several additional complications arise, however. The molten metals form drops, which must be sized, and the calculations require emissivities, which must be determined. Also, as the drop oxidizes, the surface area available for further oxidation decreases. Droplet sizes can be approximated from interfacial tension data, and the reduction of surface area can be calculated as the oxidation proceeds.

When the calculation is complete, the amount of metal-water reaction is known, subject to the approximations used in the derivations and in data such as emissivities and interfacial tension. Tables VI-2 and VI-3, for example,

* The authors of reference 38 noted that the units on this equation are not correct since an error in the original assumption resulted in the lower limit of the equation being taken for 373°K rather than 298°K. Accordingly, the Lustman values calculated are slightly high at the lower temperatures.

Table VI-2 TIME AND PERCENTAGE REACTION FOR ZIRCALOY-2-CLAD FUEL ELEMENT[38]
(Decay Heat = 0.374 cal/g/sec)

Temp., °K	HESP,* cal/g O	$k(T)$	$n(T)$	t_0, sec	t, sec	Total oxidation, g O/cm^2	Total oxidation, %
800–1000	4090	3.1×10^{-4}	0.33	0	25.5	9.03×10^{-4}	0.45
1000–1200	3920	4.15×10^{-4}	0.38	7.7	29.3	1.64×10^{-3}	0.81
1200–1400	3740	6.31×10^{-4}	0.462	7.9	20.1	2.95×10^{-3}	1.5
1400–1600	3580	9.6×10^{-4}	0.552	7.7	11.0	4.85×10^{-3}	2.4
1600–1800	3410	1.52×10^{-3}	0.66	6.1	4.6	7.26×10^{-3}	3.6
1800–2000	3230	2.5×10^{-3}	0.784	3.9	2.0	10.0×10^{-3}	5.0
2000–2200	3040	4.36×10^{-3}	0.945	2.4	0.7	12.7×10^{-3}	6.3
2200–molten	3040	4.36×10^{-3}	0.945	3.1	3.0	24.04×10^{-3}	11.9

*HESP = heat entering solid phase; Lustman's values.

Table VI-3 COOLING DATA FOR A DROPLET OF ZIRCALOY-2[38]
(Radius = 0.215 cm, Emissivity = 0.67, Decay Heat = 0.374 cal/g/sec)

Temp., °K	HESP (cal/g O)	$k(T)$	$n(T)$	t, sec	Total g O	Total reaction, %
2200–2000*	3040	4.36×10^{-3}	0.945	4.0	9.38×10^{-3}	9.8
2000–1800	3230	2.5×10^{-3}	0.784	1.1	10.84×10^{-3}	11.3
1800–1600	3410	1.52×10^{-3}	0.660	1.4	11.85×10^{-3}	12.4
1600–1400	3580	9.6×10^{-4}	0.552	2.1	12.62×10^{-3}	13.2
1400–1200	3740	6.31×10^{-4}	0.462	3.3	13.20×10^{-3}	13.8
1200–1000	3920	4.15×10^{-4}	0.38	6.0	13.63×10^{-3}	14.2
1000–800	4090	3.1×10^{-4}	0.33	13.8	14.02×10^{-3}	14.6

*Includes solidification.

show the reaction history of a Zircaloy-2-clad element and a drop of molten Zircaloy-2.

SRE Shutdown

During a normal power run on the SRE in May, tetralin coolant from the main primary pump shaft seal leaked into the primary sodium system. The reactor was shut down and the pump seal coolant system converted from tetralin to NaK. It was started up again in mid-July to remove tetralin decomposition products through careful low-power operation and cold trapping. Anomalies were noted during the run as expected. When several weeks of operation failed to clear the anomalies, the reactor was shut down to inspect fuel elements.

Since shutdown in late July, all the fuel elements have been removed from the reactor. Twelve of the 43 were found to be severely damaged by high temperature. The mechanism of damage has been established as partial blockage of reactor coolant flow passages by tetralin decomposition products, followed by local overheating of the fuel elements, resulting in formation of an iron-uranium eutectic (m.p. 1340°F) and parting of the type 304 stainless-steel cladding.

Samples of the fuel, cladding, and other components of the fuel assemblies have been metallurgically examined, and coolant and coolant contaminants have been chemically analyzed.

The results of these investigations will be given in a report by the SRE *Ad Hoc* Review Committee scheduled for publication in December. The report will be reviewed in the March 1960 issues of *Power Reactor Technology* and *Nuclear Safety*.

References

1. Research and Development in Reactor Safety, U. S. Atomic Energy Commission, February 1959.
2. S. G. Forbes, Instability in SPERT-I, *Nucleonics*, 15(1): (January 1957).
3. W. A. Horning and H. C. Corben, Theory of Power Transients in the SPERT-I Reactor, IDO-16446, Aug. 20, 1957. (Unclassified AEC report.)
4. F. Schroeder et al., Experimental Study of Transient Behavior in a Sub-cooled, Water-moderated Reactor, *Nuclear Science and Engineering*, 2(1): 96-115 (February 1957).

5. F. Schroeder, Stability Tests with the SPERT-I Reactor, IDO-16383, July 1957. (Unclassified AEC report.)
6. C. R. Montgomery et al., Summary of the SPERT-I, -II, and -III Reactor Facilities, IDO-16418, November 1957. (Unclassified AEC report.)
7. W. E. Nyer and S. G. Forbes, Idaho Operations Office, September 1957. (Unpublished.)
8. M. E. Remley et al., Program Review of the Water Boiler Reactor Kinetic Experiments, NAA-SR-1525, Mar. 15, 1956. (Unpublished.)
9. M. E. Remley et al., Experimental Studies on the Kinetic Behavior of Water Boiler Type Reactors, A/CONF.15/P/1079, Second United Nations International Conference on the Peaceful Uses of Atomic Energy, Geneva, September 1958.
10. H. A. Bethe, Reactor Safety and Oscillator Tests, APDA-117, Atomic Power Development Associates, Inc., October 1956.
11. H. V. Lichtenberger et al., Operating Experience and Experimental Results Obtained from a NaK-cooled Fast Reactor, *Proceedings of the International Conference on the Peaceful Uses of Atomic Energy, Geneva, 1955*, 3: 345 (1955).
12. F. W. Thalgott et al., Stability Studies on EBR-I, A/CONF.15/P/1845, Second United Nations International Conference on the Peaceful Uses of Atomic Energy, Geneva, September 1958.
13. R. E. Rice et al., EBR-I, Mark-III Design Report, ANL-5836, March 1958. (Unclassified AEC report.)
14. R. E. Skinner and D. L. Hetrick, The Transfer Function of a Water Boiler Reactor, *Nuclear Science and Engineering*, 3(5): 573 (May 1958).
15. S. H. Fitch, Safety Device Tests in KEWB-I, NAA-SR-2476, Jan. 28, 1958. (Unclassified AEC report.)
16. S. H. Fitch, Hanford Safety Device Summary Report, NAA-SR-2463, Apr. 1, 1958. (Unclassified AEC report.)
17. S. H. Fitch and T. H. Springer, Thermal Transient Behavior of the Neutron Sensor of a Reactor Safety Device, NAA-SR-2689, June 7, 1958. (Unclassified AEC report.)
18. G. E. Creek, W. J. Martin, and G. W. Parker, Experiments on the Release of Fission Products from Molten Reactor Fuels, ORNL-2616, July 22, 1959. (Unclassified AEC report.)
19. S. J. Rodgers and G. E. Kennedy, Fission Product Release During a Simulated Meltdown of a PWR Type Core, Technical Report 63, MSA Research Corp., Oct. 20, 1958.
20. N. M. Feder, N. R. Chellew, and M. Ader, Interim Report: Purification of Nuclear Fuels by Melting in Refractory Oxide Crucibles, ANL-5255, March 1954. (Unclassified AEC report.)
21. A. M. Saul, Pyrochemical Separations Methods. III. The Removal of Fission Products from Molten, Irradiated Uranium by Solid Oxides, NAA-SR-1361, September 1955. (Unclassified AEC report.)
22. G. A. Freund, TREAT, A Pulsed Graphite-moderated Reactor for Kinetic Experiments, A/CONF.15/P/1848, Second United Nations International Conference on the Peaceful Uses of Atomic Energy, Geneva, September 1958.
23. Alexis W. Lemmon, Jr., Studies Relating to the Reaction Between Zirconium and Water at High Temperatures, BMI-1154, Jan. 3, 1957. (Unclassified AEC report.)
24. George Long, Explosions of Molten Aluminum in Water — Cause and Prevention, Metal Progress, May 1957.
25. B. Lustman, Zirconium–Water Reaction Data and Application to PWR Loss-of-Coolant Accident, WAPD-SC-543, May 1957. (Unclassified AEC report.)
26. H. M. Saltsburg, Metal–Water Reactions, KAPL-1495, Apr. 2, 1956. (Unclassified AEC report.)
27. H. M. Saltsburg, The Kinetics of Molten Metal–Water Reactions: A Report on Na_2K–Water Vapor, KAPL-1763, Apr. 30, 1957. (Unclassified AEC report.)
28. H. M. Higgins and R. D. Schultz, The Reaction of Metals with Water and Oxidizing Gases at High Temperatures, IDO-28000, Apr. 30, 1957. (Unclassified AEC report.)
29. F. B. Porzel, Design Evaluation of BER (Boiling Experimental Reactor) in Regard to Internal Explosions, ANL-5651, January 1957. (Unclassified AEC report.)
30. R. J. Larson and W. E. Olson, Measurement of Air Blast Effects from Simulated Nuclear Reactor Core Excursions, WASH-747, September 1957. (Unclassified AEC report.) (Ballistic Research Laboratories Memorandum Report No. 1102, Aberdeen Proving Ground, Maryland.)
31. H. B. Karplus, The Velocity of Sound in a Liquid Containing Gas Bubbles, COO-248, June 11, 1958. (Unclassified AEC report.)
32. N. R. Zabel, Containment of Fragments from Runaway Reactor, SRI-1, Apr. 2, 1958. (Unclassified AEC report.)
33. Walter R. Wise, Jr., An Investigation of Strain-Energy Absorption Potential as the Criterion for Determining Optimum Reactor-vessel Containment Design, NAVORD-5748, June 30, 1958. (Unclassified AEC report.)
34. R. H. Stresau and H. Napadensky, A Technique for the Observation and Measurement of the Behavior of Porous Materials When Rapidly Compressed, ARF-132D11-1, August 1958. (Unclassified AEC report.)
35. W. E. Baker and F. J. Allen, The Response of Elastic Spherical Shells to Spherically Symmetric Internal Blast Loading, WASH-746, November 1957. (Unclassified AEC report.) (Ballistic Research Laboratories Memorandum Report No. 1113, Aberdeen Proving Ground, Maryland.)

36. W. E. Baker and J. D. Patterson, II. Blast Effects Test of a One-quarter Scale Model of the Air Force Nuclear Engineering Test Reactor, Ballistic Research Laboratories Report No. 1011, Aberdeen Proving Ground, Maryland, 1957.
37. J. R. Bohannon, Jr., and W. E. Baker, Simulating Nuclear Blast Effects, *Nucleonics*, 16: 75-79 (1958).
38. E. F. Hillner and J. N. Chirigos, Westinghouse Electric Corp., December 1958. (Unpublished.)
39. B. Lustman, Zirconium–Water Reactions, WAPD-137, Dec. 1, 1955. (Unclassified AEC report.)

Review of Shielding Art

In reference 1 is a review of analytical shielding methods. Each method is discussed, and some are used in predicting the results of experiments. The comparisons cover multiregion, multilayer, and multimaterial shields; ducts and porous plugs; air and ground scattering; shield heating; and other subjects of lesser interest in power reactor shield design. All comparisons include neutron and gamma dose rates with the addition of two comparisons of measured and calculated fast-neutron energy spectra. The calculational methods are not described in detail, but all methods are referenced.

Although the specific configurations investigated are of little interest to the designer of large power reactors, the calculation techniques used give striking agreement with experimental results, even in situations which are quite complex. There is little doubt that these techniques would be valuable in the civilian power reactor program and would constitute a real advance over those presently in use.

Reference

1. R. H. Clark, General Electric Atomic Products Div., July 1958. (Unpublished.)

Radiation Effects on Semiconductors

Nuclear radiation poses a severe problem in the application of semiconductors to control and instrumentation systems in the nuclear field. Because of the susceptibility of semiconductor materials to radiation damage, an understanding of the permissible limits of radiation exposure and of the changes in characteristics of the semiconductor is required. The Radiation Effects Information Center (REIC) has reported in two earlier memorandums[1,2] on some of the effects of radiation on semiconductor materials and more recently has issued a memorandum on the effects of radiation on semiconductor diodes.[3] Transient, semipermanent, and permanent diode parameter changes occur as a result of exposure.

Reference 3 has made the following summary of semiconductor diode behavior under nuclear radiation:

1. Fast neutrons affect semiconductor diode forward characteristics through changes in the bulk material, and they affect the reverse characteristics through changes in the junction region.
2. Where fast- and slow-neutron fluxes are of the same order of magnitude, the slow neutrons are not a major factor contributing to the deterioration of semiconductor devices.
3. Gamma radiation causes transient surface damage in semiconductor diodes which results in changes in leakage currents; recovery may occur when the device is removed from the radiation field.
4. Germanium diodes fail in the reverse direction because of changes in reverse resistance of several orders of magnitude after exposure to integrated neutron fluxes of 10^{13} fast neutrons/cm^2 or higher.
5. If germanium diodes are employed in electronic circuitry exposed to integrated fluxes as great as 10^{13} fast neutrons/cm^2, the circuit design must be such that (a) the circuit performance is not seriously affected by changes in the reverse characteristics of the germanium diodes and (b) the diodes are protected individually from self-destruction resulting from excessive power dissipation when the radiation deteriorates the reverse characteristics.
6. Failure in silicon rectifying devices results primarily from deterioration of the forward characteristics. For applications where an increase in forward resistance does not seriously affect operation, silicon diodes probably can be used to 10^{13} fast neutrons/cm^2. Equipment which utilizes silicon diodes and which will be exposed to integrated fluxes to 10^{13} fast neutrons/cm^2 must be capable of performing satisfactorily with diode reverse leakage currents as large as approximately 0.2 μa at about 30 volts.

   Some silicon diode types are highly radiation resistant and have usable forward characteristics to 10^{13} fast neutrons/cm^2 in addition to usable reverse characteristics. If the forward characteristics are important to equipment performance, radiation-resistant units such as the NSP type 1N137A silicon diode should be employed.
7. Radiation-invoked ionization of air molecules adjacent to semiconductor diodes will result in collection of ionized molecules on bare diode leads, other conduction surfaces, and terminals and will cause currents to 2 orders of magnitude larger than those created inside the diode envelope by radiation. Proper insulation virtually eliminates such currents.
8. A major factor determining the radiation resistance of semiconductor diodes appears to be the manufacturing process employed.
9. Materials currently used in the fabrication of diodes are relatively ineffectual for shielding against the effects of neutron and gamma radiation.

Radiation Effects on Magnetic Materials

Magnetic materials are used in motors, amplifiers, transducers, and other actuators and instruments in the nuclear field. When these materials are exposed to large amounts of neutron radiation, some changes in properties of the materials can be expected.

The REIC has summarized in a technical memorandum[4] some of the effects of nuclear radiation on the structure-sensitive properties of magnetic materials, such as permeability,

remanence, and coercive force. Radiation effects on magnetic core materials of nickel-iron, silicon-iron, aluminum-iron, and ferrite were reviewed. Important changes in the magnetic properties of the nickel-iron alloys were noted after exposure to 10^{17} fast neutrons/cm^2. No damage was observed in the operation of magnetic amplifiers to exposures of 10^{15} fast neutrons/cm^2.

Corrosion of Stainless Steel in a Nitrogen Atmosphere

Battelle Memorial Institute (BMI) has recently reported on corrosion tests on stainless-steel fuel-element cladding materials for the Gas-cooled Reactor Experiment (GCRE).[5] The fuel elements for this reactor experiment will be cooled by nitrogen, and the clad surface temperature is expected to be as high as 1650°F. Preliminary screening of stainless steels having satisfactory high-temperature properties were conducted at atmospheric pressure and elevated temperature with nitrogen gas containing additions of oxygen and water vapor. The results of these tests are shown in Tables VIII-1 and VIII-2.

As a result of the screening tests, AISI type 318 stainless steel was selected for further study. A general indication of the corrosion rate of this material as a function of temperature and time is provided by the data of Tables VIII-3 and VIII-4. The addition of small amounts of oxygen was shown to inhibit nitriding and result in the preferential oxidation of the stainless steel.

The data obtained are encouraging for short-time use of this material at high temperatures. However, at 1500°F, the preliminary data indicate that this material is still not suitable for long-term service in a power reactor using nitrogen coolant unless the corrosion rate drops significantly with time.

The general conclusions made by BMI as a result of the screening study are quoted below.[5]

1. Type 318 stainless steel has better resistance to oxidizing attack in wet and dry oxygen-containing nitrogen atmospheres than do type 347, type 316, Timken 16-15-6, and Timken 16-25-6 alloys. Type 347 stainless was nearly as satisfactory as type 318.

2. The relationship between depth of attack and time of exposure seems to be diffusion controlled, indicating that the rate of attack decreases with time. This relationship may be disturbed adversely by spalling, the occurrence of which would cause the rate to increase.

3. Within wide limits the surface finish does not affect the rate of oxidation of type 318 stainless in wet or dry oxygen-containing nitrogen atmospheres.

4. Nitriding reaction is inhibited when small amounts of oxygen are present in a nitrogen atmosphere. Some nitrogen diffuses into the metal, but nitrides do not appear to form. The resulting oxidation attack is much less severe than the nitriding attack.

5. The concentration of oxygen in nitrogen which was found to be optimum from the standpoint of minimum oxidation attack and inhibition of nitriding was 0.5 vol.%. The concentration of oxygen found to be most effective was 5 vol.%, followed by 0.1 and 0.05 vol.%. The results obtained when 5 vol.% oxygen was added to the atmosphere would warrant trying out dry and moist air atmospheres in the future.

6. The addition of 0.6 vol.% water vapor to a dry nitrogen atmosphere does not affect to any great extent the rate of attack of type 318 stainless as

Table VIII-1 MAXIMUM DEPTH OF OXIDATION OF VARIOUS FERROUS ALLOYS EXPOSED FOR 100 HR IN NITROGEN CONTAINING SMALL AMOUNTS OF OXIDIZING GASES*[5]

	Maximum depth of penetration after 100 hr in nitrogen having addition shown (mils)											
	0.07 vol.% H_2O			0.2 vol.% H_2O	0.05 vol.% oxygen		0.1 vol.% oxygen			0.5 vol.% oxygen		
Alloy	1500°F	1650°F	1800°F	1650°F	1650°F	1800°F	1500°F	1650°F	1800°F	1500°F	1650°F	1800°F
Type 316 S.S.	†	0.5	1.6	†	0.2	1.0	0.05	†	2.0	0.1	0.15	†
Type 318 S.S.	0.05	0.05	5.0	0.15	0.05	0.2	0.05	0.05	0.25	0.05	0.05	0.15
Type 347 S.S.	†	0.05	5.0	†	0.6	0.4	0.05	†	0.3	0.05	0.2	†
Timken 16-15-6	0.3	0.1	1.3	0.5	0.15	0.9	0.1	0.3	1.0	0.2	0.6	0.9
Timken 16-25-6	0.3	0.3	0.6	0.3	0.3	0.5	0.15	0.3	0.5	0.1	0.4	0.6

*Specimen surface was ground to 240-grit finish.
†Material was not tested.

Table VIII-2 MAXIMUM DEPTH OF OXIDATION OF VARIOUS FERROUS ALLOYS EXPOSED TO OXIDIZING NITROGEN ATMOSPHERES FOR 500 HR AT 1650°F*[5]

Atmosphere composition, vol.%	Maximum depth of penetration in alloy shown (mils)				
	Type 316	Type 318	Type 347	Timken 16-15-6	Timken 16-25-6
Nitrogen +0.07 H_2O	1.3	0.6	1.5	0.6	0.7
Nitrogen +0.1 oxygen	1.2	0.6	1.0	0.6	0.7

*Specimens were ground to 240-grit finish and annealed at 2150°F in hydrogen for 1½ hr.

Table VIII-3 MAXIMUM DEPTH OF ATTACK OF TYPE 318 STAINLESS STEEL EXPOSED AT SEVERAL TEMPERATURES TO DRY NITROGEN ATMOSPHERES CONTAINING 0.5 VOL.% OXYGEN[5]

Test	Specimen	Preanneal temp.,* °F	Exposure temp., °F	Exposure time, hr	Depth of attack, mils
1	5	2150	1750	215	0.45
	6	2150	1750	376	0.7
	44	2150	1750	479	0.7
	7	2150	1750	580	0.95
	41	2150	1750	683	1.1
	27	2150	1750	843	1.3
	8	2150	1750	1059	2.1
2	17	2150	1650	216	0.4
	18	2150	1650	478	0.5
	37	2150	1650	980	0.75
	76	2150	1650	1032	1.6
	58	2150	1650	2468	1.0
	20	2150	1650	2626	0.8
	40	2150	1650	3180	1.8
	19	2150	1650	3658	2.9
3	54	2450	1650	238	0.7
	77	2450	1650	417	0.5
	55	2450	1650	662	0.9
	73	2450	1650	1089	0.8
	56	2450	1650	1334	1.0
4	64	2450	1500	258	Nil
	80	2450	1500	417	0.25
	65	2450	1500	930	0.2
	72	2450	1500	1176	0.6
	66	2450	1500	1347	0.4
	67	2450	1500	1434	0.5

*All specimens were annealed in hydrogen. Those annealed at 2150°F were held for 2 hr and furnace-cooled. Specimens annealed at 2450°F were held for 5 hr, cooled to 1850°F, and held for 2 hr, and then furnace-cooled.

measured by the maximum depth of penetration, but it does result in a more nonuniform attack.

7. On the basis of limited work, it can be said that nitrogen atmospheres with addition of small amounts of carbon monoxide cause shallower oxidation attack than do nitrogen atmospheres containing small amounts of oxygen.

Table VIII-4 MAXIMUM DEPTH OF ATTACK OF TYPE 318 STAINLESS STEEL EXPOSED AT SEVERAL TEMPERATURES TO NITROGEN ATMOSPHERES CONTAINING 0.5 VOL.% OXYGEN PLUS 0.6 VOL.% WATER VAPOR[5]

Test	Specimen	Preanneal temp.,* °F	Exposure temp., °F	Exposure time, hr	Depth of attack, mils
5	29	2150	1800	50	0.6
	30	2150	1800	210	2.8
	31	2150	1800	616	5.4
	32	2150	1800	808	5.6
6	33	2150	1650	50	0.15
	34	2150	1650	210	0.4
	79	2150	1650	417	0.9
	35	2150	1650	616	1.1
	74	2150	1650	1080	0.7
	36	2150	1650	1498	0.75
	52	2150	1650	1971	1.8
	50	2150	1650	2120	2.0
	43	2150	1650	2377	1.8
7	84	2450	1500	65	Nil
	68	2450	1500	210	Nil
	83	2450	1500	319	0.3

*All specimens were annealed in hydrogen. Those annealed at 2150°F were held for 2 hr and furnace-cooled. Specimens annealed at 2450°F were held for 5 hr, cooled to 1850°F, held for 2 hr, and then furnace-cooled.

8. Several conclusions concerning the mechanism of attack can be drawn from the X-ray diffraction and fluorescence analyses of the oxidation products. These are:

a. The initial oxidation of the alloy produces an oxide film in which the major phase is of the R_2O_3 type. An oxide of the R_2O_3 spinel type is a minor component in the initial film. The metal constituents of the initial film are presumed to be essentially those of the alloy.

b. Preferential diffusion of chromium and manganese from the base metal into the oxide layer during the next step results in the formation of increasing amounts of the R_3O_4 type oxide.

c. The amount of preferential diffusion is reduced significantly by the addition of water vapor to the oxidizing gas mixtures. Diffusion is only slightly decreased by increasing the oxygen content of the gas over the range 0.05 to 5.0 vol.%.

d. At 1650°F, the composition of the oxide layer reaches a maximum in chromium and manganese and a minimum in iron and nickel after 500 to 600 hr of oxidation.

e. The composition of the adherent oxide, after 500 to 600 hr of oxidation, varies considerably due to spalling of parts of the oxide layer.

f. Oxidation of the thicker noncoherent oxide layer results in the formation of a chromium-rich R_2O_3 oxide.

9. Specimens that were preannealed at 2150°F in hydrogen appeared to be slightly more resistant to attack than specimens preannealed in hydrogen at 2450°F.

References

1. F. J. Reid, J. W. Moody, and R. K. Willardson, The Effect of Nuclear Radiation on Semiconductor Materials, REIC-1, Battelle Memorial Institute, Dec. 20, 1957.
2. L. W. Aukerman and F. J. Reid, Energy Levels Produced in Semiconductors by High-energy Radiation, Technical Memorandum No. 4, Battelle Memorial Institute, July 15, 1958.
3. J. E. Drennan and S. E. Harrison, The Effect of Nuclear Radiation on Semiconductor Diodes, Technical Memorandum No. 6, Battelle Memorial Institute, December 1958.
4. F. J. Reid and J. W. Moody, The Effect of Nuclear Radiation on Magnetic Materials, Technical Memorandum No. 12, Battelle Memorial Institute, December 1958.
5. D. L. Keller, ed., Corrosion of Stainless Alloys in High-temperature Nitrogenous Environments, BMI-1361, July 14, 1959. (Unclassified AEC report.)

PROGRESS ON SPECIFIC REACTOR TYPES

LIGHT-WATER REACTORS

The Belgian BR-3

The Belgian BR-3 nuclear power plant is presently under construction at Mol, Belgium, and should commence initial operation during the summer of 1960. Reference 1 contains recent information on the design of the plant. The following organizations are responsible for the designated phases of the operation.

Plant owner	Centre d'Étude de l'Énergie Nucléaire (CEN), Brussels, Belgium
CEN's consulting engineers	Bureau d'Études Nucléaires (BEN) Société Belge pour l'Industrie Nucléaire (Belgo-Nucléaire) Société de Traction et d'Électricité (TE), Brussels, Belgium
Designer of nuclear equipment and systems	Westinghouse Electric Corp., Atomic Power Division (WAPD), Forest Hills, Pa.
Architect-Engineer for Westinghouse	Gibbs and Hill, New York, N. Y.
Plant container designer	Sargent & Lundy, Chicago, Ill.

The reactor is a PWR type employing light water as the coolant and moderator. Other design details can be found in Table IX-1.

Boric acid solutions are used for two purposes in the design. The first system injects boric acid into the primary coolant to achieve shutdown to room temperature for refueling purposes, since the control rods are not adequate to keep the clean, cold reactor in a subcritical condition. A second system supplies borated water to the reactor for core cooling in the event of loss of coolant through a rupture in the primary-coolant plumbing. This latter system is actuated manually when the system pressure has fallen to 800 psia.

Table IX-1 DESIGN DETAILS FOR BR-3 REACTOR

Reactor thermal power	40,900 kw
Gross electric power	11,500 kw
Net electric power	10,500 kw
Steam pressure at throttle	525 psia
Steam temperature at throttle	472°F
Steam flow rate	154,500 lb/hr
Feed-water temperature	330°F
Reactor coolant conditions (nominal):	
Pressure	2000 psia
Inlet temperature	491°F
Outlet temperature	515°F
Flow rate	5×10^6 lb/hr
Average heat flux	94,200 Btu/(hr)(sq ft)
Peak heat flux	441,800 Btu/(hr)(sq ft)
Fuel-element geometry	Stainless-steel tubes containing UO_2 pellets
No. of tubes per assembly	~110
No. of assemblies per core	32
Enrichment:	
Outer zone	4.4 wt.%
Inner zone	3.7 wt.%
Core life	7000 equivalent full-power hours
Control	12 rods plus boric acid
Reactivity change; cold, clean to hot, end of life	19 per cent
Containment-shell dimensions, H/D	107 by 54 ft
Containment-shell maximum design pressure	45 psig

Reference

1. P. Dozinel and J. Storrer, Safety Aspects of the Belgian BR-3 Reactor, presented at the International Symposium on the Safety and Location of Nuclear Plants, June 1959.

One of the most important aspects of boiling-water reactors is the stability of power output. Considerable progress has been made in this field; the subject is reasonably well understood qualitatively, and it is possible to design large high-output boiling reactors, as well as the smaller reactors, without fear of encountering instability in the operating range. Nevertheless, the designer is still chary of those design features which are thought to promote instability, and, as a result, the design area is perhaps more restricted than is necessary.

The subject of boiling-reactor stability has been discussed in previous issues of this Review (*Power Reactor Technology*, 1(1): 14-16 (December 1957); 1(3): 21-22 (June 1958); 1(4): 10-14 (September 1958)). Recently, several new reports have been issued which make contributions to the understanding of the subject.

Design Considerations

The closest relation between questions of stability and reactor design may be expressed in terms of the steam coefficient of reactivity, sometimes called the void coefficient of reactivity. When steam exists in a reactor, the reactivity will, in general, differ from the reactivity when there is no steam present. If the steam in the reactor core occupies a fraction $\Delta V/V$ of the volume available for occupancy by H_2O and, in doing so, causes a change of reactivity $\Delta k_{eff}/k_{eff}$, then the steam coefficient of reactivity is defined as $(\Delta k_{eff}/k_{eff})/(\Delta V/V)$. If the coefficient is negative, as it must certainly be if the reactor is to be inherently stable, then any increase in reactor power which will increase the steam content of the reactor will decrease the reactivity; this, in turn, will tend to decrease power. In other words, the reactor will tend to regulate its power to a constant value if no reactivity changes are imposed by outside sources. The regulation will not occur instantaneously since there are various thermal and hydraulic time delays in the process.

It is both customary and useful to consider (1) the externally imposed reactivity variations to constitute the input signal, and (2) the reactor power output to constitute the response, of a servo loop which includes those reactor characteristics involved in the reactivity-power relation (Fig. 12). In this representation the net

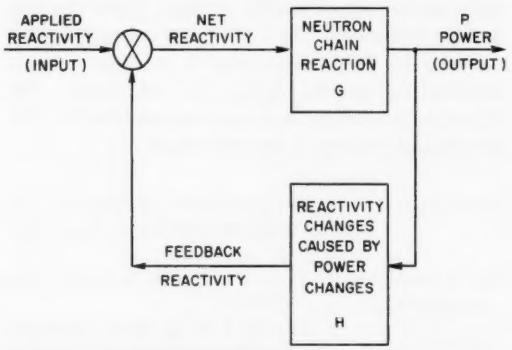

Figure 12—Representation of the reactivity-power relation in terms of a servo system.

reactivity is applied as a driving force to the neutron chain reaction, producing the appropriate variation in neutron flux and, hence, in reactor power. Those processes (e.g., change of steam content) which, as a result of a power change, produce a reactivity change are considered to constitute a feedback circuit, whose output, the feedback reactivity, combines algebraically with the externally applied reactivity (the input signal); this combination yields the net reactivity applied to the neutron chain reaction. In this representation the thermal and hydraulic time delays appear as phase lags in the frequency characteristics of the feedback loop. It is characteristic of such systems that they may oscillate unstably for certain combinations of phase shifts and gain of the feedback circuit. In general, the tendency toward instability will increase as the gain is increased. In the case of any particular boiling reactor, the steam content of the reactor is roughly pro-

portional to the operating power. Consequently, the fractional change in reactivity which results from a fractional change of power (which may be considered the gain of the feedback loop) is roughly proportional to the product of the power times the steam coefficient of reactivity. That is to say, if time lags in the system are such that instability is possible, then the point of instability will be approached more and more closely as reactor power is increased. Since, in general, the designer wishes to achieve a relatively high power density in the reactor, and since he is aware that a stability limit probably exists which acts as a limit on the product (power) × (steam coefficient of reactivity), his incentive is to make the steam coefficient of reactivity as low as possible. Hence there is a tendency to design boiling reactors for a steam coefficient of reactivity which is low in magnitude and negative in sign.

If one considers the reactivity change which may occur in a water-moderated reactor when some of the water is displaced by steam — the reactivity change which determines the steam coefficient of reactivity — several contributions to the change may be recognized. The parasitic neutron absorption by water will be decreased, and the fast-fission factor may be slightly increased; both of these effects make a positive contribution to the reactivity change. The resonance absorption in U^{238} will increase, and the leakage of neutrons out of the reactor and the leakage of neutrons into control rods and other lumped absorbers which may be present will increase; these effects make negative contributions to the reactivity change. The relative importance of these effects will vary with the characteristics of the reactor design.

In particular, if the reactor fuel contains a fertile material, the relative importance of parasitic absorption by water and of resonance absorption by the fertile material can be adjusted by adjusting the ratio of fuel to water. Higher fuel-to-water ratios will accentuate the effect of resonance absorption and cause the negative component of the steam coefficient to predominate, whereas low fuel-to-water ratios will accentuate the parasitic absorption of water and cause the positive component to predominate. In such a reactor the net steam coefficient of reactivity can be adjusted to any desired value over a rather wide range by suitable adjustment of the fuel-to-water ratio. It is evident from the same consideration that the steam coefficient of reactivity will not remain constant as the amount of steam in the reactor increases, but that it will become more and more strongly negative as the average density of water in the reactor is decreased by an increase in steam content. A similar effect will result from a temperature increase which decreases the water density. In a high-pressure boiling reactor the decrease in average water density may be some 25 per cent as a result of the temperature change from room temperature to operating temperature, and a further decrease of something like 15 per cent may result from the operating steam content. Consequently, the steam coefficient may be much more strongly negative under full-power operating conditions than it is at room temperature. Characteristically, the reactor designer is faced with a choice between (1) designing for a very low negative coefficient at room temperature and accepting a somewhat higher negative coefficient than he desires under operating conditions and (2) designing for the desired low negative coefficient under operating conditions and accepting a positive coefficient at room temperature. If the latter course is taken, a hazard question may arise because of the possibility of an autocatalytic reactivity accident at low temperature, and it may be necessary to forego operation of the reactor at low temperature and provide auxiliary heating to bring the reactor up to an acceptable operating temperature.

In so far as the fuel-to-water ratio must be chosen to yield the desired steam coefficient of reactivity, other design goals which are affected by fuel-to-water ratio may be compromised. One of the important goals of this kind is high conversion ratio. If there is no restriction on fuel-to-water ratio, the conversion ratio may be increased by increasing the fuel-to-water ratio. The improvement in conversion ratio results from increased resonance absorption in the fertile material, which, in turn, allows the use of a higher fuel enrichment with correspondingly smaller fractional loss of neutrons to parasitic absorbers. Fortunately, the fuel-to-water ratios which yield acceptable steam coefficients of reactivity also give reasonably high conversion ratios (in the neighborhood of 0.7) if low-absorption (Zircaloy) jackets are used for the fuel. Nevertheless, greater freedom in adjustment of conversion ratio through adjustment of fuel-to-water ratio (or more precisely through adjustment of the resonance escape probability) would be desirable.

It must be evident, from the above considerations, that overconservatism in the physics design of the boiling reactor, i.e., the striving for an extremely low steam coefficient of reactivity in order to avoid encroachment on the gray area in which stability is questionable, entails penalties in reactor cost and performance. Equally important penalties may arise from overconservatism in the thermal design.

The conservatism in the design of the Experimental Boiling Water Reactor (EBWR) has been thoroughly demonstrated, and such a degree of conservatism was certainly appropriate for an early boiling reactor built as an experiment. It is not appropriate for a commercial power reactor. Such a reactor is ordinarily built to a specified power capacity, and for economic reasons it should be the least reactor which will yield that capacity reliably and safely. Further, in such a practical machine, other factors which limit power output will, in the economic design of the reactor, be harmonized with the supposed stability limitations and will, thereafter, probably limit the reactor capacity to the design value. For example, in order to minimize fuel cost, the UO_2 fuel pellets will probably be made as large as is permissible within the limitations of center melting at the design power density. Thereafter the fuel temperature will limit the power output even if operation of the reactor demonstrates that a considerably higher output would be permissible from the standpoint of stability.

In summary, although boiling reactors can be designed on the basis of present knowledge to compare favorably with other reactor types, the lack of complete understanding of stability does prevent design optimization. The deficiency affects not only the design of specific reactors but also the forecasting of the ultimate value of the reactor type; it also affects the choices between types of boiling reactors (e.g., forced circulation versus natural circulation) for a given application. For these reasons, new information on boiling-reactor stability is always of considerable interest to the reactor designer.

Experimental Boiling Water Reactor

References 1 to 3 are a series of reports related to the EBWR and to the transfer-function measurements which were made on that reactor. Reference 1 describes the measurements themselves; reference 2 describes the major dynamic characteristics of an EBWR type reactor from the theoretical point of view and derives approximate expressions for the transfer functions of the important contributors to the dynamic behavior. In reference 3 the theoretical approach of reference 2, with some modification, is applied to an analysis of the measured EBWR transfer functions; by a semiempirical approach, rational values for the major dynamic components are derived.

The transfer function of a reactor is simply the frequency response of the reactor power, with respect to amplitude and frequency, to a sinusoidal oscillation of reactivity, which is produced in this case by the oscillation of a control rod. As is well known from other applications of frequency-response techniques, such measurements can be used to indicate the frequency regions of potential instability of a dynamic system when the system is operating at a gain lower than that which marks the threshold of instability. Such analyses can, of course, also be used as a basis for inferring the more fundamental dynamic characteristics of the system.

As has been implied earlier, the dynamic response of a reactor to an impressed reactivity oscillation can be considered to be made up of two major components. The first of these is simply the response of the neutron chain reaction to the oscillation of reactivity. For small oscillations to appear in the frequency range of practical interest, it depends only on the delayed-neutron characteristics and the effective prompt-neutron lifetime. All other dynamic effects result from reactivity changes, which themselves are caused by the changes in reactor power, and add to or subtract from the impressed reactivity oscillation. These effects are properly thought of as feedback effects that may modify the reactor power response drastically from the response of the "zero-power" neutron chain reaction.

The relation between the chain-reaction response and the feedback effects can be expressed diagrammatically by the usual conventions of servomechanism theory as in Fig. 12. In this diagram, G represents the complex response, or the transfer function, of the neutron chain reaction, and H represents the net power-reactivity transfer function. That is to say, H is the transfer function which shows the combined

effect of all the processes that may result in a change of reactivity because of a change in reactor power. In general, the gain of all these feedback effects is proportional to the operating power level. Consequently, since the kinetic behavior of the neutron chain reaction is independent of power level, it is a relatively simple matter to determine the G function explicitly simply by measuring the reactor transfer function at such sufficiently low power that the feedback effects are negligible. For this reason the G function is often referred to as the "zero-power" transfer function of the reaction. If G has been so determined, and if a further transfer-function determination is made at an appreciable power level, then it is theoretically possible to determine the H function for that power level by separating the G function from the reactor transfer function. The equation which relates the reactor transfer function, P, to G and H is

$$P = \frac{G}{1 + GH}$$

It is to be understood that this is a symbolic equation; since each point of each transfer function (at a given frequency) is specified in terms of an amplitude and a phase relation, the indicated mathematical manipulations are to be carried out in the complex plane.

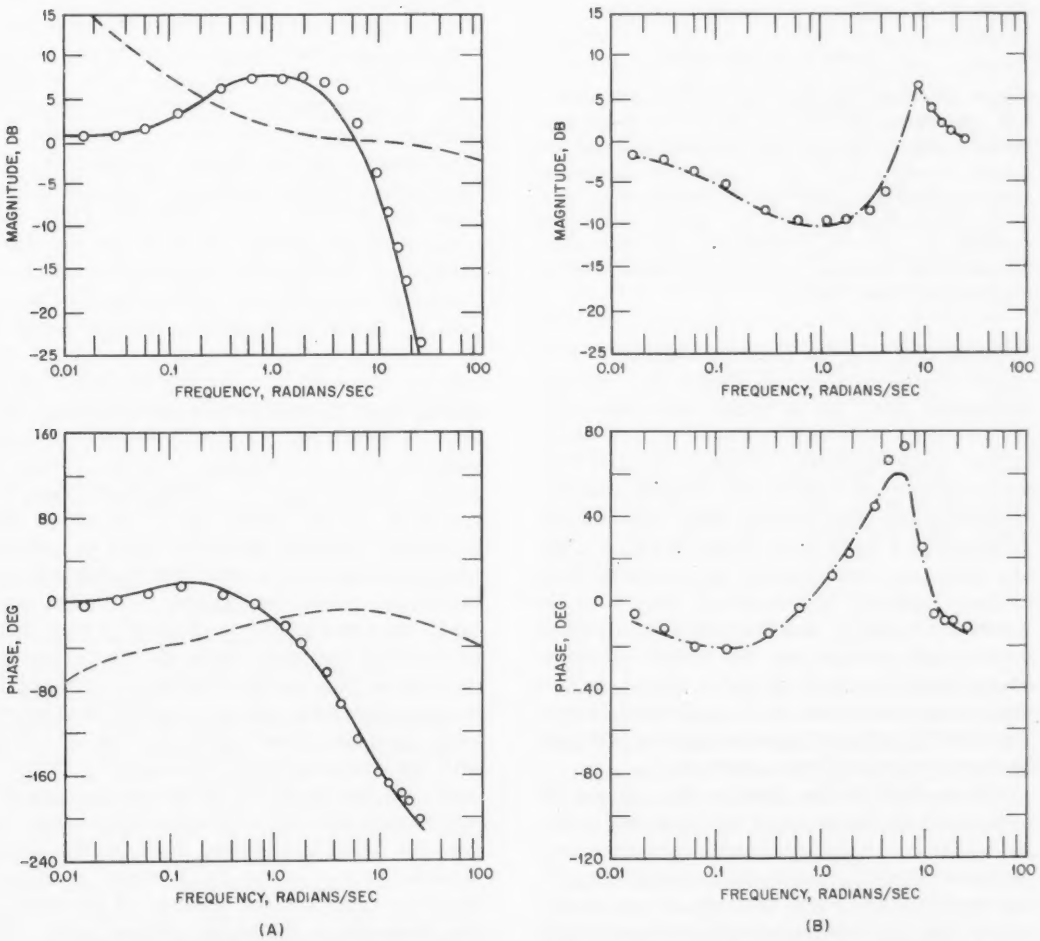

Figure 13—EBWR transfer functions, 20 Mw(t), 300 psig. ——, feedback transfer function (H). ----, zero-power transfer function (G). —·—, power transfer function (P). Data are taken from reference 3.

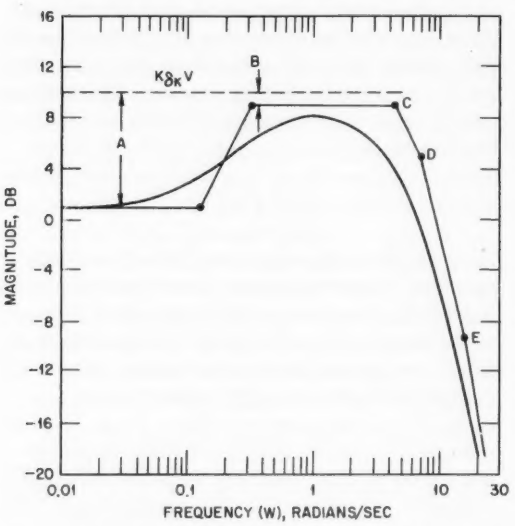

Figure 14—Bode diagram for EBWR feedback function, 20 Mw(t), 300 psig. *A*, reduction of apparent steam coefficient of reactivity by "void flashing" and change of nonboiling length. *B*, reduction of apparent steam coefficient of reactivity by "void flashing" only. *C*, $w = 1/T_h$, where T_h is a fuel heat-transfer time constant. *D*, $w = 1/T_{pv}$, where T_{pv} is a fuel heat-transfer time constant. *E*, $w = 1/\tau$, where τ is the steam transit time constant.[3]

Needless to say, the determination of H by the above procedure requires rather accurate experimental data, for in some cases the value of H results from rather small differences of rather large numbers. Reference 3 discusses this problem as well as the method used for smoothing the experimental data. The results, although they may have some imperfections, are extremely useful since they relate directly to those dynamic factors which determine the reactivity feedback, and they allow one to gain a considerable insight into the details of the dynamic behavior and, to some extent, to test theoretical predictions of the individual factors. The results of these procedures are illustrated by Figs. 13 and 14 (from reference 3).

The curves on the right in Fig. 13 are the experimentally determined reactor power transfer function. The plotted points are those experimentally determined. On the left in Fig. 13, the derived feedback function H is shown. Again, the experimental points are marked by circles. On these same grids are plotted, as dashed lines, the zero-power or chain-reaction transfer function G. The solid lines of the H function are derived from a semiempirical theory, in which specific physical components of the feedback dynamics are recognized, and the form of their behavior is calculated from first principles; but, the particular constants which enter the description of their behavior are chosen to yield a good fit with the experimental H function. The lines plotted for the reactor transfer function in Fig. 13 are those derived from the solid H curves.

An understanding of the effects taken into account in the derivation of the H function can be gained from Fig. 14. In Fig. 14, the amplitude of the H function has been replotted along with a straight-line approximation to the amplitude curve generally referred to as a Bode diagram. The straight-line approximation has the virtue of identifying certain individual feedback components and of marking on the frequency plot the frequencies which correspond to the inverse time constants characterizing those components. Starting from the left side of the figure and progressing toward higher frequencies, the components of the feedback which have been taken into account can be identified. First, note the dashed line marked $K_{\delta k}V$. $K_{\delta k}$ is the steam coefficient of reactivity expressed in dollars of reactivity per cubic foot of steam in the reactor core. V is called the power void coefficient. It is expressed as the steam content of the reactor and is expressed in cubic feet per megawatt of reactor power, multiplied by the operating power level in megawatts to give a factor consistent with the power-independent analysis. The product $K_{\delta k}V$ is simply the steady-state change in reactivity which would be produced by unit fractional change in the power level. $K_{\delta k}$ may be considered the steady-state steam coefficient of reactivity. Under the dynamic condition, however, the effect of this coefficient is very much reduced, as indicated by the difference between the dashed line and the left-hand portion of the straight-line approximation. This reduction results from two effects, both of which have to do with the change in reactor pressure with power level. As the pressure increases because of a power increase, the saturation temperature increases also; in addition, some of the steam already formed in the fuel channels must condense to raise the temperature of the water in the channels to the higher boiling point. This effect is referred to in reference 4 and in Fig. 14 as the "void flashing" effect. The second effect is a change in the nonboiling length

in the coolant channel. As the pressure increases, the subcooling of the water entering the coolant channels will be increased, and the average length of the nonboiling region in the fuel channels will increase appropriately. Conversely, if power were reduced, the pressure would fall, there would be some flashing of water to steam in the fuel channels, and the average length of the nonboiling region in the fuel channels would decrease. Both of these effects are counter to that of the primary steam coefficient of reactivity. If the power change in question were a step change which remained in effect indefinitely, then the pressure would, in the case postulated, eventually reach an equilibrium value, the total body of water would again reach thermodynamic equilibrium with the steam, and the effects on the steam content of the reactor would disappear except for a small residual effect on the length of the nonboiling region caused by the slight change in subcooling of the reactor feed water. That is to say, the effects discussed are not directly related to pressure per se, but they are related to the rate of change of pressure.

The effect on nonboiling length depends upon the introduction into the fuel channels of the subcooled recirculating water. If the frequency of oscillation is increased to a point at which the sinusoidal period is comparable with the recirculation time of the water, then the effect begins to decrease. This decrease is represented on the straight-line approximation by the line segment covering the frequency range from about 1.3 to 3.0 radians/sec. At higher frequencies the effect of variation of the nonboiling length has disappeared in the straight-line approximation, and the feedback magnitude is almost as great as $K_{\delta k} \times V$, being smaller only because of the residual steam flashing effect. This effect does not depend on the water recirculation but depends only upon the rate of change of steam pressure in addition to those variables which affect steam generation. The effect therefore persists to higher frequencies.

At frequencies of about 4.5 and 7 radians/sec, two time constants, T_h and T_{pv}, enter which introduce phase lags in the formation of steam. These two time constants include the effects of heat storage in the fuel plates as determined by the heat capacity in the plates and the heat flow characteristics which are determined both by the thermal conductivity of the plates and cladding and by the heat-transfer coefficient from fuel plate to water. However, the effects of thermal conductivity and heat-transfer coefficient are not identified explicitly. The thermal inertia identified by these time constants reduces the magnitude of the feedback function rapidly, as the frequency is increased. At a frequency of about 17 radians/sec, a further time constant, τ, enters as a further phase lag. τ is identified as the time constant related to the steam transit time in the reactor, that is, the time associated with the escape of generated steam from the reactor. At frequencies higher than about 20 radians/sec, the combined effects of thermal time lags and steam transit time have reduced the amplitude of the feedback function to a practically negligible point; at higher frequencies, the reactor transfer function (the right-hand side of Fig. 13) would be expected to be identical with the zero-power transfer function to within the limits of observation. For frequencies greater than about 20 radians/sec, the self-regulating characteristic of this boiling reactor is virtually absent.

Analyses similar to that represented by Fig. 13 are reported in reference 3 for a number of reactor operating conditions, and the time constants and associated feedback parameters are derived for the several operating conditions by making experimental fits to the feedback transfer functions. The data so derived are of considerable interest and should provide further insight into the behavior of the boiling reactor, even though a rather simplified picture of the feedback system has been employed and even though the method of empirically determining the quantitative characteristics does not give unique results.

BORAX Reactors

Reference 4 is a report on the operation of the BORAX-IV reactor and covers both the steady-state performance and the transient performance of the reactor. These experiments gain added significance because the reactor has many design characteristics in common with the previous BORAX reactors and because the effects of the specific design changes which were made are reasonably well isolated. The fundamental change made in the transition from the previous reactors to BORAX-IV was the change from a highly enriched uranium-aluminum plate type of fuel element to an element composed of thoria–

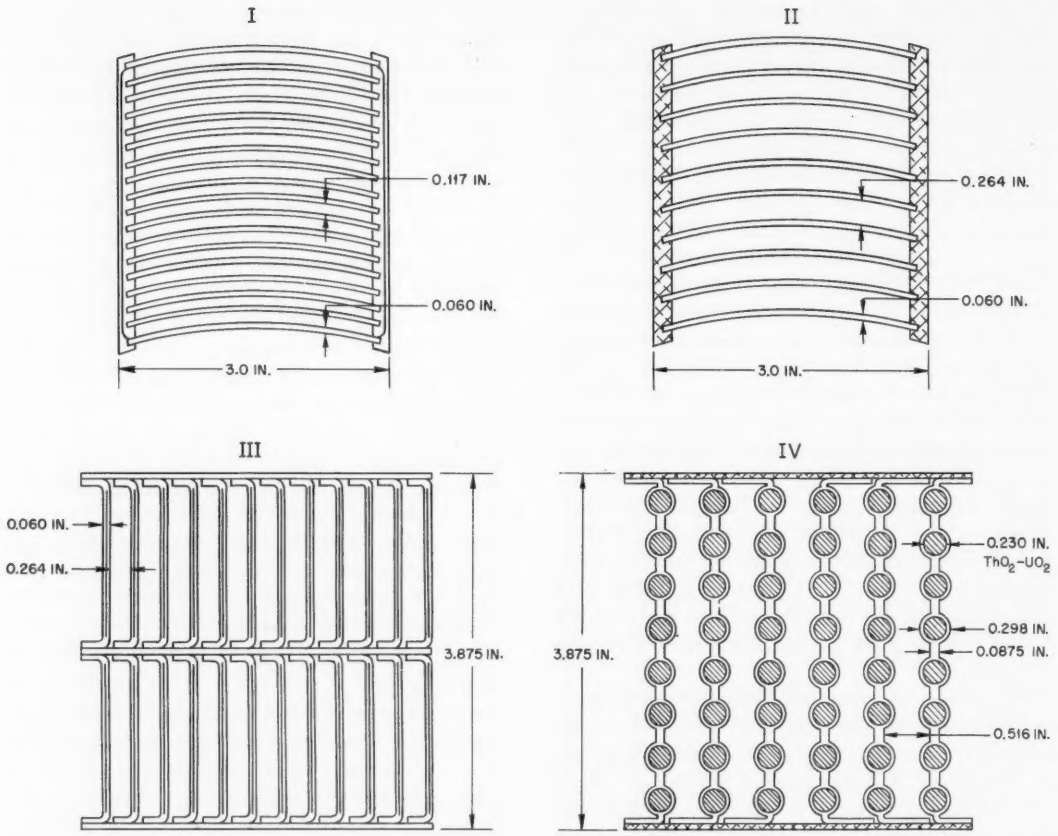

Figure 15—Fuel elements of the four BORAX reactors.

highly enriched urania pellets jacketed in aluminum. The additional heat capacity of the thoria diluent combined with the relatively low thermal conductivity of the thoria-urania sintered compact resulted in a thermal time constant which is several times that of the previous plate type fuel elements. A secondary result of the new fuel structure was a steam coefficient of reactivity which was rather highly negative (comparable to that of BORAX-I), even though the BORAX-IV core is relatively large and even though the neutron leakage is relatively low. The more negative void coefficient is due primarily to the high density of U^{235} in the core, which reduces the importance of the neutron absorption in H_2O, and to the resonance absorption in the thorium, which adds a negative component to the steam coefficient which was not present in the previous BORAX reactors. Cross-sectional drawings of the fuel elements used in the series of BORAX reactors (I to IV) are shown in relative scale in Fig. 15.

With regard to reactor stability, the most striking result of the experiments was the very large amount of excess reactivity which could be compensated by steam in stable operation at a pressure of 300 psi. For the highest power run, this amounted to about 6.9 per cent k_{eff} and gave a power output of 20.6 Mw(t) from a core consisting of 69 fuel elements. The power corresponded to a power density of about 69 kw/liter of coolant. Previous BORAX reactors had not been operated with more than 3 per cent reactivity compensated by steam, and it appeared evident in these reactors that further additions of reactivity would lead to instability, although the largest of the reactors (BORAX-III) was never taken to the actual point of instability.

The power performance of the series of BORAX reactors is summarized in Table X-1,

Table X-1 CHARACTERISTICS OF FOUR BORAX REACTORS[4-7]

	A	B	C	D	E	F	G	H
Reactor	Operating pressure, psig	Power density in core, kw/liter	Coolant vol. / Core vol.	Power density in coolant, kw/liter	Reactivity compensated by steam $(\Delta k_{eff}/k_{eff})$	D/E $\left(\frac{\text{kw/liter}}{\Delta k_{eff}/k_{eff}}\right)$	Steam coefficient of reactivity*	F × G, kw/liter of steam
BORAX-I	135	11	0.84	13	0.028	465	−0.24†	112
BORAX-II	300	27	0.702	38.5	0.030	1284	−0.10,† −0.19‡	128−244
BORAX-III	300	29	0.711	40.8	0.020	2040	−0.07,† −0.10‡	143−204
BORAX-IV	300			54.6	0.056	975	−0.28‡	273
BORAX-IV	300			68.7	0.069	1000	−0.28‡	280

*$(\Delta k_{eff}/k_{eff})$/(steam volume/coolant volume).
†From reference 5.
‡From reference 7.

which is derived from the data of references 4 to 7. It is quite evident that very substantial increases have been made in the maximum power density attainable, as was predicted after the earliest boiling-reactor tests. It should be noted that the BORAX-I results are not strictly comparable with the others, since that reactor was operated at 135 psi, whereas the later reactors were operated at approximately 300 psi. If the maximum power density in the coolant is divided by the amount of reactivity compensated by steam at that operating condition, the result reflects the variation in steam coefficient of reactivity from reactor to reactor. Thus the quantity increases progressively from BORAX-I to BORAX-III, reflecting the decreasing value of steam coefficient in this series of reactors. It was this progressive reduction in steam coefficient which accounted for most of the improvement in attainable power density in the series. In the case of BORAX-IV, however, the ratio drops appreciably, illustrating the fact that the higher power density of BORAX-IV was attained because of the higher permissible amount of reactivity compensated by steam and was attained despite the higher steam coefficient of reactivity. This is equivalent to saying that the higher power density resulted at least in part from greater reactor stability.

It appears, however, that the greater stability is not responsible for all the improvement in performance. If one takes the ratio (kilowatts per liter of coolant volume)(steam coefficient of reactivity)/(reactivity compensated by steam), the result should be the average number of kilowatts of heat generated per liter of steam contained in the core, and if the rate at which steam can flow out of the core were constant, one would expect this ratio also to be approximately constant. The last column of Table X-1 shows that this ratio increases gradually over the series of BORAX reactors as might be expected because of the increasing fuel-plate spacing over the series. The implication is that an increase in fuel-plate spacing increases the velocity of steam flow out of the core.

It must be stated that too much significance cannot be read into comparisons like those discussed above in which only the gross variables are taken into account. One significant factor which is not taken into account and which may have a large effect on the stability, as well as on the general thermal performance, is that the first three reactors were fueled with mixtures of fuel elements of rather widely different fuel loadings. In some cases this probably led to rather high peak-to-average power density ratios. Furthermore, the steam coefficients of reactivity are calculated values rather than measured values and are average values over the core rather than true effective values. The relation between average and effective values would be expected to vary over the series of reactors.

A rather extensive investigation of the stability of BORAX-IV at atmospheric pressures is also reported in reference 4. Although this condition, as an operating condition for power reactors, is not an interesting one, it is nevertheless worth investigating because the stability characteristics become poorer as pressure is decreased. Several theoretical studies of boiling-reactor stability have concluded that the stability characteristics of a reactor at atmospheric pressure are qualitatively different from those at high pressure and that no great concern

need be felt because the low-pressure characteristics are relatively poor.[8] It would, nevertheless, be comforting to understand in detail the low-pressure instabilities and to be able to predict the operating pressure at which they become insignificant and at which other effects become predominant.

It appears that, at atmospheric pressure, BORAX-IV can tolerate no greater reactivity compensation by steam than that tolerated by previous BORAX reactors. Indeed, the instability which has in the past been referred to as "chugging" was observed when the reactivity compensated by steam was no more than about 1.5 or 1.6 per cent, whereas BORAX-I had on occasion operated well above 2 per cent at atmospheric pressure without encountering instability. The power density attainable with a given amount of reactivity compensated by steam was, however, considerably higher for BORAX-IV than for BORAX-I, which was the only other reactor for which atmospheric-pressure power measurements were made. Reactor IV attained a power density of some 25 kw/liter of coolant when the reactivity compensated by steam was about 1.2 per cent. With this reactivity compensation, BORAX-I attained a power density of only about 8 kw/liter of coolant.

The transfer function of BORAX-IV was measured at atmospheric pressure over the power range from effectively 0 to 3.4 Mw(t). Although the measured transfer functions did not have the highest precision because of the necessity for using relatively crude equipment and because of the "noise" inherent in a boiling system, significant data were obtained which are summarized in Fig. 16. As reactor power was increased, a marked variation in the transfer function was observed. At powers of approximately 1 Mw and higher, a maximum was observed in the gain curve, corresponding to a damped resonance of the reactor power with the impressed reactivity oscillation. As power increased, the amplitude of the resonance increased, as did also the resonant frequency. The solid line in part A of Fig. 16 is the reciprocal of the gain at the resonant frequency as a function of reactor power. The gain is defined as the fractional increase in reactor power divided by the fractional increase in k_{eff} which produces

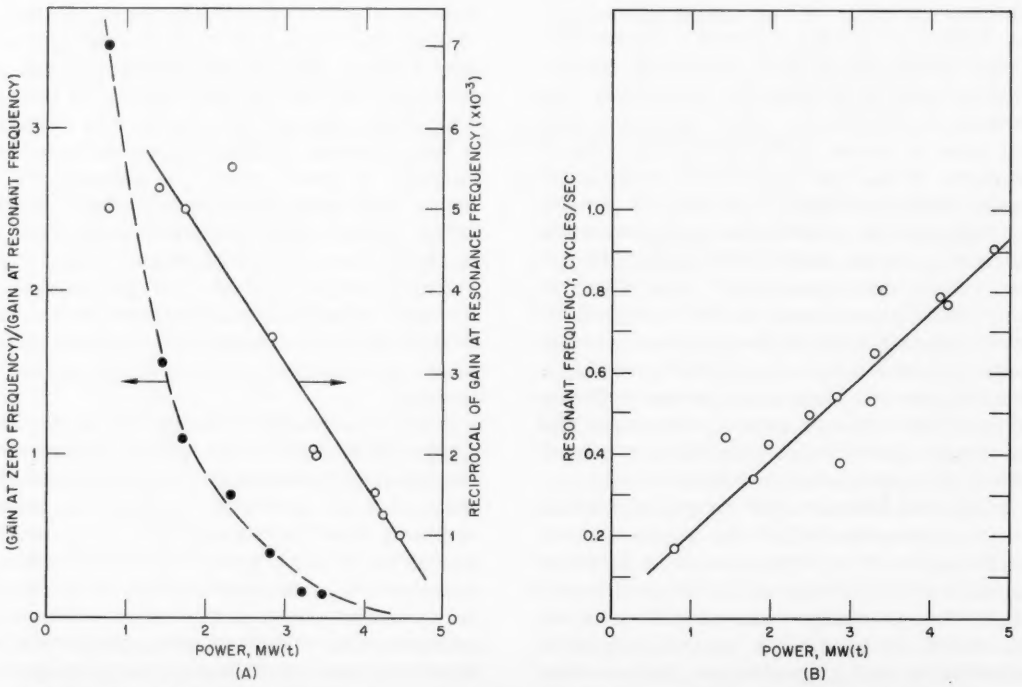

Figure 16—Behavior of gain and frequency of the transfer function with power for BORAX-IV at atmospheric pressure.[4]

the power change (gain = $(\Delta P/P)/(\Delta k_{\text{eff}}/k_{\text{eff}})$). The extrapolation of the line to zero reciprocal gain would mark the approximate power at which instability would be expected. The dashed line in part A of Fig. 16 shows the ratio of the gain at zero frequency to the gain at the resonant frequency. As reactor power is increased, the self-regulating effect of the steam production becomes more and more pronounced. That is to say, the gain of what may be considered the steam feedback loop in the self-regulating system of the reactor increases, and the net gain of the system, $(\Delta P/P)/(\Delta k_{\text{eff}}/k_{\text{eff}})$, decreases at the frequencies which are low enough to allow the self-regulating effect to operate as a stable, effective system. Consequently, the zero frequency gain of the system decreases as power is increased, and the ratio of the zero frequency gain to the resonant frequency gain decreases more rapidly than the reciprocal of the resonant frequency gain. Part B of Fig. 16 shows the resonant frequency as a function of reactor power. The very marked increase in resonant frequency with power is something that could not be adequately demonstrated by the observations which had previously been made on the self-excited oscillations of other reactors, and it demonstrates the usefulness of the oscillator technique in such studies. It seems probable that this change of resonant frequency may be an important manifestation of the basic physical processes involved and may make an important contribution to the understanding of stability in such a reactor.

Methods of obtaining reactor transfer functions other than by use of a reactivity oscillator were investigated. One of these methods called the ringing method is a well-known technique in other applications; the method consists simply of applying a sudden impulse or perturbation to the system (in this case a rapid insertion of reactivity) and observing the transient response of the system. A transfer function can be derived by appropriate observations and mathematical manipulations of the transient. A second method[9–12] is to derive the transfer function from the autocorrelation function for the normal fluctuations in the reactor power which are caused by the boiling "noise" in the reactor. In essence this method is much the same as the ringing method, but the perturbations which excite the ringing are the boiling fluctuations in reactivity, and the autocorrelation analysis is necessary in order to separate the response of the reactor to a typical impulse of this kind from its response to previous and subsequent impulses. The methods may be useful for reactors which are not equipped with suitable reactivity oscillators.

Review of ANL Experience

Reference 7 contains a review of experimental information obtained from the boiling reactors which have been operated by Argonne National Laboratory and also contains a theoretical consideration of the stability question. The experimental section of the report includes a useful collection of information on the design characteristics and observed behavior of the EBWR and the BORAX reactors, much of which is not available elsewhere. This section of the report also performs a useful service in redirecting attention to some of the dynamic characteristics, such as the boiling fluctuations of power and the small-amplitude oscillations which characterize the boiling reactor when its power level is well below the stability limit. In this connection, Table X-2, which summarizes some of the phenomena by which one might evaluate the degree of stability of a reactor, also gives an indication of the characteristic behavior that one might observe in the stable operation of a typical natural-circulation boiling reactor. The values given in the table were those observed for the EBWR at a thermal power of 45.6 Mw and an operating pressure of 600 psig.

Table X-2 MEASURES OF EBWR STABILITY[7]

ζ from ringing tests	+0.13
P_R for $R = 1.0364$	0.34 sec^{-1}
Root-mean-square value of p, i.e., $\sqrt{\overline{P^2}}$ (includes noise as well as the dominant oscillatory frequency)	0.83 Mw
Half-width of the resonance in the power spectrum from autocorrelation techniques	18 counts/sec
Properties of the transfer function G:	
Value at resonance	55.4 db
Half-width of resonance	0.38 counts/sec

Some of the symbols of Table X-2 require explanation. If a "ringing" test is made on the reactor by applying a sudden reactivity increase, a power transient of approximately the form

$$P(t) = (\text{constant}) \exp(-\zeta wt) \sin wt$$

may be expected. ζ is the damping constant for the transient oscillation and, as may be seen from Table X-2, had a value of 0.13 for the conditions in question. When the reactor is operating steadily, the power is subject to fluctuations from the "boiling noise" and, at times, from the effects of oscillations. P_R is the probability per second that the power will exceed a value R times the average power. The symbol p is used to designate the power fluctuation, that is, the instantaneous deviation from the average value. Statistical analysis of these deviations reported in the reference shows that their distribution is Gaussian. The root-mean-square value of 0.83 Mw for p is 1.8 per cent of the average power. The magnitude of the reactor transfer function at the resonance frequency is given as an absolute quantity in decibels. The amplitude of the transfer function is the ratio of the fractional amplitude of the power oscillation to the fractional amplitude of the reactivity oscillation, $(\Delta P/P)/(\Delta k_{\text{eff}}/k_{\text{eff}})$, and the magnitude in decibels is equal to 20 $\log_{10}(\Delta P/P)/(\Delta k_{\text{eff}}/k_{\text{eff}})$. This absolute specification of the transfer-function magnitude is not universally used. For example, in reference 3, the 0-db gain is defined as the amplitude of the zero-power transfer function in the region of its plateau (at a frequency of approximately 20 radians/sec in Fig. 13). The absolute amplitude of the transfer function in the plateau region is, for any reactor, $1/\beta$, where β is the delayed neutron fraction. Thus $1/\beta$ is approximately 140 or about 43 db. The magnitude of the transfer function at the resonance point quoted in Table X-2, 55.4 db, is therefore about 55.4 – 43 = 12.4 db above the zero-power plateau value. Thus the observed fractional amplitude of the power oscillation at the resonance frequency was higher by a factor of about 4.2 than the fractional amplitude of the zero-power oscillation which would have been produced by the same reactivity oscillation.

The theoretical section of reference 7 treats the derivation and application of a theoretical transfer function which neglects effects caused by pressure variations (and therefore is limited in applicability to the higher frequencies) but which treats the heat-transfer, steam-production, and steam-escape processes in more detail than was done in reference 3. In particular, the boiling and nonboiling regions of the fuel channels are treated separately. The theoretical transfer functions for the EBWR and the BORAX-II, -III, and -IV reactors are computed numerically for various operating conditions. The EBWR computations agree reasonably well with the experimental amplitude transfer functions. The BORAX-II and -III calculations show resonances at about 40 radians/sec. It is not obvious whether the calculation indicates an impending instability for these cases, but it can be said that the computed frequencies are considerably higher than the observed oscillation frequencies just before the onset of instability in these two reactors. The application of a common stability theory to a series of reactors is, however, a very worthwhile endeavor, for it will be difficult to have complete confidence in the prediction of stability until a consistent theory is available which explains the stability limits of all those boiling reactors which have been investigated.

Reference 13 is a theoretical study of the dynamics of boiling reactors which treats in some detail the dynamics of heat flow, steam flow, and the flow of water in the fuel channels and in the recirculation path. Reference 13 does not consider the effects of pressure changes in the steam space above the top reflector of the reactor; in fact, the reference is applied primarily to the understanding of the unpressurized BORAX and SPERT experiments. It has generally been thought that the hydrodynamic forces would be most important in such low-pressure reactors, and, consequently, such an application of the theory is a logical one. The analysis is not made by the transfer-function approach, but, rather, the analysis sets up the appropriate equations for the reactor power and solves them by machine computation for specific transient operational cases such as the sudden or ramp addition of reactivity or the sudden addition of cold water. In the case of ramp addition of reactivity to the mathematical model of the subcooled SPERT reactor, the response of the reactor appeared to be smooth, and no instability was found up to the limit of the reactivity addition which amounted to more than 9 per cent k_{eff}. This, of course, is contrary to the observed SPERT behavior. It is postulated in the reference that the unstable behavior of SPERT and BORAX-I at atmospheric pressure was due primarily to a hydrodynamic instability connected with the natural-circulation boiling, which, although it certainly would couple with the other dynamic factors in the reactor, could produce an oscillation in steam content of the

reactor even without such coupling. Such oscillation of the steaming rate has been observed in laboratory tests on boiling channels but has been observed only at steam contents considerably higher than those thought to exist in the BORAX and SPERT reactors at their instability points. The reference considers this instability from the theoretical standpoint and shows that it becomes a possibility when the steam content of the channel becomes high enough that a further increase in steam content will lead to a decrease of recirculation velocity, because the increment of flow resistance resulting from the extra steam content is greater than the corresponding increment in recirculation head.

The reference also makes some applications of the dynamic theory to a heavy-water boiling reactor; the reference also points out some possible differences between heavy-water boiling and light-water boiling reactors. It suggests that, whereas the closely packed fuel channels of the light-water reactor would be expected to act in concert with respect to hydrodynamic instabilities, then the segregated channels of some heavy-water boilers might be expected to act individually.

References

1. J. A. DeShong, Jr., Power Transfer Functions of the EBWR Obtained Using a Sinusoidal Reactivity Driving Function, ANL-5798, January 1958. (Unclassified AEC report.)
2. Eric S. Beckjord, Dynamic Analysis of Natural Circulation Boiling Water Power Reactors, ANL-5799, March 1958. (Unclassified AEC report.)
3. J. A. DeShong, Jr., and W. C. Lipinski, Analyses of Experimental Power-Reactivity Feedback Transfer Functions for a Natural Circulation Boiling Water Reactor, ANL-5850, July 1958. (Unclassified AEC report.)
4. B. S. Maxon, O. A. Schulze, and J. A. Thie, Reactivity Transients and Steady-state Operation of a Thoria-Urania-fueled Direct-cycle Light-water-boiling Reactor (BORAX-IV), ANL-5733, February 1959. (Unclassified AEC report.)
5. J. R. Dietrich, H. V. Lichtenberger, and W. H. Zinn, Design and Operating Experience of a Prototype Boiling Water Power Reactor, *Proceedings of the International Conference on the Peaceful Uses of Atomic Energy, Geneva, 1955*, 3: 56 (1955).
6. J. R. Dietrich and D. C. Layman, Transient and Steady State Characteristics of a Boiling Reactor. The BORAX Experiments, 1953, AECD-3840, February 1954. (Unclassified AEC report.)
7. J. A. Thie, Dynamic Behavior of Boiling Reactors, ANL-5849, May 1959. (Unclassified AEC report.)
8. J. W. Weil, ed., Boiling Water Reactor Stability, GER-1468, General Electric Co., 1957.
9. M. N. Moore, The Determination of Reactor Transfer Functions from Measurements at Steady Operation, NAA-SR-1972, Aug. 15, 1957. (Unclassified AEC report.)
10. M. N. Moore, The Determination of Reactor Transfer Functions from Measurements at Steady Operation, *Nuclear Science and Engineering*, 3(4): 387 (April 1958).
11. Charles Erwin Cohn, Determination of Reactor Kinetic Parameters by Pile Noise Analysis, *Nuclear Science and Engineering*, 5(5): 331 (May 1959).
12. J. A. Thie, Statistical Analysis of Power-reactor Noise, *Nucleonics*, 17(10): 102 (October 1959).
13. J. A. Fleck, Jr., The Dynamic Behaviour of Boiling Water Reactors, University of California Radiation Laboratory, Livermore, California, May 1959.

Report of the Fluid Fuel Reactors Task Force

In the fall of 1958, the U. S. Atomic Energy Commission organized the *Ad Hoc* Advisory Committee on Reactor Policies and Programs. The Committee reviewed the AEC's civilian power program and recommended immediate and long-range programs. One of the Committee's recommendations is quoted: "The aqueous homogeneous, molten-bismuth, and molten-salt reactors all offer the possibility of reducing the cost of the fuel cycle, and the last two offer the possibility of high-temperature operation. These three concepts for power reactors should be critically compared and work concentrated on the concept that appears the most promising."

In accordance with this recommendation, the Evaluation and Planning Branch of the Civilian Reactors Office, Division of Reactor Development, organized the Fluid Fuel Reactors Task Force in January of 1959. The Task Force had as its assignment and objective the comparison of three reactor concepts: the aqueous homogeneous reactor (AHR), the molten-salt reactor (MSR), and the liquid-metal-fuel reactor (LMFR). The comparison was to determine, as follows: the present state of development and technical feasibility; the technical feasibility of breeding; the cost of power for an optimized system; and the research and development program necessary to achieve this cost. In order to study the concepts, it was necessary to have reference designs prepared. This design work was done by three project groups, one for each concept. The report of the Task Force has recently become available.[1]

Reference Designs

1. *Molten-salt Reactor.* The reference-design molten-salt reactor is an INOR-8 vessel containing a graphite assembly 12.25 ft in diameter by 12.25 ft high, through which molten-salt fuel flows in vertical channels. The fuel salt is a solution composed of 0.3 mole % UF_4, 13 mole % ThF_4, 16 mole % BeF_2, and 70.7 mole % Li_7F. The fuel salt is heated from 1075 to 1225°F in the core and is circulated from the reactor vessel to four primary heat exchangers by four fuel pumps. A barren coolant salt is used as the intermediate heat-exchange fluid, which superheats and reheats steam in a Loeffler boiler system. The reactor develops 760 Mw of heat. By using 2000-psig, 1000/1000°F steam in a reheat cycle, the net electrical output is 318 Mw(e); the net efficiency is 41.9 per cent.

2. *Liquid-metal-fuel Reactor.* The liquid-metal-fuel reference-design reactor is fueled with a slurry containing approximately 3 wt.% ThO_2-UO_2 in bismuth. The reactor core vessel is 14 ft in diameter and 14 ft high, containing a graphite core and reflector assembly. The fuel slurry is heated from 750 to 1050°F through channels in the reactor core and is circulated through three primary heat exchangers by three primary variable-speed pumps. The reactor develops 825 Mw of heat. Sodium is used as the intermediate heat-transfer coolant. The steam from the secondary heat exchangers supplies a non-reheat, 2000-psi, 1000°F steam turbine which produces 312 Mw of net electricity. The net efficiency is 37.8 per cent.

3. *Aqueous Homogeneous Reactor.* Three concepts of aqueous homogeneous reactors were presented to the Task Force: a two-region, solution-core, slurry-blanket reactor; a two-region, slurry-core, slurry-blanket reactor; and a one-region slurry reactor. Heavy water is the fuel carrier and moderator in all cases. The design group chose the two-region, solution-core, slurry-blanket reactor as the reference design. This reactor consists of a 4-ft-diameter by 12-ft-long zirconium alloy core tank in an 8-ft-diameter by 16-ft-long pressure vessel. A 5 g/liter solution of uranyl sulfate in heavy water is circulated through the core of the reactor, and a thoria slurry containing 1000 g of thorium per liter is circulated through the blanket. Heat is removed from the core solution in two circulating systems, each of which contains

a steam generator and a circulating pump. The blanket slurry is recirculated through one similar heat-removal circuit. Steam is generated at 400 psia and 435°F and sent directly to the turbogenerator. The heat-generation rate for one reactor is 380 Mw(t): 320 Mw(t) in the core and 60 Mw(t) in the blanket. Three reactors provide steam for one turbogenerator in the reference station to produce 317 Mw(e) net. The slurry-fueled reactors are similar but larger; for each type, one 1140-Mw(t) reactor satisfies the requirements of the reference station.

Present State of Development and Technical Feasibility

For fluid-fuel reactors, the critical factors are fuels and their containers. Table XI-1 lists estimated technical difficulties for the three systems. The larger ratings represent smaller probabilities of technical success.

Table XI-1 RELATIVE TECHNICAL DIFFICULTIES—FUELS AND MATERIALS[1]

	AHR			
	Solution core (reference)	Slurry core (alternate)	MSR	LMFR
Materials:				
Internal	5	2	2	1
External	3	2	1	3
Total materials	8	4	3	4
Fuel	7	5	2	4
Total	15	9	5	8

The internal material for the MSR and LMFR is graphite, and the AHR uses Zircaloy. The basic container and piping for the AHR is INOR-8 (79 per cent Ni, 12 per cent Mo, 7 per cent Cr, 5 per cent Fe), whereas the LMFR employs Croloy and the AHR employs stainless steel. The relatively poor rating for the AHR on internal structure, a value of 5, comes from the difficulty of assuring integrity of the Zircaloy core tank for all operating conditions.* The LMFR is penalized by mass transfer in the external piping loops while stress-corrosion cracking and hydrogen embrittlement of stainless steel is a problem on the AHR. The low (numerical) rating for the MSR on internals and externals is due to the good corrosion and mass-transfer properties of INOR-8 in the presence of fused salts.

The MSR has, in addition, a good rating for fuel, principally because its fuel is a solution. Both the AHR and LMFR have slurry problems, the magnitude of which "can hardly be defined at this time." The rating of 7, assigned to the solution core of the AHR, is caused by the extreme care necessary to maintain the fuel solution within proper chemical control to prevent damage to the Zircaloy core tank. The alternate AHR, with a slurry core, is in a somewhat better situation, since corrosion of Zircaloy in the slurry case seems to be substantially less than in the case of the solution fuel. The slurry fuel for the AHR, however, is considered a more difficult problem than that of the LMFR (5 versus 4) due to the fact that the aqueous slurries have faster settling rates than the liquid-metal slurries. On the basis of Table XI-1, the MSR has been rated as the "best possibility" for developing satisfactory fuel and containing materials.

Maintenance is cited as the most important factor influencing the practicability of any of the three concepts. The problem basically arises from the fact that the fluid-fuel reactor circulates a highly radioactive stream of fuel around the plant. The aqueous homogeneous reactor experiments have demonstrated many remote maintenance techniques employing water as a shield (wet maintenance), but the feasibility of dry maintenance has not been proven. The large plants under consideration would consist of floors of equipment stacked one above the other; successful maintenance would be contingent upon remotely operated robots, manipulators, and other devices. Another maintenance technique would be to spread the plant out on one floor, allowing overhead access—a costly procedure. It is stated that: "The liquid-metal, molten-salt, and aqueous homogeneous concepts are not feasible unless remote welding or substitute methods of closure are perfected." Another difficult problem, as yet unsolved, is to provide remote inspection of the remotely made closures. The MSR and LMFR have an advantage over the AHR in that the solid fuels, when cool, retain most of the fission products.

A considerable discussion of hazards and containment is presented in reference 1. The AHR is considered to be potentially the most hazardous system because of the large amount

*See the section on the Homogeneous Reactor Test, p. 58, for additional details.

of energy stored in the primary system at the operating condition. The AHR also produces radiolytic gas, an explosion hazard, and is more susceptible to nuclear instabilities arising from hydrodynamic flow perturbations. The latter is caused by the fact that the flow is directed through the entire AHR core, whereas the other systems employ flow in channels, thereby minimizing hydrodynamic fluctuations. The ability of frozen metallic and salt fuel to retain many fission products also is an advantage should an accident occur.

The last area of technical feasibility discussed[1] is chemical reprocessing of fuel. In this area there are some differences of opinion; these differences primarily concern the location of the processing plant (on-site versus off-site) and the amount of process costs. The AHR employs the Thorex process, so modified as to maintain the desired purity of the heavy water. The MSR uses the fluoride volatility process, and the LMFR uses a modified Thorex process.

Technical Feasibility of Breeding

For comparison three kinds of systems can be defined, as follows:

1. Converters (conversion ratio <0.95)
2. "Hold own" breeders (conversion ratio ≅1)
3. Doublers (doubling time <20 years)

The need for these various kinds of breeder reactors depends on how rapidly the production of nuclear power expands, on the status of uranium reserves available to this country, and on the degree of fuel utilization available in other reactors which may be in operation.

The degree of breeding, as measured by the breeding ratio or conversion ratio, depends on neutron utilization; of the three concepts, the AHR makes the best showing since it can reduce parasitic losses to a minimum. The optimum breeder reactors were found to be two-region machines; a one-region breeder was technically feasible but was of too large a size (physical and electrical) to be considered very attractive. Of the three concepts, only the AHR could be considered a doubler, the other two being, at best, hold owns in their present forms. The possibility of making the MSR and LMFR into doublers by reducing the fuel inventory by means of internal cooling has been considered. The externally cooled reactors are penalized by having large amounts of fuel in the primary circuit outside the core. The size of the external circuit is affected strongly by considerations of remote maintenance and thermal stress. If the primary heat exchanger could be incorporated in the core structure, the resulting internally cooled reactor could have a reduced fuel inventory and, hence, a shorter doubling time if the breeding ratio remained constant. This is not, however, an easy development. If it were successful, the resulting reactors might have doubling times roughly equal to that presently predicted for the AHR.

The above conclusions are predicated on a value of 2.28 for η (number of neutrons produced per neutron absorbed) of U^{233}. The feasibility of thermal breeding is affected strongly by the value of η, not only at thermal but at epithermal neutron energies, since the MSR and LMFR have substantial amounts of nonthermal fission. British measurements in DIMPLE and GLEEP have indicated considerably lower values of η for U^{233}. (For a more detailed discussion see *Power Reactor Technology*, 2(2): 16 (March 1959).) However, recent U. S. results derived from critical experiments[2] support the thermal value 2.28 or a slightly higher one. Reference 1 concludes that all the fluid-fuel systems could probably at least be hold own breeders, even with the uncertainty in η, since, at an η value of 2.28, conversion ratios were 1.05 for the LMFR and MSR and 1.07 to 1.10 for the AHR.

Cost of Power

The cost studies were done to compare the relative cost potential of the three reactor systems, and it is stated that the cost data should not be compared with costs of conventional or other nuclear plants, since the emphasis in the studies was placed on relative, rather than absolute, numbers. Table XI-2 lists the power costs presented by the Task Force.

As indicated previously, the design groups disagree with the Task Force on chemical processing costs for the MSR and LMFR. The LMFR project estimates that processing can be done for "much less than the Task Force estimates," and the MSR project estimates are about 1 mill lower on processing costs. Although, if correct, these would place the nonaqueous reactors in an even more advantageous position costwise, the Task Force states that the differences in power-cost estimates among the three concepts are so small in relation to the probable accuracy of the estimates that they are not considered a de-

Table XI-2 SUMMARY OF POWER COSTS
(FOR REFERENCE REACTORS: 333 Mw(e), GROSS)

	Mills/kw-hr		
	LMFR	MSR	AHR
Power-plant investment	5.72	6.24	6.70
Chemical- and waste-disposal-plant investment	0.71	0.71	0.89
Fuel inventory use and burn-up	1.36	1.37	0.90
Chemical-plant operation and maintenance	0.76	0.76	0.96
Power-plant operation and maintenance	1.46	1.57	1.66
Total power costs, gross	10.0	10.7	11.1
Total power costs, net	10.7	11.1	11.5

termining factor. It should be pointed out that the AHR reference design is for a breeder, whereas the other two reactors are converters.

Research and Development Programs

The time and cost estimates for research and development programs are given in Table XI-3.

program, to be known as the Thermal Breeder Reactor Program, has been assigned to the Commission's Oak Ridge Operations Office.

The new program has as its objective the development of a thermal breeder reactor capable of converting thorium to fissionable fuel material at a doubling time of not more than 25 years.

The new program also involves a reorientation of work on the Fluid Fuel Reactor Program previously conducted for the Commission by the Brookhaven National Laboratory, Upton, N. Y., and The Babcock & Wilcox Company, Lynchburg, Va., on the Liquid Metal Fuel Reactor (LMFR) concept and by the Oak Ridge National Laboratory, Oak Ridge, Tenn., on the Aqueous Homogeneous Reactor (AHR) and Molten Salt Reactor (MSR) concepts. Much of the work on these projects has been directed toward the development of reactors of these concepts for the production of economic electric power. During Fiscal Year 1960, research and development on the AHR, MSR, and LMFR concepts, except as applicable to the new program, will be discontinued and a transition of financial support made to the new program.

The Commission's decision to reorient the Fluid Fuel Program and toward implementation of the

Table XI-3 TIME AND COST ESTIMATES

	AHR			MSR			LMFR		
	Start	End	Cost, 10^6 dollars	Start	End	Cost, 10^6 dollars	Start	End	Cost, 10^6 dollars
R&D for reactor experiment		July 1963	18		July 1963	19		April 1962	14
Design, construction, and operation of reactor experiment	July 1961	July 1966	15	July 1959	December 1965	18		September 1964	14
R&D for prototype	1962	1967	35	1963	1968	35		1964	17
Design, construction, and operation of prototype	1964	1969	59	1965		50	1963	1971	45
R&D for full-scale plant	1968	1971	5	1968	1971	Not given	1965	1969	10+
Total			132			122(+?)			100+

Conclusions

With the completion of the Task Force study, evaluation of the fluid-fuel concept, as compared with other power reactor concepts, should be possible. The following quotations, taken from an AEC press release, outline a new program to develop thermal breeder reactors:[3]

> "The Atomic Energy Commission has initiated a long-range program to develop effective thermal breeder reactors which would make full use of the latent energy in thorium. Responsibility for the

Thermal Breeder Reactor Program was based on the results of a study by a special task force of scientists and engineers convened by the Commission in January 1959 to make a comparison of the reactor concepts included in the Fluid Fuel Program. As a result of task force estimates of the power costs of large-scale fluid-fuel reactors and on the cost and scope of research and development compared with that of other reactor concepts in advanced stages of development, the Commission concluded that there is little incentive for further development of fluid-fuel reactors as an approach to the attainment of low-cost nuclear power in the near

future. Therefore the Commission decided to reorient its fluid-fuel effort toward the use of the latent energy in thorium and natural uranium through a long-range development program. Because all three of the fluid-fuel reactor systems were found by the task force to be potentially capable of development as breeder reactors, the new Thermal Breeder Program may include one or more of the concepts included in the Fluid Fuel Program.

In the initial phases, the new program will be a basic research and development effort and will include an evaluation of reactor technology to determine the most promising type of thermal breeder reactor for continued long-range development. Any work continued on present fluid-fuel reactor concepts will be conducted in the framework of the broader Thermal Breeder Program.

The Homogeneous Reactor Test

The AHR concept was reviewed in a previous edition of this publication.[4] Since that review, additional technical information has been accumulated pertinent to the reactor type, the data coming from the Homogeneous Reactor Test (HRT) operations and supporting development work.[5–8] The previously discussed Task Force report cited the materials and fuel stability problems of the AHR as being major problems, and therefore this discussion will be oriented toward those areas.

The first power run of the HRT, run 13, was started on Feb. 7, 1958. This run was initiated without any copper recombination catalyst in the fuel so that recombination rate constants could be evaluated as copper was added. High stainless-steel corrosion rates were experienced (up to 166 mils/year), but these were reduced to about 1 mil/year in subsequent runs by the addition of copper sulfate and an increase in the oxygen feed to the stream. Run 13 was terminated on February 13 when the nickel concentration became too high for reliable chemical analysis. Run 14 was initiated with fresh fuel on March 24; during the intervening month, about 1000 ft of electrical wiring was replaced due to faulty insulation. The wet maintenance philosophy made this possible without a single case of personnel overexposure. On April 4, the power was increased to the nominal design value of 5 Mw(t). After 0.5 hr at this power a leak developed between the core and blanket regions of the reactor through the Zircaloy core tank, and the reactor was shut down. The leak was subsequently determined to be a nearly round hole between 1 and 2 in. in diameter at the elevation of the weldment of the 30- and 90-deg flow transition cones at the bottom of the core tank. Mounted in these transition cones, perpendicular to the flow direction, were a total of nine Zircaloy flow-diffuser screens. Probing revealed that the first, second, and fifth screens were not attached to the core. Runs 15 and 16 were undertaken to establish the feasibility of operating the reactor in the damaged condition with fuel in both the core and blanket regions. These runs proved that such operation was feasible.

During the several runs, power surges had been experienced; the most drastic run was from a power set point value of 3.8 to 5.6 Mw. In addition, chemical analysis of the fuel stream showed that the concentration of uranium in circulation was erratic and did not correspond to the amount that should have been present by material balance. The amount of "lost" uranium appeared to increase with increasing power. Run 17 was undertaken to examine these problems further and to expose corrosion samples that were placed in the core and blanket regions prior to the run.

At the end of the run it was ascertained that 22 of the original 48 corrosion specimens had become separated from the titanium sample holder and had fallen onto the top diffuser screen. Severe corrosion was observed on the top screen and adjacent core region, and a hole cutter was used to cut 2-in. samples out of the top six screens. It was concluded[5] that:

1. Localized sections of the titanium specimen holder had been heated to a temperature above the melting point during reactor operation, causing a reaction between the holder and the steam–heavy water environment.

2. When the heat source (probably a deposit containing a high concentration of uranium) was removed as a result of the reaction, the reaction quenched out, indicating that the reaction was not self-sustaining.

3. The damage observed on the Zircaloy-2 mechanical-property specimens, originally supported on the titanium specimen holder, was caused by the "burning" of the specimen holder and not by a reaction of the specimens with their environment.

4. The damage observed on the top screen of the core tank, due to a high-temperature excursion, was caused by an event associated with the titanium specimen-holder spike.

5. The exfoliation observed on the screen specimens was caused primarily by corrosion or hot spots occurring in the cracks and laminations that

existed in the screens as installed in the vessel. The cracks and laminations were formed primarily during the punching of the holes during manufacture.

With respect to the fuel stability problems, the following data[6] are applicable.

It is concluded that uranium separates reversibly from the fuel solution in a manner which is related to the composition of the fuel and to the reactor power. From the criticality data, it appears that much of the separated uranium collects on the metal surfaces of the core tank, presumably because they are at high temperature. After the fuel solution has lost a kilogram or more of uranium, power excursions occur that can be attributed to shifting of the material in the core or to redissolution with resulting changes in reactivity. If enough uranium collects in one place on a metal surface in the core, the nuclear heating causes the temperature to rise uncontrollably, and the metal melts. Examination of the interior of the core with periscopes and metallographic examination of the corrosion specimens and pieces removed from the perforated plates in the core inlet indicate that some of the metal has been heated to temperatures above 1000°C. There is reason to believe that the hole in the core tank and the severe corrosion of the perforated plates in the core inlet resulted from overheating.

Run 18 was designed to study fuel instability problems and was conducted at a maximum power of 1.6 Mw. No power excursions were detected above background, about 400 g of uranium was "lost," and changes in fuel composition were small.

Run 19 was started to investigate core and blanket circulation rate, but low flow in both systems caused shutdown. It was found that the core circulation pump had been electrically connected in reverse. Examination of the blanket circulation pump revealed that about three-fourths of the titanium impeller had been consumed, apparently by combustion.

Although the exact circumstances which resulted in the damaged titanium probably cannot be determined, it is conjectured that the pump became gas bound in a high oxygen atmosphere, and that the protective oxide layer on the titanium was scratched, exposing metal to the oxygen. Newly exposed titanium metal can be expected to burn in an oxygen atmosphere.[5]

Several designs for a replacement for the core and pressure vessel have been prepared. They provide for the sweeping of the inside of the core tank with inlet fuel in one design and also for the using of the blanket as a core tank coolant in another design. Using the blanket as a core tank coolant would be accomplished by fabricating the core tank with two concentric spherical shells and then by pumping blanket material through the annular space before discharging the material to the main blanket region. In the interim, consideration is being given to the repair of the existing reactor by plugging the hole in the core tank as follows:[5]

1. The screen system will be surveyed with periscopes to determine which screens are already loose and to note any special problems.
2. The screens will be cut loose from the wall.
3. By holding the loose screens out of the way, photographs and a cast impression of the hole in the core tank will be made to enable a well-fitting patch to be machined.
4. The loose screens will be sectioned or dissolved and removed.
5. The hole will be plugged.

Needless to say, this procedure would require a considerable number of special tools, such as remote cutters, millers, nibblers, and loose-screen manipulators. A special core-hole impression device has been designed to press a thermoplastic material into the hole, to heat the plastic to soften it, and then to cool the mold prior to removal from the hole. Another tool has been constructed to toggle-bolt a patch over the hole using a gold gasket for sealing. The tool has been successfully used in the HRT mock-up. An ultrasonic thickness gauge to measure core-wall thickness has been built and tested successfully. Another interesting device is the remote weld-impression device, designed to take an impression of the welds in the top of the pressure vessel. This is accomplished by employing a block of thermoplastic which is heated by an embedded resistance heater.

If a successful repair is accomplished, it is obviously of more than passing interest to assure that another hole is not burned in the core tank. Hydraulic tests in the HRT mock-up have resulted in the following conclusions:[5]

As a result of the above investigations, it was concluded that satisfactory hydrodynamic operation of the HRT core could be achieved only by removing the top five or more screens and reversing the direction of flow. The importance of preventing solids deposition in a region of high power density may be appreciated by considering that the power density in corrosion products containing 4 per cent uranium is approximately 20 times that of the fuel solution.

References

1. Report of the Fluid Fuel Reactors Task Force to the Division of Reactor Development, TID-8507, February 1959. (Unclassified AEC report.)
2. D. W. Magnuson and Reginald Gwin, Comparison of Critical Experiments for the Determination of Eta of U^{233}, *Transactions of the American Nuclear Society*, 2(1): 146 (June 1959).
3. AEC Initiates Long Range Program to Develop Thermal Breeder Reactors, Atomic Energy Commission Press Release, Aug. 10, 1959.
4. *Power Reactor Technology*, 1(2): (February 1958).
5. Homogeneous Reactor Project Quarterly Progress Report for Period Ending April 30, 1959, ORNL-2743, Aug. 8, 1959. (Unclassified AEC report.)
6. Homogeneous Reactor Project Quarterly Progress Report for Period Ending October 31, 1958, ORNL-2654, Feb. 24, 1959. (Unclassified AEC report.)
7. Homogeneous Reactor Project Quarterly Progress Report for Period Ending January 31, 1959, ORNL-2696, Apr. 16, 1959. (Unclassified AEC report.)
8. Homogeneous Reactor Project Quarterly Progress Report for Periods Ending April 30 and July 31, 1958, ORNL-2561, Feb. 4, 1959. (Unclassified AEC report.)

NEW REACTOR CONCEPTS: THE FLUIDIZED-BED REACTOR STUDY

The fluidized-bed reactor (FBR) has been under study at Martin Nuclear Division for some time, and reference 1 is a report of recent progress. The reactor primarily consists of a cylindrical tank with retaining screens placed across each end. When operating the reactor, fuel pellets are placed in the tank and water is pumped into the tank from the bottom. At a certain velocity the drag of the water (or other coolant) flowing through the bed compensates gravitational attraction, and the pellets become suspended; also, they are continuously agitated by the turbulent flow of coolant. Reference 1 contains fluid-flow, heat-transfer, and nuclear analyses directed at determining the feasibility of such a concept. The preliminary studies were so sufficiently promising that a reference reactor was designed. Pertinent design data are presented in Table XII-1.

Table XII-1 FBR DESIGN DATA[1]

Reactor power	1366×10^6 Btu/hr; 400 Mw(t)
Gross electrical output, Mw	117
Steam pressure at full load at steam generator, psia	615
Normal reactor-coolant-system operating pressure, psia	2000
Reactor-coolant-system design pressure, psia	2500
Total number of loops	3
Steam generators per loop	1
Pumps per loop	1
No. of loops operating for design power of 117 Mw	3
Flow per loop at design power, lb/hr	5.07×10^6
Estimated reactor pressure drop, psi	75
Estimated steam-generator pressure drop, psi	45
Estimated primary-pipe pressure drop, psi	20
Estimated throttling, psi	40
Total estimated pressure drop, psi	180
Steam-generator inlet temperature, °F	565.5
Steam-generator outlet temperature, °F	491.5
Velocity in main loop piping at 528.0°F, ft/sec	30.2
Reactor coolant flow (total), lb/hr	15.21×10^6
Reactor inlet temperature, °F	491.5
Reactor outlet temperature, °F	565.5
Steam-generator size (total), sq ft	55,500
Primary-piping diameter, in.	16
Pressure-vessel diameter, ft	10.5
Pressure-vessel length, ft	13
Weight of fuel, lb	63,736
Core diameter, ft	8.5
Core height, ft	6.0
Fuel-pellet material	UO_2
Fuel-pellet diameter, mils	250
Enrichment, %	1.5
Volume fraction of coolant	0.70

The pressure vessel is constructed of SA-353 clad with 304 stainless steel. A bottom grid retains the pellets upon shutdown, and a top retaining grid prevents loss of fuel in the event of pump runaway. A particle separator is incorporated into the structure above the core; this is a cyclone separator which helps to remove fuel particles from the coolant before it leaves the vessel. Provisions are made for continuously slurring pellets from the core for chemical processing and for returning fresh fuel pellets to the core.

The control-system analysis for this reactor is particularly interesting since the nuclear behavior is closely related to the flow rate of coolant through the parameter of bed porosity. A considerable number of analog-computer runs were made to ascertain whether the reactor could be shimmed and/or scrammed by controlling the primary-coolant flow rate. The scram conditions analyzed were a cold-water accident, a high-power scram trip event, and a ramp insertion of positive reactivity. The response of the system, using flow rate control only, to increase power from 35 to 90 per cent, was determined. Within the assumptions made in solving the system-response equations, the technique of controlling the reactor by controlling the primary-coolant flow appeared satisfactory.

The reactor contains about 64,000 lb of UO_2, with a resulting specific power of about 12.5 Mw(t) per ton of oxide. This is typical of other water-cooled reactors of low enrichment (Dresden: 10.5, Yankee: 21.6). The specific power attests to the good heat-transfer properties of

fluidized beds. Although the superficial coolant velocity* was about 1.40 ft/sec in the bed, the large heat-transfer area and large amount of turbulence promoted high heat-transfer rates.

One of the main advantages sought in this reactor type is reduced fuel cost primarily through reductions in both fabrication and processing costs; however, improvements of neutron economy, which would reduce the net burn-up cost, are also visualized. The amount of cost improvement which these anticipated reductions represent depends strongly on the attainable fuel life in the more conventional reactors. The Yankee reactor fuel costs, for example, are composed of roughly 40 per cent element fabrication costs and 60 per cent processing, burn-up, and transportation costs. Of these costs, both the fabrication and processing costs, when referred to unit energy production, vary approximately inversely with fuel lifetime. These variations are illustrated in Table XII-2, which shows the estimated Yankee fuel-cost breakdown as a function of fuel lifetime.

Table XII-2 YANKEE FUEL-CYCLE COSTS[2]

Irradiation level, Mwd/ton	Initial U^{235} assay, %	Cost, mills/kw-hr: Fuel-element fabrication	Transport	Chemical processing and uranium conversion	U^{235} burn-up	Pu credit	Total
2,000	2.33	7.44	0.74	2.01	3.28	−1.32	12.15
4,000	2.48	3.72	0.37	1.00	2.64	−1.14	6.59
6,000	2.60	2.48	0.25	0.67	2.50	−1.08	4.82
8,000	2.77	1.86	0.19	0.50	2.36	−1.01	3.90
10,000	2.90	1.49	0.15	0.40	2.29	−0.94	3.39
12,000	3.05	1.24	0.12	0.33	2.23	−0.85	3.07
14,000	3.20	1.06	0.11	0.29	2.17	−0.77	2.86

A key point in the fluidized-bed reactor concept is the fuel element. The economic success of the reactor could well depend on obtaining a fuel pellet that did not seriously contaminate the coolant system through the release of fission products by one means or another. The importance of obtaining satisfactory fuel pellets was recognized in the feasibility study, and considerable space was devoted to a discussion of fuel pellets. A major problem connected with the unclad UO_2 pellet fuel is abrasion of the pellets caused by the relatively violent conditions in the bed. Erosion and corrosion of UO_2 pellets by water alone was found to be insignificant at the operating conditions of the reactor. The problem, of course, can be partially solved by minimizing the effect of fines in the system as well as by securing a more abrasion-resistant pellet. The former could be accomplished by processing a side stream for removal of fines, designing the primary loops to ensure no "dead spots" for trapping of fines, providing efficient fines removal equipment in the reactor cyclone system, achieving satisfactory decontamination techniques, etc. The current design of the FBR called for a maximum of 500 ppm fines in the main coolant loops. Preliminary abrasion tests on UO_2 pellets in small fluidized beds at room temperature indicated that the pellets lost from about 0.5 to 1.5 per cent of their weight per day. A 1 per cent loss yields a fines concentration of 4000 ppm in the reference design, and hence abrasion resistance must be improved if the design condition is to be met. It was recognized that testing at elevated temperatures and in radiation fields is a necessary part of a fuel-pellet development program.

Several experiments to clad the UO_2 pellets with nickel were described. The process is called "electroless nickel plating" and is accomplished as follows:

1. The UO_2 pellets are cleaned in hot alkaline solution and washed in distilled water.
2. Dilute palladium chloride is used to activate the UO_2 surface.
3. The pellets are placed in nickel sulfate–sodium acetate–sodium hypophosphate for 1.5 hr.

* The superficial velocity is the velocity the fluid would have, at a given mass flow rate, if there were no particles in the container.

The resulting nickel cladding, of about 1 mil in thickness, is mechanically bonded to the UO_2 surface. Although the cycling and abrasion tests were of fairly short duration, several thermal-cycling tests and abrasion tests were reported, and the results were encouraging.

The UO_2 pellets were prepared by two methods. The first method was one of cold compacting followed by sintering, and the second method was a capillary-drop method. This latter method consists of dropping a water suspension of UO_2 into a water repellent bed and drying the drop while it retains a spherical shape; these events are followed by sintering. Both methods produced UO_2 pellets having densities of about 90 per cent of the theoretical density. Additives were tried in both methods in an attempt to improve the physical properties. The additives studied were TiO_2, CaO, CaF_2, and CeO_2; these additives increased sintered densities to about 95 per cent. It was also hoped that the additives would permit increased bonding at the grain boundaries leading to increased abrasion resistance. ThO_2-UO_2 pellets were also made by the cold-compacting process and had densities of 98 per cent of the theoretical density following sintering.

As pointed out in reference 1, either jacketed or unjacketed fuel pellets might be considered for a fluidized-bed reactor, and much of the investigation summarized in the reference covers problems which would be common to both systems. However, the two systems would differ greatly in many of their characteristics and problems; the systems should probably be considered as two distinct reactor types.

If jacketed fuel elements were used, the possible advantages of the fluidized-bed system would include the elimination of control rods, the compensation of fuel burn-up by the loading of new fuel in small increments, some reduction in parasitic neutron absorption, and perhaps lower unit cost for fuel fabrication. An inherent problem, in addition to those problems (which were investigated in the reference) stemming directly from the characteristics of a fluidized bed, would seem to be that there is no obvious method of selecting old or damaged fuel pellets for removal as new fuel is added. Apparently, in such a reactor one would approach an equilibrium situation in which new fuel pellets are added at appropriate intervals and fuel pellets are removed in whatever order may be dictated by chance. It would appear that, in such a system, operation with some fraction of defective fuel elements would be necessary; that the average fuel lifetime, whether determined by fuel-pellet failure or by burn-up of fissionable material, would be considerably shorter than the maximum lifetime of individual pellets.

If, however, the use of unjacketed ceramic fuel in a water-cooled reactor is deemed attractive, then the fluidized-bed approach is one which naturally suggests itself, since the more conventional arrangement of fuel in a fixed solid structure is probably not easy to attain without the use of a metallic supporting structure of some kind. The problems of fission-product contamination which accompany unjacketed pellets must then be faced. The problem of selecting fuel for removal may be automatically solved, if attrition of the fuel by abrasion is severe; presumably, the fuel, on the average, will wear away at a more or less constant rate. Indeed, if the abrasion rate amounted to approximately 1 per cent per day, as in the case of the pellets investigated in the reference, the average fuel life in the reference reactor would be only about 1200 Mwd/ton, even if fuel pellets could be left in until they were completely worn away. It is doubtful that such a short fuel life could be tolerated, even if fuel fabrication costs were quite low. Consequently, the improvement of abrasion resistance appears to be necessary from the standpoint of fuel cost as well as from the standpoint of system contamination.

The discussion of pellet fuel elements for the Pebble Bed Reactor[3] (reviewed in *Power Reactor Technology*, 2(3): (June 1959)) may also be pertinent to the FBR, since there appears to be no fundamental reason why UO_2 is the only material that can be used for preparing fuel pellets.

References

1. M. R. Scheve, Fluidized Bed Reactor Study, Phase I — Feasibility, MND-FBR-1696, February 1959. (Unclassified AEC report.)
2. Costs of Nuclear Power, TID-8506, July 1959. (Unclassified AEC report.)
3. Sanderson and Porter, Design and Feasibility Study of a Pebble Bed Reactor Steam Power Plant, NYO-8753(Vol. I), May 1, 1958. (Unclassified AEC report.)

LEGAL NOTICE

This document was prepared under the sponsorship of the U. S. Atomic Energy Commission. Neither the United States, nor the Commission, nor any person acting on behalf of the Commission:

A. Makes any warranty or representation, expressed or implied, with respect to the accuracy, completeness, or usefulness of the information contained in this report, or that the use of any information, apparatus, method, or process disclosed in this report may not infringe privately owned rights; or

B. Assumes any liabilities with respect to the use of, or for damages resulting from the use of any information, apparatus, method, or process disclosed in this report.

As used in the above, "person acting on behalf of the Commission" includes any employee or contractor of the Commission, or employee of such contractor, to the extent that such employee or contractor of the Commission, or employee of such contractor prepares, disseminates, or provides access to, any information pursuant to his employment or contract with the Commission, or his employment with such contractor.

☆ U. S. GOVERNMENT PRINTING OFFICE O—1959-521976/2

NUCLEAR SCIENCE ABSTRACTS

The U. S. Atomic Energy Commission, Technical Information Service, publishes *Nuclear Science Abstracts (NSA)*, a semimonthly journal containing abstracts of the literature of nuclear science and engineering.

NSA covers (1) research reports of the U. S. Atomic Energy Commission and its contractors; (2) research reports of government agencies, universities, and industrial research organizations on a world-wide basis; and (3) translations, patents, books, and articles appearing in technical and scientific journals.

Complete indexes covering subject, author, source, and report number are included in each issue. These are cumulated quarterly, semiannually, and annually providing a detailed and convenient key to the literature.

Availability of *NSA*

SALE *NSA* is available on subscription from the Superintendent of Documents, U. S. Government Printing Office, Washington 25, D. C., at $18.00 per year for the semimonthly abstract issues and $15.00 per year for the four cumulated-index issues. Subscriptions are postpaid within the United States, its territories, Canada, Mexico, and all Central and South American countries, except Argentina, Brazil, British and French Guiana, Surinam, and British Honduras. Subscribers in these Central and South American countries, and in all other countries throughout the world, should remit $22.50 per year for subscriptions to semimonthly abstract issues and $17.50 per year for the four cumulated-index issues.

EXCHANGE *NSA* is also available on an exchange basis to universities, research institutions, industrial firms, and publishers of scientific information. Inquiries should be directed to the Technical Information Service Extension, U. S. Atomic Energy Commission, P. O. Box 62, Oak Ridge, Tennessee.

POWER REACTOR TECHNOLOGY may be purchased ($2.00 per year, $0.55 per issue) from the Superintendent of Documents, U. S. Government Printing Office, Washington 25, D. C. The use of the coupon below will facilitate the handling of your order.

POSTAGE AND REMITTANCE: Postpaid within the United States, Canada, Mexico, and all Central and South American countries except as hereinafter noted. Add $0.50 per year, or $0.15 per single issue, for postage to all other countries, including Argentina, Brazil, British and French Guiana, Surinam, and British Honduras. Payment should be by check, money order, or document coupons, and MUST accompany order. Remittances from foreign countries should be made by international money order, or draft on an American bank, payable to the Superintendent of Documents, or by UNESCO book coupons.

order form

SUPERINTENDENT OF DOCUMENTS
U. S. GOVERNMENT PRINTING OFFICE
WASHINGTON 25, D. C.

Enclosed:
document coupons ☐ check ☐ money order ☐

Charge to Superintendent of Documents No. _____

Please send me a one-year subscription to

POWER REACTOR TECHNOLOGY
($2.00 a year; $0.55 per issue.)

SUPERINTENDENT OF DOCUMENTS
U. S. GOVERNMENT PRINTING OFFICE
WASHINGTON 25, D. C.

(Print clearly)

Name _____

Street _____

City _____ Zone ____ State _____